PHD

The effects of ultrasound on mammalian cells

Ives, Katherine Jane

Award date:
1999

Awarding institution:
University of Bath

The Effects of Ultrasound on Mammalian Cells

submitted by

Katherine Jane Ives

for the degree of PhD
of the University of Bath

1999

K. J. Ives

ProQuest LLC
789 East Eisenhower Parkway
P.O. Box 1346
Ann Arbor, MI 48106-1346

To my parents

&

Bill and Joan.

ACKNOWLEDGEMENTS

I would like to thank so many people that I run the risk of producing an award acceptance speech, so I will attempt to make this brief. First and foremost I would like to thank Bill for his encouragement, enthusiasm, guidance, wit, friendship and vast knowledge of all things biochemical. Not to mention his willingness to recommend alcohol as either a celebration or commiseration. I am also indebted to the following Drs for their advice and assistance; Anne Tinsley-Bown at CAMR, Francis Duck at the RUH, Bath, Clarie Doody at the University of Bath and David Darling at King's College, London. While Ursula Potter at Centre for Electron Optics at the University of Bath must be credited for her help and expertise in electron microscopy.

My sincere thanks to Magali and Joan for their help and friendship throughout my time in the lab and numerous games of badminton. Thanks also to all the people who passed through 1:45 making it a happy place to be, especially Iggy and Suzie Sue (also a badminton player). No memory of days in the lab would be complete without Prof. Robert Eisenthal who kept me smiling even when I thought I would scream. I shall truly never forget funny walks, dances, phrases, sayings and stories but "Let the ball roll" will always be my favourite.

I must apologise for moaning and thank a number of people for listening. My flatmates: Natalie, Iggy, Magali (especially as she had to work with me too), Diana (for coordinating things in Bath), Brian, Spenny (for his computing skills), Stuart and Steve. My family: Jane, Rob, Philip, Grandpa and my parents without whom none of this would have been possible both in the conventional sense and in view of their words of wisdom particularly when it came to bugs and germs. My e-mail buddies Ed, Girly Steve, Roy, Audrey, Chris (who is always there), Russell, Simon, Claire, Gary and finally Ju, with whom I consumed several bottles of fine (?) wine, ate substantial amounts of good food, debated a number of highly intellectual issues (they know who they are) and created havoc. Last but not least, Ruth, John and Jacob for entertainment and sanctuary.

Gratitude is due to the BBSRC, CAMR and my parents for funding.

Finally, thanks to Steve for driving me up and down the hill, late night discussions, making me laugh and most memorably, asking numerous thought provoking questions regarding the well-known vital stain trypan *purple*.

ABSTRACT

This project had two major objectives, firstly to address the bioeffects of ultrasound on mammalian cells and secondly to investigate the possibility that ultrasonic energy could be used to heat microcarriers within a biofermentation system. The former having far reaching implications for the use of ultrasound in medicine where research has been sparse.

The use of ultrasound parameters similar to those employed therapeutically as a heating agent in the biofermentation of mammalian cells was investigated. Mathematical modelling showed that it was not possible to heat the polystyrene microcarriers available on the market to a temperature which would sustain cell growth using ultrasound under these conditions. However, it was possible to subject cells to ultrasound without any detectable effects on their health depending on the design of the experimental exposure system.

An overview of general cell health was obtained under conditions where the physical ultrasonic wave was less 'clean'. Alterations in the integrity of the cell membrane were observed by trypan blue exclusion and the successful stable transfection of foreign DNA into host cells. The latter also indicated that DNA breaks were induced, at least transiently, and there was also evidence of an upregulation in the rate of integration. Increases in PARP activity showed that chromatin structure was quite clearly damaged by cellular insonation. Cell lysis and sonoporation were attributed to mechanical (non-thermal, non-cavitational) effects of ultrasound, less severe damage to the plasma membrane was suggested to be due to the mechanical effects associated with cavitation, while DNA damage was thought to be due to the action of hydrogen peroxide, at least in part.

Scanning electron microscopy was employed to compare the permeabilisation of cells by ultrasound with standard chemical techniques. Cells were clearly holed, divided or fragmented in response to ultrasonic exposure. This technique, in particular, revealed the severity of the physical damage insonation can produce.

ABBREVIATIONS

[^{3}H]NAD	tritium labelled nicotinamide adenine dinucleotide
ADP	adenosine diphosphate
ADP-ribose	adenosine diphosphate ribose
ALARA	as low as reasonable achievable
ATP	adenosine triphosphate
ATPase	adenosine triphosphatase
cDNA	complementary deoxyribonucleic acid
CHO	Chinese hamster ovary
CPM	counts per minute
CW	continuous wave
DNA	deoxyribonucleic acid
DTT	dithiotreitol
EDTA	ethylendiamine tetraacetic acid
EGTA	ethylene glycol-bis(oxyethylenenitrilo)tetraacetic acid
EM	electron microscope
ERA	effective radiating area
ESWL	extracorporeal shock wave lithotripter
FACS	fluorescence-activated cell-sorting
FCS	foetal calf serum
G418	gene which confers resistance to geneticin
GFP	green fluorescent protein
Gray(Gy)	The SI unit of absorbed dose of ionizing radiation, defined as the absorbed dose when the energy per unit mass imparted to the matter by ionizing radiation is 1 joule per kilogram.
Hepes	*N*-(2-hydroxyethyl)piperazine-*N*'-(2-ethanesulforic acid)
MEM	minimal essential medium
NAD	nicotinamide adenine dinucleotide

NCRP	National Council on Radiation Protection and Measurements
neper	The SI unit which denotes the attenuation of an amplitude A_1 to an amplitude A_2 as N nepers, where $N=\log_e(A_2/A_1)$. 1 neper = 8.686 decibels.
NPL	National Physics Laboratory
PARP	poly(ADP-ribose) polymerase
PBS	phosphate buffer saline
PVC	polyvinyl chloride
rayl	An SI unit of sound impedance (ratio between the wave pressure and the particle velocity it produces). The impedance is 1 rayl if unit pressure produces unit velocity. 1 rayl = $1kgm^{-2}s^{-1}$.
rpm	revolutions per minute
RPMI	Roswell Park Memorial Institute
RUH	Royal United Hospital
SEM	scanning electron microscopy
SOD	superoxide dismutase
SONAR	sound navigation and ranging
SSB	single strand break
TCA	trichloroacetic acid
TEA	triethanolamine
watt(W)	The SI unit of power, defined as a power of 1 joule per second.
WFUMB	World Federation of Ultrasound in Medicine and Biology

CONTENTS

CHAPTER ONE

INTRODUCTION

1.1 Sound, ultrasound and its applications

1.1.1 Sound

Mechanical or acoustic waves consist of pressure and particle displacement, produced when the particles, of which a medium is composed, are supplied with energy and are driven to vibrate. Wave propagation ensues when these particles transfer some of the energy to those adjacent to them. Mechanical waves which propagate within solid bodies are referred to as vibrations, whereas those which propagate in liquids and gases are known as sound.

Some basic wave properties are illustrated in figure 1.1. The amplitude of a wave is the maximum excursion either above or below its undisturbed value and determines its power (energy). A wavelength (λ) is the repeat distance from any measurable point to the same point after it has travelled through one cycle of negative and positive displacement. The number of wavelengths which pass through any given point in one second determines the wave frequency (f). Once generated, the frequency of a wave remains constant. It should be noted that wave velocity (v) is not dependent on frequency though they are related by the equation

$$v = f\lambda.$$

Hence it follows that, since frequency remains constant, if the velocity changes as the wave moves from one medium to another so too does the wavelength.

Sound waves are longitudinal in that particle vibration is in the same direction as wave propagation allowing regions of compression and regions of rarefaction.

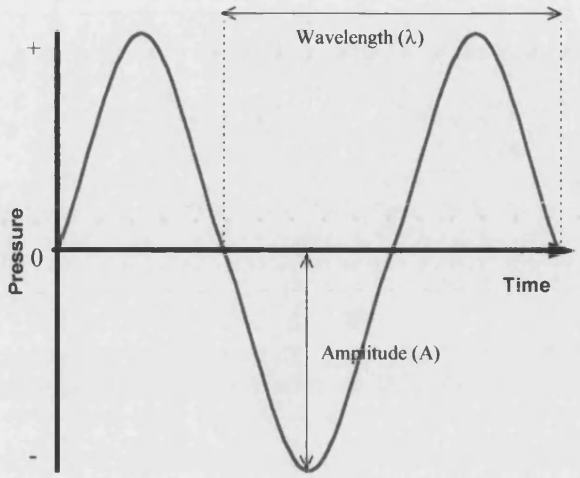

Figure 1.1: Schematic diagram of a wave.

The wavelength (λ) is defined as the length of one repeating unit consisting of a peak and a trough, while the amplitude (A) of the wave is defined as the maximum excursion of any portion from its original resting position. Adapted from Williams, 1983.

1.1.2 Ultrasound and its applications

The term ultrasound, is used to describe ultrasonic waves of greater frequency than those audible to the human ear (16 Hz-20 kHz), while infrasound describes those of lower frequency. In nature, there are several animals who utilise ultrasound, for example, bats navigate by the use of sound in the range of 30-70 kHz. Similar pulse-echo principles have been employed by mankind in sound navigation and ranging (SONAR) allowing under water imaging to take place and providing easy location of submarines, fish, mineral and oil deposits. In industry, ultrasound has a wide range of applications including drilling, grinding, cutting, cleaning, welding and metal testing, while chemistry has a specialised branch known as sonochemistry which is devoted to the use of ultrasound in synthesis, polymerisation and catalysis. However, the most well-known applications of ultrasonic waves lie in the field of medicine and involve sound waves in the low megahertz frequency range (0.2-20 MHz).

Ultrasonic waves have been successfully employed in medicine over the past 40 years and the diversity of their application is ever broadening. Therapeutic applications include the disintegration of gall or urinary stones, using high amplitude low frequency waves from an extracorporeal shock wave lithotripter (ESWL) (Coleman and Saunders, 1992; Delacretaz *et al*, 1995) and physiotherapy in which ultrasound has a wide range of uses from the control of pain (Gray, Quayle and Hall, 1994) and muscle strains to alleviation of inflammation (Williams, 1983), stimulation of tissue repair and promotion of wound healing (Ernst, 1995). Ultrasound is employed diagnostically to provide internal body images. In this context it is used in the initial location of gall and urinary stones, the identification of various organ abnormalities, the imaging of blood flow and identification of occlusions within vessels (Goldberg and Kimmelman, 1988) and also plays an important role in the monitoring of surgical tools during complex procedures such as cryosurgery (Onik, Downey and Fenster, 1996). Further to these areas ultrasound has been described to be potentially useful in a number of other experimental fields such as phonophoresis, the use of ultrasound in percutaneous drug delivery (Meidan, Walmsley and Irwin, 1995); sonodynamic therapy, the enhancement of anti-cancer drugs in the presence of ultrasound (Umemura *et al*, 1992; Tata *et al*, 1996); tumour targeting and abolition (Malcolm and ter Harr, 1996; Chen *et al*, 1998*)*; targeted drug and gene delivery (ImaRx Pharmaceutrical Corp., 1997; M^{c}Creery *et al*, 1998a+b) and very high frequency acoustic microscopy (Chandraratna *et al*, 1998).

The most common medical application of ultrasound is foetal imaging in pregnant women (Merritt, Kremkau and Hobbins, 1992). This procedure utilises a pulse-echo technique and provides accurate and detailed information on the progression of the pregnancy including foetal size, detection of multiple pregnancies, placental location, diagnosis of uterine tumours and identification of various foetal abnormalities (e.g. Down's Syndrome, cardiac problems, abdominal wall defects). In Britain, every pregnancy is routinely scanned at 12-20 weeks gestation and in high risk cases several images may be carried out. To date ultrasound has been perceived as a totally safe method of non-invasive foetal assessment, however it does have the potential to cause adverse bioeffects. These bioeffects are categorised into two groups by their mechanisms; thermal and non-thermal.

1.2 Mechanisms of ultrasound induced bioeffects

Although, strictly speaking the mechanisms by which ultrasound may cause bioeffects are categorised into two groups, for simplicity's sake they are described here in three sections: thermal mechanisms, non-thermal cavitational mechanisms and non-thermal non-cavitation mechanisms.

1.2.1 Thermal mechanisms

Thermal bioeffects arise due to the attenuation of the ultrasonic beam as it travels through tissue losing energy as heat. During ultrasound treatment this thermal gain is dependant on frequency, intensity and area of the beam, the duration of therapy and also the rate of heat removal due to blood perfusion or conduction. Clearly ultrasound induced rises in tissue temperatures *in vivo* have the potential to be damaging just as hyperthermia induced by any means has teratogenic properties (World Federation for Ultrasound in Medicine and Biology (WFUMB), 1998).

The human body maintains a nearly constant core temperature which is achieved by complex metabolic and neural mechanisms which balance heat loss and internally generated heat. Variability of this core temperature is limited to a very few degrees. Brief periods of temperature elevation, up to 40.5 °C, result in reversible cell and tissue damage, while sustained temperatures above 41.5 °C are barely compatible with life and ultimately result in the collapse of most organ systems. At tissue level, rises in temperature result in cell death or other significant biological defects such as, increased metabolic activity and cell cycling rates, increased heart rate and altered blood perfusion rates, increased leakage of proteins through capillary membranes, oedema formation and the production of heat shock proteins (Barnett *et al*, 1994). Non-proliferative metabolically active tissues are more resistant to damage by heat than actively proliferating tissues (WFUMB, 1992). This indicates that areas of proliferative activity in embryonic as well as adult tissues are most at risk. Such risk tissues in adults include the gut epithelium, bone marrow, testes, endometrium and skin. However, focal loss of cells in these areas is unlikely to cause significant tissue

damage as repopulation from adjacent undamaged cells is probably prompt and complete. Exposure of pregnant animals to hyperthermia can cause adverse reactions including prenatal death and resorption, stillbirth and small or malformed offspring (WFUMB, 1992). Tragically, embryonic or foetal death, resorption or abortion can occur after hyperthermia at any stage of gestation, while malformation generally occurs only after exposure during organogenesis and foetal tissue disruption occurs following hyperthermia in later stages of development. Ultimately, teratogenic damage is highest in the early stages of organogenesis when the central nervous system is most at risk (WFUMB, 1992), although local damage can produce lesions in most tissues (Barnett *et al*, 1994).

Many defects caused by hyperthermia in animals have been observed in children following febrile episodes *in utero*, especially neural tube defects (WFUMB, 1998). However, there is uncertainty whether the temperature threshold for damage is best represented by the absolute temperature reached by the embryo or by the elevation above normal body temperature. In animals which are popularly studied, normal body temperatures differ between species, ranging from 37.5 °C in humans to 39.5 °C in sheep, rabbits and guinea pigs. Although few studies have been designed to calculate thermal thresholds in humans due to the difficulties involved, data from whole body hyperthermia experimentation has demonstrated that a rise in body temperature of 1.5-2.5 °C is hazardous to embryonic and foetal development in animals (WFUMB, 1998). Since it is unclear whether an absolute temperature is critical for normal biochemical processes and development of all mammalian systems or if the catalysts for biochemical reactions (e.g. enzyme systems and biomolecular messengers) have operating temperatures that are optimised for each species, with similar limited tolerance ranges (WFUMB, 1998), interpretation of the relevance of the results from animal experimentation with regard to human risk is extremely difficult. However, much of the variation between species in threshold absolute temperature for teratogenic damage appears to be accounted for by the variation in normal temperature between the species. The best indication of risk, therefore, seems to be the temperature elevation above normal in that particular species. Accordingly, above an established threshold temperature, there is a very definite dose response

relationship between temperature elevation and the severity of tissue damage and also the duration of exposure and the degree of damage (WFUMB, 1998).

There are many uncertainties involved in the extrapolation of biological effects of whole body hyperthermia to the risk from ultrasound induced heating. With regard to experimentation in animals, whole body heating is an extremely slow process as compared with the absorption of ultrasound where substantial elevations in temperature occur within a few seconds. The issues of heating due to ultrasound are further complicated by the fact that absorption is greater in dense tissue such as bone and cartilage than it is in soft tissue and therefore the degree of heating across the tissues is not uniform (Barnett *et al*, 1997). Heating is greatest at soft tissue-bone interfaces making the central nervous system particularly susceptible to damage due to its close proximity to bone. One implication of this is that it may be prudent to perform ultrasound scans during pregnancy prior to the formation of foetal bone in order to protect the developing central nervous system. However, this must be considered in parallel with the fact that early ultrasound examinations led to the exposure of a far greater proportional volume of an early embryo, whereby cell death and delayed proliferation may result in depletion of cells below the critical mass required for a developmental event such as closure of a neural tube or formation of an organ (WFUMB, 1992).

Naturally body temperatures do, of course, vary greatly. For example, during exercise or in response to disease states where temperatures of 40-41 °C can be observed (Merritt, Kremkau, Hobbins, 1992). However, these elevations arise from an adaptive reversible response triggered by pyrogen from leucocytes and resulting in a resetting of the body's 'thermostat'. Indeed, it is thought that fever during illness, the most common cause of hyperthermia in humans, is an effective reaction to viral or bacterial infection since such organisms cannot tolerate high temperatures (Barnett *et al*, 1994). Conversely hyperthermia due to fever during pregnancy is seldom beneficial, but instead is recognised as a human abortifacient (WFUMB, 1992). In contrast to pyrexia induced by disease and exercise, during environmentally induced hyperthermia (e.g. hot water, sunshine) no pyrogen is produced and no thermostat resetting occurs, although protective heat shock proteins are produced. The expression of heat-shock

genes which is mediated by heat-shock factor is reported to be activated by a temperature increase rather than an absolute temperature. The precise temperature rise required is thought to be related to the protein degeneration profile characteristics of each cell type (WFUMB, 1998), adding weight to the argument that teratogenic effects occur in response to temperature elevation rather than absolute values. Regardless of their method of production, under normal hyperthermic conditions, heat-shock proteins are produced to protect the cell from damage. Sadly, ultrasonic absorption leads to heating on a time scale of seconds which is too rapid to allow any thermo-protective mechanism to act, thus making tissue more susceptible to damage (Barnett *et al*, 1994).

Unfortunately temperature rises within the body in response to exposure to an ultrasonic field are rather difficult to predict accurately and hence risk to patient health is a complex issue which continues to be addressed.

1.2.2 Non-thermal cavitational mechanisms

Cavitation is the formation and dynamic life of gaseous or liquid vapour bubbles within a medium exposed to an ultrasonic field (Suslick, 1988). Two categories of microbubble activity are generally described, the first of which is referred to as non-inertial cavitation, gas body activation or stable cavitation. This occurs where a pre-existing bubble undergoes periodic and regular changes in volume in response to applied acoustic pressures, causing the bubble radius to vary around an equilibrium value as it oscillates within the acoustic field (Figure 1.2(a)). The bubble exists for many acoustic cycles and subjects the liquid around it to microstreaming and high shear stresses (1.2.3). This process is induced at relatively low acoustic intensities, while at higher intensities the second category of bubble activity known as, inertial or transient cavitation occurs. Here bubbles oscillate in an unstable manner and experience periodic but qualitatively different changes in volume causing their radii to grow rapidly over a period of a few cycles and leading to their violent collapse (Figure 1.2(b)). These microbubbles may be of much smaller than resonant size and can be considered to be cavitation nuclei. When the bubble is compressed to its minimum radius, pressures of thousands of bars and simultaneous localised temperatures in the

order of thousands of degrees Kelvin are experienced inside the bubble and are sufficient to allow energy transfers to other forms to occur. Light flashes known as sonoluminescence are emitted and the disruption of chemical bonds allows the formation of free radicals (atoms or molecules with one or more unpaired electrons) which subsequently yield reactive sonochemicals. This process of energy re-radiation is known as scattering (WFUMB, 1998). In addition, high pressure liquid jets travelling at great velocities frequently pass through a bubble as it undergoes collapse. Notably, a stably oscillating bubble has the ability to become inertial and collapsing inertial bubbles can produce many smaller stable bubbles. Ultimately, these processes convert the low-energy density of a sound field into high-energy density in the interior and surrounding of a collapsing bubble (Riesz and Kondo, 1992). It is clear that these high-energy 'hot spots' have the potential to elicit damage in biological tissue. Indeed, there are a number of possible mechanisms by which damage could be induced including, bubble associated microstreaming and radiation forces, which will be dealt with in 1.2.3, and the production of free radicals and sonochemicals.

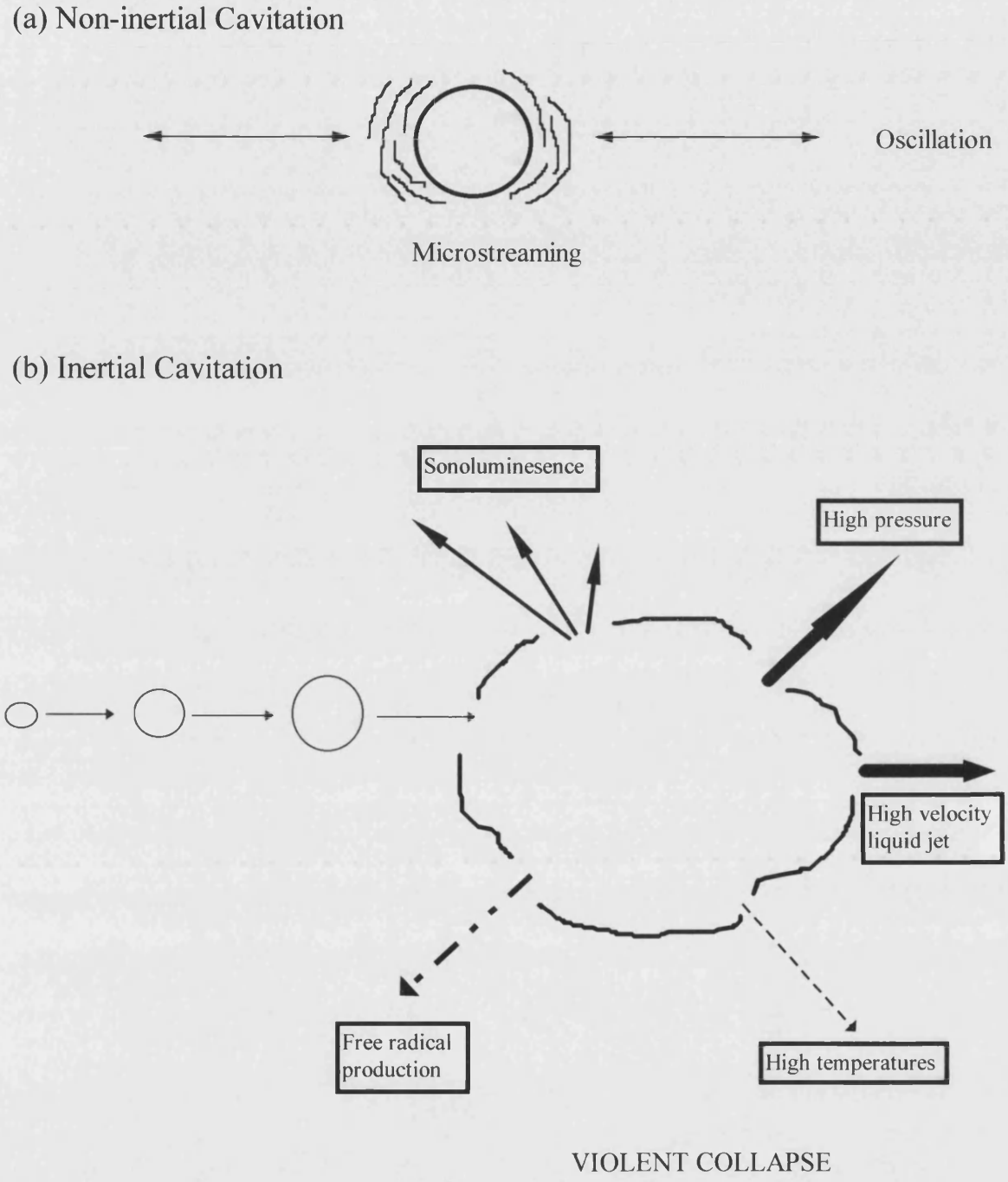

Figure 1.2: Schematic representation of cavitation.

(a) depicts a gas body oscillating stabily within a field at relatively low acoustic intensities and (b) shows the growth and eventual collapse of a bubble undergoing inertial or unstable cavitation.

In water, the transient high temperatures and gas shocks produced upon microbubble collapse produce hydroxyl radicals and hydrogen atoms due to the thermal decomposition of water molecules, subsequently these either combine to form hydrogen gas, hydrogen peroxide and new water molecules or attack solute molecules which are reduced or oxidised (Riesz and Kondo, 1992). Meanwhile sonolysis in the presence of oxygen leads to the formation of oxygen atoms which can react with hydrogen atoms to produce the acid form of superoxide anions (Riesz and Kondo, 1992), alternatively these anions can also be formed directly in water in the absence of oxygen. The production of free radicals is extremely rapid, indeed under free-field conditions ultrasonic exposure of argon saturated water allows transient cavitation and free radicals to occur within microseconds (Riesz and Kondo, 1992). It is clear that a range of free radicals are produced in response to ultrasonic exposure depending on the gaseous content of the solution. Unfortunately, the extent of free radical production remains unclear for media of the viscosity and surface tension equivalent to that found in mammalian body fluids and tissues (Edmonds and Sancier, 1983).

It is important to note that free radicals are produced naturally within cells and indeed reactive oxygen species have a role in cell signalling (Khan and Wilson, 1995). However, free radicals are also known to produce biologically detrimental effects and are implicated in a number of disease pathologies including cardiovascular, neurodengerative and chronic inflammatory disease as well as cancer. Lipids, proteins and thiols, DNA and uric acid are amongst the molecules which are subject to damage or change in response to free radicals (Rumley and Paterson, 1998). It is worrisome that alterations to these molecules could led to drastic cellular damage, in particular DNA damage may led to mutation, and as a result may have a serious impact on the health of babies exposed to ultrasound *in utero*.

Cavitation in general increases with increasing intensity of the ultrasonic beam and the threshold at which it occurs increases with increasing frequency, increasing ambient pressure, increasing temperature, increasing gas content and viscosity of the medium (Riesz and Kondo, 1992). Cavitation phenomenon is utilised by industry in ultrasonic cleaning and sonochemistry and is also used in cell disrupters. It is further harnessed

in medicine in the disintegration of gall stones. Unfortunately the very nature of cavitation and its associated energy loss mechanisms make it a potentially dangerous ultrasonic side effect *in vivo*. The most likely sites for formation of such bubbles from cavitation nuclei are low viscosity fluid environments, for example, blood and amniotic fluid and in air filled regions, such as, the lungs and the large intestine.

1.2.3 Non-thermal non-cavitational mechanisms

The propagation of ultrasound stresses the medium supporting the wave and its inhomogeneities. Particles experience not only forces in the direction of wave propagation but also shear and torque. Such stresses produce mechanisms of ultrasonic bioeffects which are neither thermal or cavitational in origin, although some special cases do occur in association with microbubbles. These mechanisms include such things as radiation pressure, radiation force, acoustic torque, acoustic streaming and shear stresses.

Radiation pressure is the pressure which is exerted upon any object immersed within an acoustic field, while radiation force is the term used to describe the force experienced by such an object. The direction and the magnitude of this radiation force are dependent on the parameters of the field and also the size and shape of the object. The direction of propagation is normally, although not always, away from the transducer and is proportional to the intensity of the wave in magnitude. Such radiation forces can result in the aggregation of particles and their subsequent separation from the rest of the media undergoing sonication, which has implications for biological cells in fluid spaces, for example blood (Barnett *et al*, 1994). Particles are also known to agglomerate around gaseous bodies during cavitation due to a specialised form of radiation forces, which may be particularly important where the particles are biological cells (Barnett *et al,* 1994; WFUMB, 1998). Radiation forces can also cause free bubbles to move around and fuse with each other. Near a solid boundary, the radiation force exerted on a bubble may draw it towards the boundary. *In vitro*, free bubbles move across experimental tanks extremely quickly and subsequently persist until the ultrasonic exposure is discontinued, although this is less likely to occur *in vivo* due the constrictions of tissue (WFUMB, 1998).

Acoustic torque is produced due to the non-uniformity of an ultrasonic field and causes a twisting action, which could lead to cellular rotation or movements of the intracellular structure *in vivo* (Barnett *et al*, 1994).

Acoustic streaming describes the movement of fluid within an ultrasonic field and is particularly important where the fluid encounters a solid body or boundary. For example, this may occur as plasma travels through a blood vessel, a high velocity gradient can be reached as the plasma (fluid) streams against the vessel wall (boundary) causing shear stresses. Significant biological consequences may also occur at the embryonic epithelia as it acts as a boundary in amniotic fluid during ultrasonic scanning to produce streaming effects (Barnett *et al*, 1994). Furthermore, unusual acoustic microstreaming patterns are known to occur around cavitating bubbles which have unknown biological consequences, although it is possible that the high velocity gradients and shear stresses could lead to severe membrane damage if the bubble activity occurs near a cell (Barnett *et al*, 1994). Streaming velocities of up to 10 cms^{-1} have been recorded in water using diagnostic ultrasound (WFUMB, 1998). Indeed, streaming velocities in blood may exceed those in water as attenuation and viscosity are greater, although it is thought that the types of exposure in common usage *in vivo* are likely to produce similar results to those seen in water (WFUMB, 1998).

1.3 Evidence of ultrasound induced bioeffects

1.3.1 In humans

Widespread exposure of babies to ultrasound in the womb in the U.K., and to a lesser extent in the U.S.A., over the past twenty five years does not appear to have led to serious physical or mental abnormalities in children. Nor have any serious side-effects been reported due to the use of diagnostic ultrasound which has been practised for more than 40 years (Merritt, Kremkau and Hobbins, 1992). However, recently the effects of ultrasound as used in medicine, particularly in foetal scanning have become a concern amongst the scientific (Edwards, 1999) and medical community (Salvesen *et al*, 1993) and indeed this concern has spread to the popular press (Wallace, 1996;

TV Quick, 1997) and media (This Morning, 1999). As foetal scans have provided more and more information on risks of children being born with physical or chromosomal abnormalities so they have been used more frequently. Indeed, mothers who are deemed to be in a high risk group will undergo ultrasound several times during the course of their pregnancy. However, some recent reports have stated that routine scanning has little or no advantage over selective scanning in terms of detection of foetal defects (Ewigman, Green and Lumley, 1993) and it is with regard to this information that women in the U.S.A. are not routinely scanned.

Reports have described cases where children who had been exposed to ultrasound *in utero* suffered from difficulties such as dyslexia (Stark *et al*, 1984) and speech delay (Wallace, 1996) or other ultrasound induced changes within the brain, leading to increased incidence of left handedness (Salvesen *et al*, 1993). These bioeffects are mild, although, it remains unknown as to what other subtle neuronal damage may be occurring in children as a consequence of ultrasonic exposure, let alone what the implications may be in later life. In all areas of diagnostic ultrasound, the risk of adverse bioeffects is increasing as the acoustic outputs from clinical scanners continue to rise dramatically, as diagnostic sensitivity improves (WFUMB, 1998). At present there is no direct evidence that the mechanisms by which bioeffects are induced occur in humans; however there is substantial circumstantial evidence based on some of its therapeutic actions and also *in vivo* experimentation in other animals. This situation is due, at least in part, to the fact that experimentation of this nature in humans is extremely difficult.

1.3.2 In vivo

A considerable body of information regarding what may happen during ultrasonic exposure in humans has been gained from *in vivo* work in animal models. Components of all mechanisms by which ultrasound may cause damage have been reported to some extent *in vivo*, for example ultrasound induced heating in mouse skull and guinea pig foetal skull-brain interfaces have been documented in experiments designed to model human foetal insonations (WFUMB, 1998). One interesting observation of this work was that degree of perfusion cooling was related to the

gestation of the pregnancy. Foetuses nearer to term had more substantially developed vasculature and were therefore able to produce more effective cooling mechanisms. Similar work has been undertaken in the cerebral cortex of sheep (WFUMB, 1998) and in monkeys the intracranial temperatures in response to low output diagnostic ultrasound have been analysed. The formation of microbubbles *in vivo* has been described in guinea-pig hind limbs (ter Harr and Daniels, 1981) and rat lungs (Holland *et al*, 1996), unfortunately the properties of these cavitation nuclei are largely unknown. Meanwhile streaming has also been observed in an *in vivo* setting in situations such as intracranial haemorrhage, cystic breast fluid and abscess, fortunately this process is thought unlikely to be harmful (WFUMB, 1998).

A plethora of *in vivo* experimentation has revealed a range of ultrasound induced effects on tissues, including; reversible biochemical changes in embryonic rat central nervous system (Margulies *et al*, 1991), altered locomotive and exploratory activity in female mice and aggressive male mice following prenatal administration (Hradzdira *et al*, 1995), ultrasonically induced lung haemorrhage in neonatal mice and swine (Baggs *et al*, 1996), intestinal haemorrhage in mice (Dalecki *et al*, 1996), delay of tumour growth in rats (Debus *et al*, 1999) and irreversible hind-leg paralysis in neonatal mice (Barnett *et al*, 1994). Stabilised gas-bodies used as contrast agents in diagnostic ultrasound have been shown to enhance vascular bioeffects seen in mouse intestine (Miller and Gies,1998), while other microbubbles have been shown to have potential in therapeutic medicine, over and above the disintegration of gallstones, since vascular transport of bubbles to a remote site led to the ablation of tissue volumes in dog brain and prostate (Fry *et al*, 1995).

Useful information has also been gained from *ex vivo* techniques, for example; significant stimulation of mouse calvaria bone formation was observed in excised bone maintained in tissue culture following ultrasound exposure (Reher *et al*, 1997), alterations in the neural circuit activity of rat brain hippocampus in culture were described following insonation (Bachtold *et al*, 1998), gross morphological abnormalities and death were observed following insonation of rat whole-embryo cultures (Ramnarine *et al*, 1998) and ultrasound induced heating in freshly excised human foetal femurs, guinea pig brain, pig liver and sheep brain have also been

confirmed (WFUMB, 1998). *Ex vivo* data is perhaps more difficult to interpret, although similar experimentation is often difficult or impossible to conduct *in vivo*.

Clearly it is possible to induce adverse bioeffects *in vivo* ultrasonically. In order to minimise the risks of ultrasonic therapy as it is currently used in medicine the ALARA (As Low As Reasonably Achievable) principle is employed, whereby the user endeavours to keep exposure time and power output to a minimum during treatment (Merritt, Kremkau and Hobbins, 1992). A number of official bodies frequently produce documents on medical ultrasound outlining safety standards and providing recommendations in order to achieve the ALARA principle (WFUMB, 1992; 1998; National Council on Radiation Protection and Measurements (NCRP), 1992a). These recommendations are produced in conjunction with health care and science experts and are based upon theoretical measurements and experimental results as well as the specific criteria of the individual exposure. Detection of the mechanisms by which ultrasound is reported to produce adverse effects are extremely difficult to either identify or predict *in vivo* particularly regarding cavitation, consequently research is continuing in these areas and recommendations must be updated in accordance with the results. It should be made clear at this point that the research described in this introduction is intended to be a representative overview of some of the more alarming observations in the literature, but is by no means complete. Indeed the field is plagued by conflicting reports and unrepeatable results.

It is notable that ultrasound scans are instrumental in the identification of a wide variety of life threatening conditions in the unborn child resulting in quick and effective treatment and that the comparative risk of any damage by the scan itself is minimal. Ultrasound also has a key role in the diagnostic and therapeutic treatment of a number of conditions in adulthood. The greatest risk to health, particularly in the case of the foetus, is misdiagnosis and for this reason health professionals involved in the administration of ultrasound are required to be sufficiently trained and educated. Furthermore, they must also be aware of changes in current practice and therefore a support system aimed at facilitating this must be available.

1.3.3 In vitro

In vitro experimentation in this field spans a number of cell types and involves a broad range of very different experimental systems (4.1), nonetheless several groups have described detrimental effects on cells following insonation. Unfortunately, it is again important to note that in some cases apparently contradictory observations have been published by other groups.

The implications of results produced *in vitro* are difficult to determine with regard to ultrasound's effects *in vivo*, nonetheless they are important in establishing thresholds and exploring damage at a cellular and molecular level. Briefly, since this work will be described in detail throughout the thesis, there are two categories into which this research falls. The first group of experiments are conducted in generally aqueous cell-free solutions whilst the second involves experiments conducted on cellular preparations. Amongst the observations obtained from cell-free solutions is the degradation of highly polymerised natural products such as starch, gum arabic and gelatin in solution and polystyrene, polyacrylates and nitrocellulose in organic solvents by ultrasound, the occurrence of double strand breaks in solutions of DNA, and the inactivation of some enzymes under certain conditions (Riesz and Kondo, 1992). As well as increased activity of enzymes exposed to ultrasound while immobilised on polystyrene beads (Schmidt, Rosenfeld and Millner, 1987).

Over the past ten years some of the most elegant work in this field using cellular matter has been described by Miller *et al* who have studied ultrasound induced single strand breaks (SSB) in the DNA of chinese hamster ovary (CHO) cells (Miller, Thomas and Frazier, 1991a+b); Miller, Thomas and Buschom, 1995).

Reports from other groups have described sister chromatid exchanges in human lymphocyte and lymphoblastoid cells (Martin *et al*, 1991), chromosomal aberrations and altered mitotic characteristics in human fibroblasts (DeDeyne and Kirsch-Volders, 1995), reversible increased agglutination and aggregation of human erythrocytes *in vitro* (Pohl *et al*, 1995), augmentation of human leukocyte adhesion to bovine aortic endothelium (Maxwell *et al*, 1994) and altered membrane characteristics in murine

neuroblastoma cell lines (Fahnestock *et al*, 1989). However, perhaps the most commonly observed bioeffect is ultrasound induced cell lysis (Miller and Thomas, 1993; Brayman, Church and Miller, 1996; Williams, Miller and Gross, 1986). Various mechanisms have been proposed to account for these effects of ultrasonic exposure, but it remains difficult to decipher if one mechanism is solely responsible in each case.

1.4 Aims of the project

The initial aim of this project was to utilise ultrasound as a heating agent during biofermentation of adherent mammalian cells on polystyrene microcarriers. The biotechnology industry manufactures a number of products from mammalian cells in bulk. Traditionally these vast cell cultures are heated to an optimal temperature of 37 °C by use of heating jackets. Recently, polystyrene microcarriers have allowed effective scale-up in such systems by increasing the total surface area available for cell growth within the vessel. This project aimed to devise a method whereby ultrasonic energy could be used to heat the microcarriers themselves, making it possible to keep the bulk of the media at 2 °C whilst maintaining the cells at 37 °C. This should reduce costs and also serve to minimise contaminations. The feasibility of heating microcarriers to sufficient temperatures to sustain cell growth by the conversion of ultrasonic energy to heat was addressed.

In addition, the elucidation of an overview of general cell health following insonation was central to the project with regard to the use of ultrasound both in biofermentation and medicine. Although a substantial amount of *in vitro* research has taken place into the effects of ultrasound clear conclusions are still not possible. To date, no investigation has attempted to view a number of cell health markers under similar conditions. The project focused on the adverse effects of ultrasound on cells, particularly concentrating on areas such as cell growth and division and alterations in membrane integrity, with a view to their reduction. Throughout the investigations the exposure of mammalian cell lines within appropriately designed experimental systems were conducted using ultrasound at frequencies between 1-10 MHz (i.e. those used in diagnostic medicine) which do not have the ability to propagate in air.

CHAPTER TWO

METHODS

2.1 General cell culture

This project has concentrated on two mammalian cell lines which are L929, a mouse areolar and adipose adherent cell line and L1210, a mouse lymphocytic leukaemia suspension cell line. The important characteristics of these cell lines with regard to this project are their mammalian origin and the ability or inability to adhere, respectively.

2.1.1 L929 cells

This cell line is a subclone of the parental L strain which was established by W.R. Earle in 1940 in continuous culture (Earle, 1943). The L strain itself was derived from normal subcutaneous areolar and adipose tissue of a 100 day old male C34/An mouse. L929 cells are permissive for pseudorabies virus and vesicular stomatitis virus (Indiana strain) and are susceptible to other viruses depending on the culture conditions employed. They exhibit the morphology of fibroblasts.

These cells were obtained from ICN Flow, High Wycombe, U.K (Sanford, Earle and Likely, 1948). They were maintained in minimal essential medium (MEM) also obtained from ICN Flow and containing 10 %(v/v) foetal calf serum (FCS) (Globepharm Ltd., Esher, U.K.), penicillin and streptomycin (Sigma-Aldrich Ltd., Irvine, UK.) at 20 μg/ml and 200 IU/ml respectively and 2 mM glutamine (ICN Flow). Cells were harvested for sub-culture by trypsinisation and medium was replenished every 2-3 days.

2.1.2 L1210 cells

These cells were established from a tumour induced in an 8 month old female 234, subline 212 of a DBA mouse. It was originally subcultured in DBA/2 mice and then adapted to suspension culture in 1960 (Foley *et al*, 1960). They are extensively used in cytotoxicity assays and have the morphology of lymphoblasts.

This cell line was also obtained from ICN Flow (Hutchison, Ittensohn and Bjerregaard, 1966) and was maintained in RPMI 1640 medium with added L-glutamine (2 mM) and 20 mM Hepes pH 7.4 (Sigma-Aldrich Ltd) supplemented with 10 %(v/v) FCS and penicillin/streptomycin (20 μg/ml and 200 IU/ml respectively). Cells were subcultured in fresh medium every 3-4 days.

2.2 Cell growth using microcarriers

Gelatin coated polystyrene microcarrier beads (Sigma-Aldrich Ltd.) were used to support an L929 culture. The beads ranged in size between 90-150 μm and had a density of 1.03 g/cm^3. Microcarriers were used at a concentration of 10 mg/ml in accordance with the manufacturers instructions. Prior to use they were soaked in medium for 1 hour at 37 °C and 5 %(v/v) CO_2 in an incubator. The medium was then discarded and the microcarriers were transferred to a 100 ml glass bottle (Life Technologies, Paisley, U.K.) in fresh medium containing L929 cells seeded at 1 x 10^5 cells/ml. The glass bottle was then fixed inside a 900 cm^3 roller bottle (Corning-Costar Corp., Cambridge, M.A., U.S.A.) and placed in a Belco Glass Inc. (Vineland, N.J., U.S.A.) 'roll-in' incubator, where they were gently rolled (2 rpm) for a period of three hours. Microcarriers were inspected, using light microscopy, to make sure that the cells had adhered before the rolling speed was increased (4 rpm). Figure 2.1 depicts a microcarrier culture at Day 6. It should be noted that all glassware was coated with 'Sigmacote' (Sigma-Aldrich Ltd.) in order to prevent microcarriers adhering to the walls of the vessels. Cells were sub-cultured either by transferring microcarriers which were already covered by confluent cells to a new culture of fresh microcarriers or by trypsinisation of the

cells from the microcarriers following their centrifugation from the culture medium and subsequent seeding of new microcarriers with cells alone. Trypsinisations were performed in calcium and magnesium free solutions. Although this technique was generally successful microcarriers did show a tendency to clump during culturing. This problem appeared to be due to the growth of cells between the beads and which may be possible to eliminate by increasing the speed of rotation.

Figure 2.1: L929 cells growing on microcarriers following 6 days of growth.

L929 cells were adhered to and grown on polystyrene microcarriers for a period of 6 days using the standard growth medium for the cell line and a 'roll-in' incubator. Cells and microcarriers are pictured here at x200 magnification The microcarriers range in size between 90-150 μm and this non-uniformity of bead size can be clearly observed.

2.3 Ultrasound Apparatus

The ultrasound unit used throughout this project was a Medi-Link therasonic machine (Electro-Medical Supplies Ltd., Wantage, U.K.) designed for use in therapeutic medicine. This consists of a control module (model no 70) and an

operating unit (model no 72). It has a maximum output power of 11.3 W, an output intensity of 2.54 Wcm^{-2} and is operational at two frequency settings of 1.1 and 3.3 MHz (referred to as 1 and 3 MHz). During this project it has been used, mainly, as a source of continuous waves although it has the ability to produce pulsed waves. It has two probes of differing sizes 0.5 and 5 cm^2.

Ultrasonic waves were generated by the machine piezoelectrically, whereby, the transducer was composed of an internal crystal whose molecules were electrically asymmetrical coated by a thin film of metallic conductor which was driven to vibrate by the application of an external electric field.

CHAPTER THREE

MATHEMATICAL FEASIBILITY OF THE USE OF ULTRASOUND TO HEAT MICROCARRIERS

3.1 Introduction

The proposal that ultrasonic energy be used to heat small microcarriers constructed from polystyrene within cell growth medium, was explored mathematically to obtain a measure of its feasibility. The literature relating to the mathematical modelling of heating within ultrasonic fields largely concentrates on the safety aspects of medicinal ultrasound. One such publication, from the National Council on Radiation Protection and Measurements (1992b), details expressions for the temperature rise produced in the vicinity of small heat sources following their conversion of ultrasonic energy to heat. The equation below gives the steady-state temperature rise at the surface of a sphere of a diameter D whose rate of heat production is Q and where heat transport is both by conduction and perfusion,

$$\Delta T = (Q/2\pi KD)/[1 + (D/2L)], \quad (1)$$

where Q is the rate at which heat is conducted outwards in watts, K is the thermal conductivity co-efficient for polystyrene in joules^{-1}second^{-1}metre^{-1}degree celsius^{-1}, D is the diameter of the sphere in metres and L is the perfusion length in metres.

This equation has been derived with a view to modelling *in vivo* situations, for example the use of contrast agents (1.3.2) within the blood stream. It and indeed associated equations are particularly appropriate in the case of water bearing tissues with low fat content, no calcification and no macroscopic gas-filled cavities. For such

tissues, the thermal diffusivity is approximately the same as it is for water. In view of these constraints, it was considered that this equation could be used to provide an appropriate "ballpark" figure for the change in temperature experienced by one polystyrene microcarrier within a biofermenter subjected to an ultrasonic field (Figure 3.1).

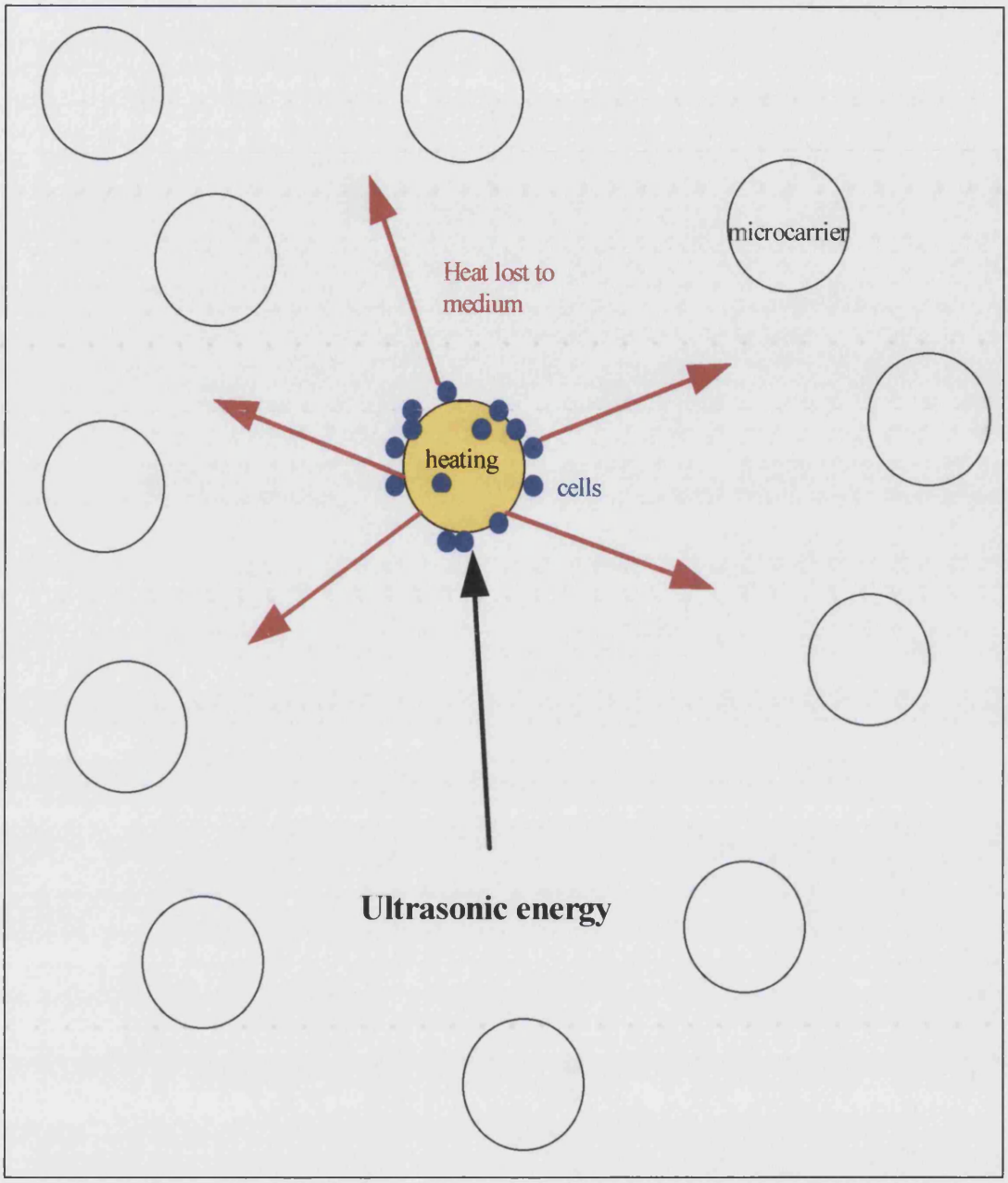

Figure 3.1: Schematic diagram of the heating caused by ultrasonic energy applied to one microcarrier within a biofermenter.

Calculations performed within this chapter have assumed that any one microcarrier within a biofermenter is exposed to a 'clean' ultrasonic beam. Such a polystyrene bead will attenuate the ultrasonic wave and its energy will be lost as heat to the surrounding medium, thus cells growing on the microcarrier will experience heating.

3.2 Calculations

In equation (1), the term *[1+(D/2L)]* describes the heat transported by perfusion. It was assumed, for simplicity's sake, that no perfusion was occurring within the biofermenter and therefore L is infinite, *(D/2L)* is zero and hence *[1+(D/2L)]* is one, producing,

$$\Delta T = (Q/2\pi KD). \quad (2)$$

In order to calculate the rate of heat production, Q, it was necessary to assess the proportion of the ultrasonic beam which would be reflected at the bead-medium interface using,

$$Reflection\ Coefficient = [(Z_1 - Z_2)/(Z_1 + Z_2)]^2, \quad (3)$$

where Z_1 is the acoustic impedance in water and Z_2 is the acoustic impedance in polystyrene (Kaye and Laby, 1973).

Acoustic impedance itself is calculated from,

$$Z = \rho c, \quad (4)$$

where ρ is the density in kgm^{-3} and c is the speed of sound in $m\ s^{-1}$.

The acoustic impedance was simple to calculate for both polystyrene and water since the density of water is 1000 kgm^{-3} (Kaye and Laby, 1973) and the speed of sound through water is 1482 $m\ s^{-1}$ (Kaye and Laby, 1973), while the density of the polystyrene beads which were employed as microcarriers (2.2) is 1030 kgm^{-3} and the speed of sound in polystyrene is 2350 $m\ s^{-1}$ (Kaye and Laby, 1973).

If Z_1 is the acoustic impedance in water, which is 1.48×10^6 rayls (1 rayl = 1 $kgm^{-2}s^{-1}$) and Z_2 is the acoustic impedance in polystyrene, which is 2.42×10^6 rayls then the

reflection coefficient is 0.06. This value is equivalent to a 6 % reflection of the ultrasonic beam and a resultant 94 % attenuation of the same beam. It has therefore been assumed that W_a, the acoustic power absorbed by the polystyrene bead is equal to the acoustic power incident on the object (W_i).

The rate of heat production in watts per unit volume (m^3) was calculated using,

$$Rate\ of\ heat\ production = 2\alpha I, \quad (5)$$

where α is the attenuation coefficient in nepers m^{-1} and I is the intensity of the ultrasound beam in Wm^{-2}.

The attenuation coefficient for ultrasound in polystyrene is calculated to be approximately 23 nepers m^{-1} at 2.5 MHz (Kaye and Laby, 1973). This value was determined to be appropriate since the thermosonic device used for all bench work operates at 1 or 3 MHz (2.3). The maximum intensity of the ultrasound beam used is 2.0 Wcm^{-2} or 2.0 x 10^4 Wm^{-2}. To obtain a rate of heat production (Q) in watts equation (5) was multiplied by the volume of the microcarrier to give,

$$Q = 2\alpha IV. \quad (6)$$

Q was calculated for a microcarrier of diameter 100 μm as described in 2.2. The volume of such a sphere is 5.235 x 10^{-13} m^3 and therefore Q is 4.8 x 10^{-7} watts.

K is the thermal conductivity co-efficient, which is the rate of heat transfer by conduction through a unit thickness, across a unit area, for a unit difference in temperature. The thermal conductivity of polystyrene does not vary greatly across a wide range of temperatures and it is this property that makes it an efficient insulator. The value for the thermal conductivity co-efficient is 0.1 $Js^{-1}m^{-1}\ ^{\circ}C^{-1}$ (Boundy and Boyer, 1952; Boyer, Keskkula and Platt, 1970).

Having calculated all of the terms required, the rise in temperature above ambient produced for a 100 μm polystyrene sphere in an infinite medium experiencing an ultrasonic field, 2.5 MHz in frequency and at an intensity of 2.0 Wcm^{-2} was calculated from equation (2),

$$\Delta T = (Q/2\pi KD) \quad (2)$$

$$= (4.8 \times 10^{-7}/2\pi \times 0.1 \times 10 \times 10^{-5})$$

$$= \underline{7.64 \times 10^{-3}\ ^{o}C.}$$

3.3 Discussion

The calculated steady state temperature rise was less than 0.01 °C which would not be sufficient to allow ultrasonic heating to be used as a cheaper alternative to conventional heating jackets in biofermenters. The value calculated is likely to be an over-estimate due to the assumptions made, for example that all ultrasonic energy would be converted to heat. Indeed it is unlikely that within a biofermenter any one bead would remain exposed directly to the ultrasonic source for a prolonged period of time. Furthermore, there may be a number of other influencing factors within the biofermenter, such as streaming and reflection from the vessel walls themselves.

A temperature rise of at least 12 °C (room temperature to 37 °C) would be required if ultrasound was to be an efficient means of heating within a biofermenter. The equations described above were used to investigate the alterations that would be required to various parameters to achieve such a temperature rise. The calculated intensity of the ultrasonic beam required to elicit a temperature increase of 12 °C is 3200 Wcm^{-2}, while a microsphere of 4000 μm in diameter would produce the same temperature rise. These values are dramatically larger than those which were convenient to employ on a small scale basis. It may be possible to enhance the temperature elevation produced by using a less sonolucent material, that is one with a higher attenuation co-efficient, to construct the microcarriers, although such materials are likely to be of greater density and may therefore not be buoyant. The implementation of a lower frequency ultrasonic source may allow greater heating, but

is also likely to produce greater cell damage. Resolving this problem is likely to involve changing a number of these parameters in order to allow optimal heating in a practically manageable system while maintaining cell health. However, further research into these areas is not within the bounds of this project.

CHAPTER FOUR

ULTRASOUND EXPOSURE SYSTEMS: PROPERTIES AND DESIGN

4.1 Introduction

It is extremely difficult to control biological or physical exposure parameters during insonation *in vivo*. Indeed, it is even troublesome to speculate upon their contribution to the experimental results. Similarly, it will be difficult to control these parameters, at least initially, in biofermenters. However, the utilisation of cell suspensions *in vitro* to study the effects of ultrasound allows the control of such environmental factors or at the very least, the opportunity to consider what their effects may be. Such systems are often very precise and can be used to explore events occurring at a cellular level. Unfortunately, the results obtained using systems *in vitro* can be of limited relevance to medical ultrasound and other complex applications and must therefore be interpreted carefully. For example, the thermal effects of ultrasound are likely to be very different in tissue as there is little fluid surrounding the cellular matter. Likewise, the conditions under which cavitation occurs are unlikely to be the same *in vivo*. Despite these problems, systems *in vitro* have proved useful in elucidating some of the effects of ultrasound and are especially relevant to fluid filled regions of the body, such as blood. Furthermore, information gleaned from such experimentation has been valuable with regard to the design of studies dealing with the bioeffects of ultrasound in both animals and humans, aimed at addressing health and safety issues. For these reasons it was proposed that systems *in vitro* could also prove to be useful tools in designing and understanding biofermenters in which ultrasound could be employed.

A considerable amount of time was devoted to the design of the experimental systems utilised within this project. The process was plagued by the conflicting demands of the physical and biological requirements that must be married in order to produce an

effective experimental set-up. However, since this is a biochemistry thesis, the physical demands of the project were secondary to ensuring that the cells would be in a condition fit for biological analysis following insonation. Nonetheless it is important to be aware of the physical distortions which may occur to the waves as a result of these constraints.

Exposure systems have varied wildly between groups, indeed, in the recent review by Miller, Miller and Brayman (1996) no less than 15 different exposure systems were described to have been used. It is partly for this reason that it is almost impossible to compare one group's experimental results with another's. To compound this problem further it is rare that the detection of ultrasonic damage is achieved by the same means or that the insonation takes place at the same frequency or intensity. Subsequently, throughout this thesis, review of the literature has proved a mammoth task since conflicting methods make comparisons between studies difficult, although where possible loosely comparable results have been described.

The ways in which the design of a system *in vitro* can alter the physical properties of the ultrasound wave, to which the test cells are ultimately exposed, are numerous and cannot all be addressed here, therefore the following paragraphs describe some of the most influential aspects of system design.

In general, cell suspensions are contained within a vessel of some description, although there are instances of cells being placed directly onto the transducer (Miller, Miller, Brayman, 1996). Notably, direct contact between the cells and the transducer during insonation was avoided throughout this project due to the early observation that substantial heating took place at the transducer face which lead to severe cell damage. Indeed transducer heating was noted as a concern by the World Federation for Ultrasound in Medicine and Biology at a recent safety symposium (WFUMB, 1998).

The containing vessel itself can have a marked effect on the character of the ultrasonic exposure due to both to its shape and its ability to either absorb or reflect the wave. For example, the vessel may be sonolucent in that its ultrasonic properties do not

differ significantly from the medium in which the cells are suspended or may be thin enough not to perturb the wave as it travels from the cell media into another easily transversible medium. Conversely, the vessel may be manufactured from a material which readily absorbs ultrasound or reflects it and may thus have a marked effect on the type of exposure the cells experience. For instance, internal reflections as a result of the difference in acoustic impedance between the vessel walls and that of the vessel contents in a tube system, where the vessel is constructed of a non-sonolucent material, will produce a wave which is reflected back along its own path allowing interference with that part of itself which has yet to reach the vessel wall. This is known as a standing wave and can result in the segregation of cells and lytically effective bubbles reducing the effect of cavitation (Miller, Miller, Brayman, 1996). The same system set-up using a sonolucent material will generally avoid standing waves if the tube is placed within a tank where an appropriate ultrasonic absorber is present. Non-sonolucent materials may also cause problems due to the conversion of ultrasonic energy to heat upon its absorption and the subsequent conduction to the cellular medium. Meanwhile, the shape of the vessel in which cells are contained can play a role in distorting the physical shape of the wavefront, while the walls may contribute to the production of cavitation nuclei and allow bubble stabilisation due to imperfections.

Air-water interfaces produced within a system, for example, in a fluid filled petri dish placed directly upon the ultrasound transducer, are likely to lead to 100 % reflection and the production of an almost perfect stationary wave. The resulting exposure will subject the cells to far greater ultrasonic intensity than expected with respect to the thermosonic settings, although bubble-cell segregation should protect cells from cavitation if the vessel in question is not rotated. However, vessel rotation will lead to increased cavitation nuclei, a property which has been exploited by many groups (Miller, Miller and Brayman, 1996).

The properties of the exposure medium are also of great importance to the ultimate physical attributes of the ultrasonic wave. A more viscous liquid will increase the cavitation threshold (Miller, Miller and Brayman, 1996), while a medium containing large amounts of dissolved gas will reduce it (Kondo and Kano, 1988). The

temperature of the medium can also alter the ultrasonic effects, in particular, the temperature history of the medium, for example, where the medium has been heated prior to exposure it may be supersaturated (Armour and Corry, 1982) reducing the cavitation threshold. The presence of certain biological molecules in aqueous solutions, such as foetal bovine serum, trypsin and human blood plasma, have been reported to produce extremely reactive free radicals during insonation (Edmonds and Sancier, 1983), thus implying that the biochemical composition of the medium is also of importance with regard to the physical properties of the wave.

Initially, great care was taken in order to produce a physically clean system, however, such systems were not always ideal for maintaining cells in a state which was compatible with the biological detection process to be employed and therefore had to be reconsidered. It is clear that a balance must be made between biological and physical perfection in order to produce an effective system.

4.2 System design

Several systems were designed during the course of this project but only three were finally involved in the production of the results described within this thesis. Each system has different properties and was employed for its compatibility with a particular biological damage detection process.

4.2.1 Waterbath exposure system

The system initially employed in chapter 7 is represented schematically in figure 4.1. It was designed to minimise heating by preventing reflection and standing wave formation whilst simultaneously maintaining cell health by use of a 37 °C waterbath. A special glass housing was designed and manufactured (Mechanical Engineering, University of Bath, U.K.) to contain the cells. Nescofilm (Nippon Shoji Kaisha Ltd., Japan) was stretched across the bottom of this housing and firmly held in place by elastic bands in order to produce minimal reflection while allowing cellular containment. The smaller transducer (0.5 cm^2) was used in this system which ought to have helped prevent reflection of the ultrasonic wave against the side of the glass tube

as the area of wave production was small as compared with internal area of the tube. On leaving the transducer, ultrasound passed straight through the cells and the nescofilm and was finally absorbed by the carpet placed at the bottom of the tank, which again prevented reflections. This system was thought to produce a relatively 'clean' physical wave (i.e. a wave which is minimally perturbed by reflection, attenuation etc. due to the system) and no bubbling or rippling was observed during the insonations. However, cells were suspended in their normal growth medium which by definition contained biological macromolecules similar to those implicated in the production of highly reactive free radicals. Cells were not observed to lyse using this system (7.2.1).

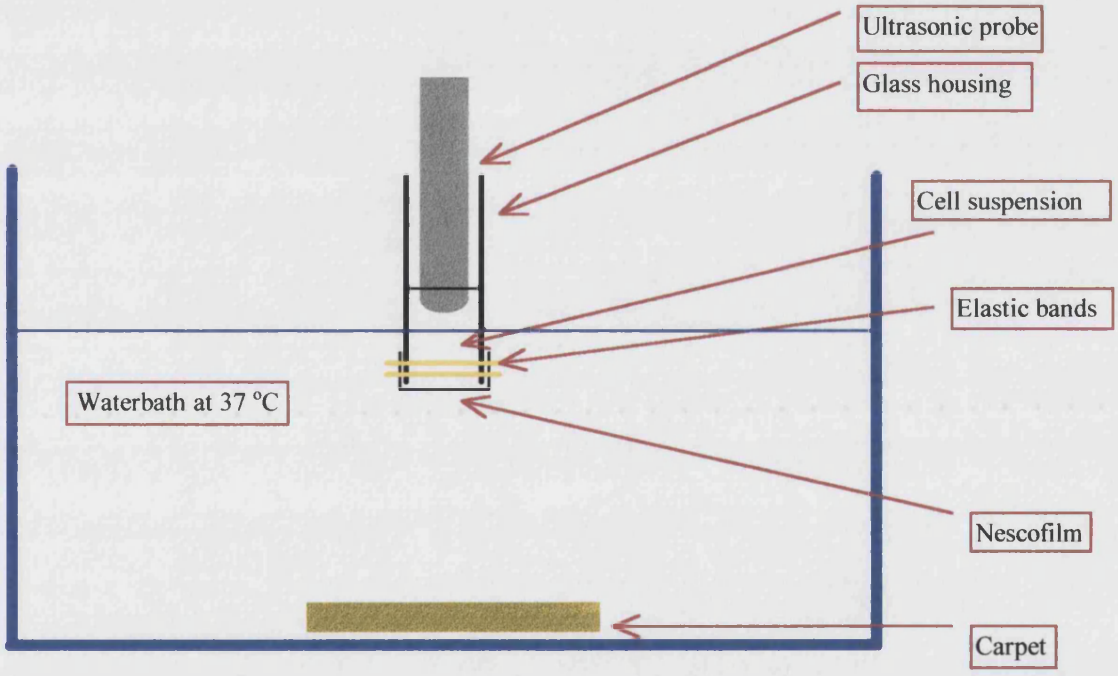

Figure 4.1: Apparatus designed for insonation of L1210 cells prior to PARP activity evaluation.

This apparatus was designed to produce as 'clean' an ultrasonic wave as possible and was utilised in the early part of chapter 7.

4.2.2 Six-well plate system

The system utilised in chapter 6 (Figure 4.2) was designed and adapted to produce cavitation within the medium, but avoided either the use of system rotation or the addition of artificial cavitation nuclei. A six-well plate (Corning-Costar Corp.) containing a cell suspension was placed directly on top of the 5 cm^2 transducer. 'Aquasonic®' water based coupling gel (Parker Laboratories, Inc., N.J., U.S.A. (Trademark of Dupont)) was used to seal the interface between the transducer and the culture plate and to allow wave propagation.

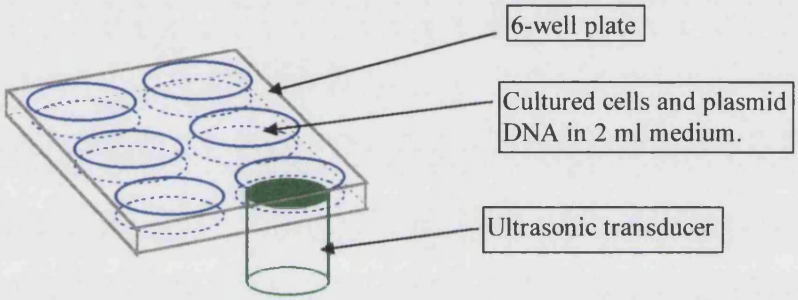

Figure 4.2: Schematic diagram of the apparatus designed for transfection of cells by insonation.

This apparatus was designed to produce cavitation and to induce transfection in cells by transiently damaging the integrity of the cell membrane and was utilised in chapter 6.

The air-medium interface produced within the tissue culture plate led to a substantially reflected wave, while the proximity of the transducer face to the cells allowed the possibility of heating due to conduction through the bottom of the tissue culture plate. Furthermore, attenuation of the ultrasonic wave as it passed through the polystyrene well also had the potential to cause cellular heating. However, following insonation, the temperature of the wells was assessed and no significant heating was found to occur. This was due partly to the short duration of exposure and also to the use of a pulsed wave whereby brief bursts of ultrasonic waves are transmitted. In this case the duration of the pulse was 2 ms, the repetition frequency (the reciprocal of the interval

between pulses) was 100 Hz and the ratio of on to off was 1:4. The surface of the medium was clearly perturbed during the insonation process and again the potential for the production of free radicals existed as exposure took place in normal growth medium.

4.2.3 Flask system

The system photographed in figure 4.3 was the most widely employed during the experimentation described in this thesis and evolved for a number of practical reasons. Principally, as the system designed in 4.2.1 produced a physically 'clean' wave and did not lead to any detectable cell damage it was not best suited as a tool in the evaluation of the detrimental effects that ultrasound has the potential to induce. The resultant design of a system which was less 'kind' to cells was therefore essential.

The 25 cm^2 tissue culture flask (Corning-Costar Corp.) used as an exposure vessel was a convenient easy way to store cells and was also an effective way of maintaining cellular sterility when required. The larger 5 cm^2 transducer was employed in this set-up which is unfortunately prone to becoming hot during prolonged insonations. In order to prevent conduction heating occurring between the probe and the bottom of the flask an 'ice-cube' bag (Sainsbury's Supermarkets Ltd., London, U.K.) was used as a cooling device (Figure 4.3). A number of cooling methods were investigated during the early part of the project including a cold water pumping system and the use of 2-3 %(w/v) agar blocks. However, 'ice-cube' bags which had been pre-chilled to 4 °C proved to be the most effective and user friendly. The interfaces between the probe and the 'ice-cube' bag and the bag and the culture flask were sealed with 'Aquasonic®' gel in order to improve wave propagation.

The air-medium interface within the flask is likely to have produced a standing wave, indeed the surface of the medium was clearly perturbed particularly when this system was used for lower frequency higher intensity insonations. Furthermore, a 'fountain effect' (Williams, 1983) was observed, whereby the flat surface of the liquid was displaced upwards by the ultrasonic field. The height of this peak is a direct measure of the intensity of the beam as the column of water rises until the upward force is

exactly equal to the weight of the water. Bubbling was seen to occur in the medium and on occasion, also within the 'ice-cube' bag which may have affected the wave's physique. Again since the insonation was conducted in cell medium there was potential for free radical formation. Finally, it is unlikely, but possible that absorption or reflection may have occurred as the wave passed through the bottom of the polystyrene tissue culture flask. This will be addressed in 4.3.

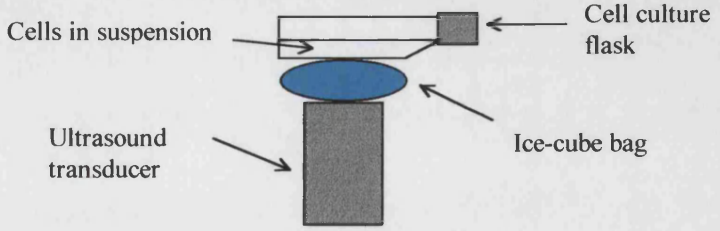

Figure 4.3: Cell culture flask exposure system.

The ultrasound machine used throughout this project is pictured during an insonation. An 'ice-cube' bag is placed between the transducer and the tissue-culture flask to prevent conduction heating. All interfaces have been sealed with 'Aquasonic®' gel. This system is shown as both a picture and a schematic diagram.

4.3 Wave quantification

Physical measurements of the waves produced by the therasonic machine employed in this experimentation were conducted in the Medical Physics Laboratories of the Royal United Hospital (RUH), Bath. These measurements were undertaken to provide an overview of the waveforms themselves and to identify ways in which the system components modified the wave properties.

4.3.1 Total acoustic power measurements

As pulses of ultrasound are transmitted through a medium or a tissue, work is performed. From a bioeffect point of view, the most important result of this work is the heating of tissues. The capacity to perform work is determined by the quantity of acoustical power produced, where acoustical power describes the amount of acoustical energy produced in a unit of time. It is therefore important to establish the actual acoustical power output of a machine rather than its theoretical output.

The large transducer has an effective radiating area (ERA) of 5 cm^2 while the smaller transducer's ERA is 0.5 cm^2. The theoretical total acoustic power can be calculated by multiplying the ERA by the intensity, while, the actual total acoustic power can be measured using a force balance (Perkins, 1989). Such instruments determine the acoustic power via the principal of radiation force, which is the force that a reflecting or absorbing target experiences when it is placed in an ultrasonic beam. This force is dependent only upon the total acoustic power, the velocity of sound in the fluid and the geometry of the target. Under known conditions the latter parameters are relatively easy to calculate. The force balance used here was designed in-house at the RUH (Perkins, 1989) and uses water as a conducting fluid. The ultrasound probe was placed against a PVC membrane and the sound wave was transmitted through a water-filled chamber to the target which was constructed of very thin metal and surrounded by a total absorber. In the path of the applied ultrasound beam, the target would tend to move backwards. This was prevented from happening by a concentric permanent-magnet/coil assembly mounted to the back of the target and energised by a

restoring current. The current required to establish target equilibrium was displayed on a large-scale analogue meter and was equivalent to the acoustic power. The balance null position was measured internally by opto emitters and detectors situated at the lower extremity of the target.

The force balance employed is used regularly to calibrate the hospital's ultrasound machines and is itself calibrated frequently in the laboratory. It had also been calibrated by the National Physical Laboratory (NPL) (Teddington, U.K.) less than a year prior to this experimentation.

Total acoustic power measurements were taken at a range of wave intensities at both frequency settings for each transducer. During these measurements the force balance pointer was observed to be rather shaky, although this is not unusual with this model of machine (personal communication with lab staff, RUH, Bath, U.K.). Figure 4.4 depicts the measured total acoustic power at a range of intensities during insonation at either 1.1 or 3.3 MHz for the large transducer. It should be noted that the therasonic display showed the frequency as either 1 or 3 MHz, when the actual frequency emitted is 1.1 and 3.3 MHz respectively. Elsewhere in this thesis the displayed frequency will be given for simplicity. The machine measured total acoustic power could have been plotted against the actual acoustic power, but since insonations throughout this project are described by intensity it was more appropriate to use intensity as the theoretical measurement. It is clear that the measured total acoustic power values are higher than those which would be calculated by multiplying ERA by intensity. Indeed, measured values range between 20 and 40 % higher. This discrepancy is reasonable and to be expected (personal communication with Dr F. A. Duck, RUH, Bath, U.K.) Impressively, the results were linear and virtually identical for both frequencies.

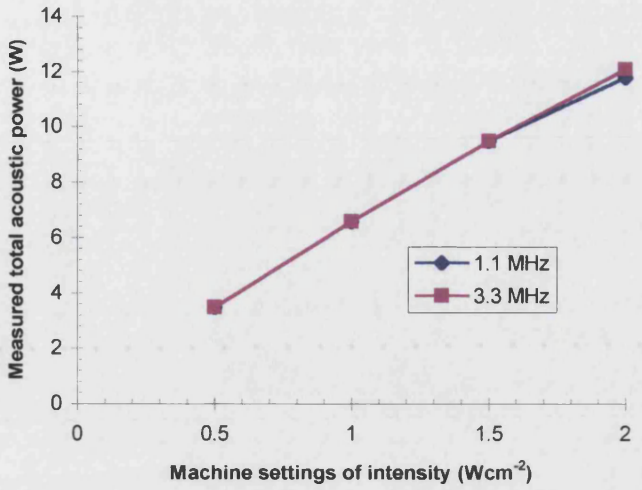

Figure 4.4: Total acoustic power of the large transducer (ERA = 5 cm^2) at 1.1 and 3.3 MHz, CW.

Total acoustic power measurements were taken using a force balance at a range of intensities. The plotted intensities are those given by the therasonic machine display, while the total acoustic power is as measured by the force balance.

Figure 4.5 shows the same total acoustic power measurements for the small transducer. The difference between measured acoustic power and calculated acoustic power (I x ERA) was far greater here, ranging from 80-100 %. However, the total acoustic power increases were still proportional to intensity. The power outputs showed greater difference between frequencies than was observed for the large transducer. Although these power measurements were not ideal they are not unusual for this model of machine (personal communication with Dr F.A. Duck).

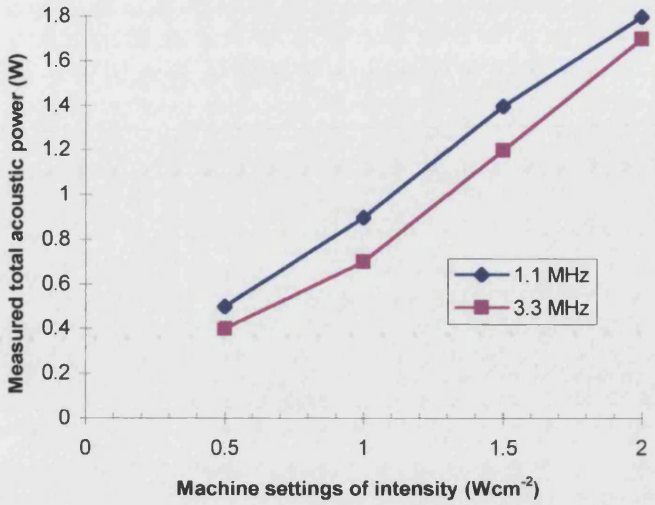

Figure 4.5: Total acoustic power of the small transducer (ERA = 0.5 cm^2) at 1.1 and 3.3 MHz, CW.

Total acoustic power measurements were taken using a force balance at a range of intensities. The plotted intensities are those given by the therasonic machine display, while the total acoustic power is as measured by the force balance.

4.3.2 Free field waveform quantifications

An NPL ultrasound beam calibrator (Preston, 1988) was used to further determine the characteristics of the waves produced by the ultrasonic apparatus. This instrument was designed to meet the need for an accurate comprehensive measurement system of the acoustic output of medical ultrasonic equipment and operates by use of hydrophone technology. It also meets the requirement that calibration is traceable to national standards.

When in use, a hydrophone is positioned in an ultrasonic field propagating in water; its active element, usually less than 1 mm in diameter, responds to the local acoustic pressure to produce an electrical signal at its output terminals which can be measured using either an oscilloscope or a digitiser. By moving the hydrophone in a plane across the ultrasonic field it is possible to determine various acoustic parameters. Although measurement analysis systems can be developed to enable these beam-

plotting measurements to be made reliably using a single hydrophone system, the whole process is time consuming and requires careful interpretation of the results to avoid significant errors. To overcome these problems an alternative system was developed by the NPL which maintained the concept of the hydrophone as the method of measurement but constituted a self-contained system. Using this system the ultrasonic field is sampled by a multielement bilaminar membrane hydrophone and the acoustic waveform is presented on a microprocessor display. As a result, storage of data and immediate processing enables acoustical parameters to be determined in a matter of seconds.

The ultrasound beam calibration apparatus employed in this project consisted of a polycarbonate test-tank 300 mm in diameter and 300 mm in depth containing degassed/deionised water which could be filled or emptied using a small water circulating pump. The hydrophonic membrane was mounted in a cradle which could be tilted and moved vertically. The membrane itself was constructed of two layers of the piezoelectric polymer polyvinylidene fluoride in between which 21 hydrophone elements were embedded. Each hydrophone was 0.5 mm in diameter and was separated from the next by a distance of 1 mm centre to centre. An acoustic absorber was placed at the bottom of the tank below the hydrophonic membrane to minimise the effects of reflected ultrasound. While under test, the transducer was supported in a positioning rig, which allowed both horizontal and vertical movement above the hydrophone membrane.

The results obtained using this system were presented in the form of two real-time graphics displays, various real-time digital readouts and a number of static system parameters. The acoustic pulse waveform at any given hydrophone element was graphically displayed alongside a beam profile constructed from the readings at each hydrophone which allowed an immediate visual representation of the acoustic field. Furthermore, the system was able to store waveform data in a separate memory which corresponded to the largest peak profile recorded, whereby when the acoustic signal at a particular hydrophone element exceeded the previous maximum level then the waveform data for the whole beam profile was stored. In this way data was constantly

updated by the apparatus while the insonation was in progress. This was also the case where averaged measurements were produced.

Although the system was capable of producing an array of acoustic measurements only a limited number were of interest as continuous rather than pulsed wave insonations were investigated. In the main, the following sections will concentrate on measurements of pressure and intensity.

Each ultrasound wave results in peak compressional and peak rarefactional pressures which are often referred to as peak positive and peak negative pressures respectively. Peak pressure values are of interest with respect to mechanical bioeffects such as cavitation and are hence normally studied during the testing of medical ultrasound machines. In practice peak positive and negative pressures are not always identical.

The intensity of an ultrasonic field describes the spatial concentration of its power and is subsequently calculated by dividing its power in watts by the area over which this power is distributed. For a continuous wave, the spatial peak intensity is the highest intensity at any given point in the ultrasound beam and is denoted I_{SP}. This value is of interest as it has the potential to be much larger than the theoretical intensity emitted from the transducer and may thus alert the user to beam 'hot spots'.

Initially, free field measurements were made using the larger transducer at a distance of 20 mm from the transducer. This separation was chosen to represent the distance between the transducer and the cells during exposure in the system described in 4.2.3. The therasonic machine was set at varying intensities at which peak negative pressures and spatial peak intensities were measured. The results depicted in figure 4.6, indicate that peak pressures rose in a linear fashion with the exception of the last point where a plateau was beginning to form. Meanwhile, spatial peak intensities showed a linear relationship to the machine setting intensity, although the values were between 3.9 and 6.0 times greater. This magnitude of discrepancy between the average and peak intensity values is common and to be expected (personal communication with Dr F. A. Duck). Clearly, such huge peak intensity values must be taken into account during the use of machines employed in medical situations.

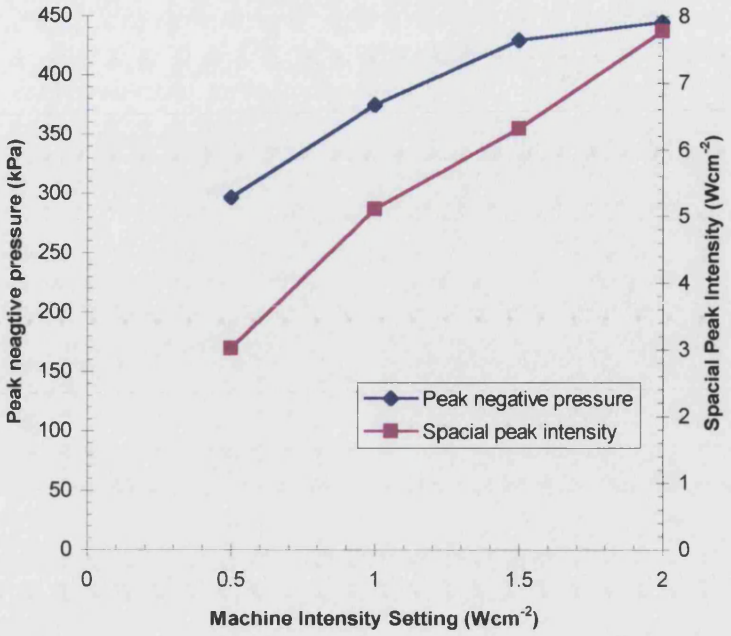

Figure 4.6: Peak negative pressure and spatial peak intensity measurements of the acoustic output of the large transducer (5 cm^2) at various machine set intensities.

Peak negative pressure and spatial peak intensities were measured using the NPL ultrasound beam calibration system. The transducer was placed 20 mm away from the hydrophone in order to simulate the system set-up described in 4.2.3. Readings were taken at various intensities according to the therasonic machine's settings.

Free field wave forms were examined for both transducers at each frequency setting using the therasonic machine. The machine intensity used was relatively low in order to try and reduce cavitation and to produce 'nice' waveforms as viewed on the real-time graphic displays. In each case the transducer-hydrophone distance was chosen to mimic the distance between the cells and the transducer in the appropriate experimental system. In the case of the larger transducer (5 cm^2) this was the system described in 4.2.3 while in the case of the smaller transducer this was the system described in 4.2.1. Despite this careful positioning, the transducer-hydrophone distance was not observed to significantly change the waveform. It is also notable that

in general the small transducer produced a smoother wave as observed by eye using the real-time displays.

The results of these test insonations are shown in Table 4.1. The upper part of the table, above the double line, shows the parameters set on the therasonic machine itself, while the lower part of the table illustrates the acoustic parameters as measured using the ultrasound beam calibration system. Measurements of peak positive and peak negative pressures are extremely similar for each waveform which is rather impressive. Peak pressure readings are greater for insonations at 3 MHz for both transducers. Measurements cannot be compared between transducers since exposures took place at different intensities. In all instances the measured frequency of an average waveform is within 3 % of the machine set frequency. For the large transducer the spatial peak intensity was six times the machine set intensity at 3 MHz and three times the intensity at 1 MHz. In the case of the small transducer the peak intensity was four times the machine set intensity at 3 MHz while at 1 MHz the peak intensity was actually smaller than the machine set intensity. In all cases the observed waveforms were as would be expected using this type of machine.

Transducer	5 cm^2	5 cm^2	0.5 cm^2	0.5 cm^2
Machine set frequency	3.3 MHz	1.1 MHz	3.3 MHz	1.1 MHz
Machine set intensity	0.2 Wcm^{-2}	0.2 Wcm^{-2}	0.5 Wcm^{-2}	0.5 Wcm^{-2}
Distance between transducer and hydrophone	20 mm	20 mm	50 mm	50 mm
Measured peak positive pressure	212 kPa	146 kPa	279 kPa	131 kPa
Measured peak negative pressure	-203 kPa	-143 kPa	-245 kPa	-119 kPa
Measured spatial peak intensity	1.28 Wcm^{-2}	0.59 Wcm^{-2}	2.08 Wcm^{-2}	0.46 Wcm^{-2}
Measured frequency of average waveform.	3.28 MHz	1.09 MHz	3.39 MHz	1.13 MHz

Table 4.1: Measured acoustic parameters of free field waveforms produced by each transducer.

An NPL ultrasound beam calibrator was used to determine the above acoustic parameters of both the 5 cm^2 and the 0.5 cm^2 transducer during insonation. The upper part of the table (above the double line) defines the values as set on the therasonic machine, while the lower part of the table (below the double line) describes the values as measured by the beam calibrator. The ultrasound beam calibrator provides 95% confidence intervals for the uncertainties of its measurements. All values shown above have uncertainties of 4 +/- % or less.

4.3.3 Effect of polystyrene on free field waveform quantifications.

Although the free field waveform parameters obtained in 4.3.2 provided an outline of the type of ultrasonic exposure experienced by cells during insonation, a number of features of the designed exposure systems may have altered the waveform before it reached the cells. The presence of polystyrene tissue culture vessels is one such feature, which occurred in the experimental systems described in 4.2.2. and 4.2.3. It should be noted that this material is somewhat different from the expanded polystyrene used to construct the microcarriers described in 2.2 and in chapter 3 and thus has very different acoustic properties.

In order to ascertain the influence that a polystyrene tissue culture vessel had on the ultrasonic wave, the lid of a six well plate was placed between the transducer and the

hydrophone membrane. Since the lid is constructed of the same material as any other tissue culture vessel it was representative of both the system described in 4.2.2 and 4.2.3. During insonation the hydrophone membrane was tilted slightly to prevent reflection, while ultrasound beam calibrations were carried out as in 4.3.2 in the presence or absence of the polystyrene lid. The smaller transducer was used for this purpose as it produced a more readily calibrated wave profile. The results are displayed in table 4.2 and show that at 3 MHz (Table 4.2(a)) an 8 % decrease in the measured spatial peak intensity value in the presence of polystyrene occurred, while at 1 MHz (Table 4.2(b)) no decrease was observed. Since absorption through plastic is frequency dependent these results were expected. The overall loss of acoustic intensity at 3 MHz was thought to be acceptable.

(a) Machine settings:- 3 MHz, 0.5 Wcm^{-2}.

	No Polystyrene	Polystyrene
Measured spatial peak intensity	15.5 Wcm^{-2}	14.3 Wcm^{-2}

(b) Machine settings:- 1 MHz, 0.5 Wcm^{-2}

	No Polystyrene	Polystyrene
Measured spatial peak intensity	0.36 Wcm^{-2}	0.37 Wcm^{-2}

Table 4.2: Effect of the presence of polystyrene on the spatial peak intensity of ultrasonic waveforms.

Both tables above represent the measured spatial peak intensity detected in the presence or absence of polystyrene using the 0.5 cm^2 transducer. The values shown in (a) were taken at machine settings of 3 MHz and 0.5 Wcm^{-2} with a transducer hydrophone distance of 50 mm and 95 % confidence intervals of +/- 3 %, while values in (b) were taken at machine settings of 1 MHz and 0.5 cm^{-2} with a hydrophone distance of 70 mm and 95 % confidence intervals of 6 %.

4.3.4 Effect of a medium-air interface on free field waveform quantifications

The experimental systems detailed in sections 4.2.2 and 4.2.3 both present the ultrasonic beam with a medium-air interface which, as discussed earlier, has the potential to cause standing waves. To address this problem air was trapped beneath the hydrophone with the result that readings were taken at a water-air interface during insonation. Waveform quantifications were carried out by employing the 5 cm^2 transducer at a distance of 20 mm away from the hydrophone and the therasonic machine set at 3 MHz, 0.2 Wcm^{-2}. The resultant waveform had little shape when viewed as a real-time profile. It was also highly unstable due to reflections, indeed a reflected wave was observed on the surface of the experimental tank. The waveform was so irregular it was impossible to determine any quantifiable acoustic parameters. It could only be speculated that, like any standing wave, this one had the ability to increase the intensity by a factor of four and the pressure amplitude by a factor of two.

4.3.5 Effect of transducer heating on peak positive pressure

It is well known that transducer heating can lead to alterations in ultrasonic power output with time (WFUMB, 1998). The 5 cm^2 transducer was used to observe the power output changes for the machine used within this project. Figure 4.7 depicts the peak positive pressures as measured at 3 MHz, 1.5 Wcm^{-2} at one minute intervals. The overall decrease in peak pressure was 10 % which is not unusual for this type of machine and should not cause any problems for the experimentation described within this thesis.

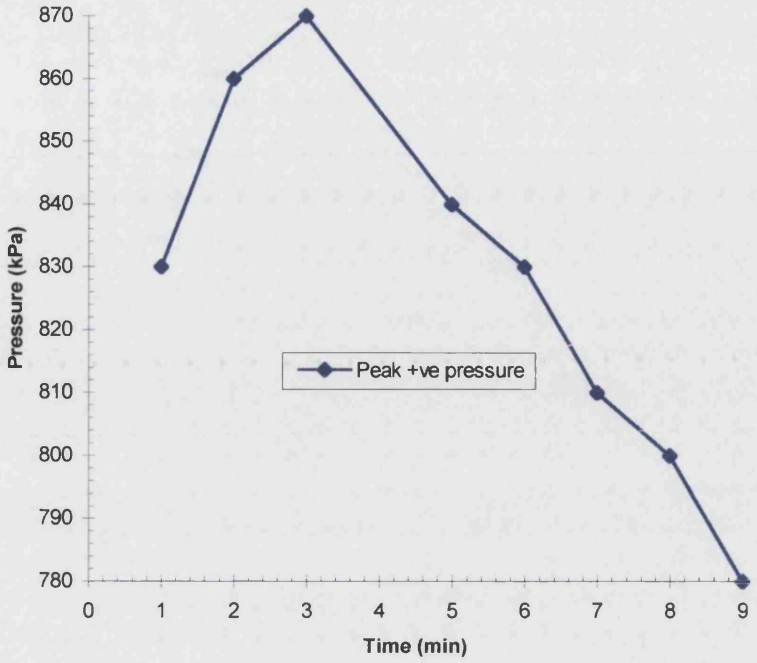

Figure 4.7: Output shift of the 5 cm^2 transducer due to heating.

Peak positive pressure readings were taken every minute while the large transducer was set at 3 MHz, 1.5 Wcm^{-2}. Transducer-hydrophone distance was 20 mm and the 95 % confidence intervals were +/- 6 % or less.

4.4 Discussion

It is clear that the therasonic machine used within the experimentation described in this thesis functioned satisfactorily as far as the wave quantifications in a free field were concerned. However, it is also apparent that some of the design features employed within the utilised experimental systems affected the physical attributes of the waveforms. In particular, air-medium interfaces produced marked alterations such that wave characteristics could not be quantified at all. This may have resulted in local intensities four times greater than the expected value. In comparison, losses due to the presence of polystyrene tissue culture ware were negligible. Thus the major distortion of the ultrasonic wave produced in the systems described in 4.2.2 and 4.2.3 was due to the air-water interface, though in the case of the six-well plate system insonation was so brief that this was not as important. The presence of an ice-cube bag in the system detailed in 4.2.3 was thought to be unlikely to perturb the wave to the same

extent as the polystyrene tissue culture flask, although this proved to be too cumbersome to investigate directly.

The waterbath system (4.2.1) did not have either air-medium interfaces or polystyrene tissue culture products and as a result cells were likely to be exposed to an ultrasonic wave with properties as defined by free field measurements. Only nescofilm was directly in the beam in this system which was virtually sonolucent. The hierarchy of systems from the cleanest physical wave to the most perturbed is therefore the system described in 4.2.1, 4.2.2. and finally 4.2.3. It is of note that cells were prone to settling on the nescofilm in the waterbath system (4.2.1), whereas the standing waves produced in the other systems meant that cells were continually circulated during insonation. Unfortunately, it is not known what effect this might have on the extent of cell damage observed, although there have been controversial reports that increasing the cell density provides cell protection (Sacks, Miller and Sutherland, 1983; Ellwart, Brettel and Kober, 1988) which are dealt with in detail in section 5.1. Finally, all insonations in all systems took place in normal growth medium and thus allowed the possibility that highly reactive free radicals may be formed.

CHAPTER FIVE

INVESTIGATION OF PLASMA MEMBRANE INTEGRITY FOLLOWING INSONATION BY TRYPAN BLUE EXCLUSION

5.1 Introduction

The integrity of the cell plasma membrane is vital to cell health, growth and development. It selectively regulates the composition of the intracellular medium by controlling the flow of molecules and ions into and out of the cell, receiving and responding to environmental stimuli and allowing communication between cells. The structure of this membrane takes the form of a lipid bilayer, in which protein molecules are embedded and to the outer surface of which, carbohydrate chains are bound, forming a glycocalyx or cell coat. The glycocalyx is involved in cell recognition and adhesion, but it is the protein content of the membrane which mediates the majority of its functions. Proteins are responsible for membrane transport, enzymatic catalysis, reception and transduction of environmental signals and structural links with the cytoskeleton. The lipid bilayer itself, provides the membrane with fluidity and thus allows interactions of embedded proteins to occur efficiently.

The plasma membrane, as a whole, is semi-permeable allowing some small water-soluble molecules and ions to be transported passively due to electrochemical gradients. Others are actively pumped through specific protein channels against such gradients or are transported by facilitated diffusion, whereby hydrophilic materials are attached to specific membrane-located carrier proteins allowing them to traverse the membrane. Meanwhile, acids and bases simply equilibriate across the membrane according to their dissociation constants and the pH of the intracellular and extracellular compartments. Clearly, alterations in either the plasma membrane

structure or electrochemical gradient can lead to problems in membrane transport and result in inappropriate responses to external environmental signals.

The physiological importance of the cell plasma membrane and the detrimental effects that any damage to it may incur, has lead to widespread research into the interactions of ultrasonic waves with both synthetic and biological membranes. Most of this work has focused on effects on membrane transport. It is known that ultrasonic waves can perturb lipid bilayers at relatively low frequencies, indeed this property is utilised in the production of liposomes from multilamellar vesicles (Szoka and Paphadjopoulos, 1978), meanwhile the action of higher frequency waves on such membranes remains unclear, despite a growing body of research (Dinno, Dyson, Young *et al*, 1989). However, at very high frequency but low intensity, no adverse effects on cells have been observed (Chandraratna *et al*, 1998) and ultrasonic waves with frequencies in the order of 600 MHz are being employed in acoustical microscopy.

Therapeutically some modifications in the properties of the plasma membrane may be beneficial, for example in inflammation, repair, pain relief and phonophoresis, where increased permeability may lead to greater second messenger activity resulting in functional changes such as increased synthesis and secretion and alterations in cell motility (Dinno, Dyson, Young *et al*, 1989). Unfortunately it is possible that other membrane alterations could adversely affect cell activity and development.

The observed effects on cell plasma membranes range from severe structural damage to far more subtle changes in membrane permeability, alterations in ionic transport and electrophysiology, depending on the experimental parameters. There are many documented reports of cell lysis in response to ultrasonic exposure both *in vitro* and *in vivo* (Miller and Thomas, 1993; Brayman, Church and Miller, 1996; Williams, Miller and Gross, 1986) whereby the cell is completely torn apart by the mechanical effects of the waves. Severe damage of this nature is easily observed. However, almost any form of damage to the cell membrane may seriously affect cellular events. A number of studies have concentrated on ultrasound frequency ranges used in diagnostic and therapeutic medicine, although such reports are hard to compare due

to widely variable experimental conditions, they are useful individually and for this reason will be briefly discussed.

There is evidence that ultrasound can elicit the uncoupling of gap junctions (Dinno, Dyson, Young *et al*, 1989), which may be particularly important during development and differentiation in the embryo, when positional information is passed in the form of chemical and electrical gradients from one cell to another. Such uncoupling can be achieved by the influx of calcium ions into the cell, a phenomenon demonstrated in fibroblasts in response to ultrasonic exposure (Mortimer and Dyson, 1988). Alterations in calcium ion transport are important, in general, since not only are they involved in development and differentiation in the embryo, but they affect synthesis of proteins in the foetus and are extremely important as second messengers throughout life. Changes in other ionic fluxes have also been observed, such as altered potassium efflux (Chapman, M^{ac}Nally and Tucker, 1979).

The sodium transport properties of frog skin epidermis have been well characterised making it an ideal model to observe any electrophysiological changes that occur under the influence of ultrasonic waves. Dinno *et al* (Dinno, Dyson, Young *et al*, 1989; Dinno, Crum and Wu, 1989) have used this modelling system to show that ultrasound causes reversible intensity dependent decreases in the transepithelial potential and resistance under open circuit conditions which represent changes in active transport across the cellular and or paracellular pathway. This is accompanied by an intensity dependent increase in the total ionic conductance under short circuit conditions which is a measure of the ease with which a particular ion crosses the epidermis by the cellular pathway only. This is also reversible. The suggestion that such a decrease in current and increase in conductance corresponds to a reduced electromotive force of the sodium-potassium ATPase pump, possibly due to inhibition of the activity of this enzyme, is consolidated by work describing the inactivation of erythrocyte ATPase in response to ultrasound (Matthews *et al*, 1993). However, this report described the effect as irreversible and was not in agreement with work by Fahnestock *et al* (1989) conducted on neuroblastoma cell membranes where no significant effect on the sodium-potassium ATPase pump was observed. These discrepancies can be accounted for by the following points. Firstly, frog skin and neuroblasts are intact

living systems which are capable of regeneration and repair, while inverted erythrocytes are not which serves to explain the irreversibility of the damage to the ATPase pump. Secondly, the preparation of inverted erythrocytes allows the removal of the cell's natural antioxidants, which may act as a defence to this kind of damage. Finally, the erythrocytes experienced cavitational attack on the cytosolic side of the membrane, due to their inversion, which may cause more severe damage.

Al-Karmi *et al* (1994) have investigated the effects which Dinno *et al* (1989) observed in the presence of calcium since a number of cellular events are dependent on free calcium ions. Their results indicate that the magnitude and kinetics involved in the increase of ion conductance due to ultrasound are influenced by calcium ions. Further electrophysiological changes have been observed in the myocardial cells of adult rats, where ultrasound exposure lead to a decrease in the stimulation threshold (Salz, Rosenfield and Wussling, 1997).

Curiously, it has been observed that ultrasound stimulates angiogenesis *in vivo*, in healing wounds, under conditions where macrophages have been shown to release growth factors *in vitro* (Dyson and Young, 1988; Young and Dyson, 1990). This would obviously serve to escalate the healing process. Conversely, it has also been observed that ultrasound can cause the augmentation of leucocyte adhesion to endothelium (Maxwell *et al*, 1994) and thus trigger the inflammation pathway. Furthermore, ultrasonic exposure of human erythrocytes has been shown to cause increased, but reversible, agglutination and aggregation both stimulated and spontaneous (Pohl, *et al*, 1995).

It should be noted that there are a number of reports which describe protective effects against ultrasonic damage when cell density is increased (Sacks, Miller and Sutherland, 1983; Ellwart, Brettel and Kober, 1988; Brayman, Church and Miller, 1996), thus it may be that the detrimental effects described above occur to a much lesser degree in patients undergoing ultrasonic therapy. However, the most recent report (Brayman, Church and Miller, 1996), emphasises that the absolute number of cells lysed increases with increasing cell concentration and it is merely the relative damage which is seen to decrease, indicating that there are still very real implications

for medicine. Furthermore, it is very difficult to predict what kind of subtle experimental changes may cause huge alterations in the results, for example work by Fahnestock *et al* (1989) on two neuroblastoma cell membranes of minimal genetic diversity showed different results. The cell lines differed only in their ability to adhere, however, in response to ultrasound treatment one line became merely permeable while the other tended to lyse.

The mechanisms which underlie the observed alterations in membrane functions and properties in response to ultrasound are generally thought to be cavitational despite the occasional report of thermal effects. However, there is some dispute as to whether these cavitational mechanisms are due to sonochemical production or to the localised streaming which will be experienced around an individual cavitation bubble. It is likely that the observed ultrasonic damage is due to a combination of these effects. Pohl *et al* have proposed that the increased permeability of model lipid bilayers to weak acids (Pohl, Antonenko and Rosenfeld, 1993) and the increased agglutination and aggregation of erythrocytes that they observed in response to ultrasonic exposure (Pohl *et al*, 1995), are due to reductions in thickness of the unstirred layers adjacent to the membrane caused by acoustic streaming. Thus the gradient of ions near the bilipid layer is increased and the membrane is effectively more permeable. This theory has also been suggested by a number of other groups including Mortimer and Dyson (1988) who proposed it to be the cause of their observed increase in calcium ion uptake in fibroblasts. It should be noted that effects such as liquid jets, microstreaming around cavitation bubbles and mechanical streaming, amongst others, can be extremely difficult to differentiate let alone determine and so all are likely to play a role in at least some of the systems described here.

In the context of this project, the underlying mechanism of ultrasonic action on membranes is of secondary importance to the investigation of any perturbations which may occur within the employed experimental systems. In order to gain some initial insight into the effects of ultrasonic radiation within these systems trypan blue exclusion was employed to assess moderate to severe cell damage.

5.2 Methods

L1210 cells were harvested during exponential growth and set at a concentration of approximately $6x10^5$ cells/ml (unless otherwise stated). This cell suspension was then dispensed in 10 ml aliquots into 25 cm^2 canted neck tissue culture flasks (Corning Costar Corporation) which were then allowed to cool on ice. The ultrasound exposure system was as described in 4.2.3, which was designed to prevent cellular damage by direct heating due to conduction from the ultrasonic transducer.

Prior to any ultrasound exposure and at various times during the 10 min exposures 50 μl samples were removed from the flasks for cell counting and temperature of the medium was taken by thermometer.

Cells were counted in the presence of an equal volume of trypan blue, a well-known vital stain, which is excluded by intact healthy cells, but taken up by non-viable cells. The stain was obtained as a 0.4 %(w/v) solution in 0.85 %(w/v) saline from ICN Biomedicals Ltd., Oxfordshire, U.K. and a stock solution was prepared by 1:1 dilution in saline, prior to filtering through a single use 0.22 μm syringe top filter (ICN Biomedicals Ltd.).

Counting was performed using an improved NeuBauer haemocytometer (Weber Scientific International Ltd., Middlesex, U.K.). In order to improve accuracy eight counting squares were used for each sample and the mean cell number/ml and the standard error of the mean were calculated in each case. Cell permeability (%) was calculated by dividing the number of stained cells by the total cell number and multiplying by 100. Permeability was also given as a mean value and standard error of the mean was used to produce error bars. It should be noted that cell counting was carried out as quickly as possible following insonation in order to reduce the period of time that the cells were exposed to trypan blue as this may lead to the staining of viable cells.

5.3 Effect of intensity during L1210 cell exposure to 3 MHz, continuous wave (CW) ultrasound

Cells were prepared and assessed as described in section 5.2. Each flask was exposed to 3 MHz, CW ultrasound, although, the intensity of the beam was altered between samples. A sham exposure was also conducted where a flask was left on the bench for the duration of the experiment, but was not insonated.

Figure 5.1(a) shows the rise in bulk medium temperature that was experienced in each flask. It is clear that increasing the intensity of a given exposure leads to a greater elevation in the temperature over a period of 10 min. The temperature in the sham insonated flask rose to just below room temperature. It is important to note that at intensities of 1.0 Wcm^{-2} and below, the temperature never rose above the 37.5 °C. It should also be noted, that the ice-cube bag was always cool to the touch following exposure, the only exception to this being the 2.0 Wcm^{-2} sample after 10 min of insonation, where the bag became hot and melted. It is therefore unlikely that heat conduction from the transducer played any part in the observed rises in bulk medium temperature at all other intensities.

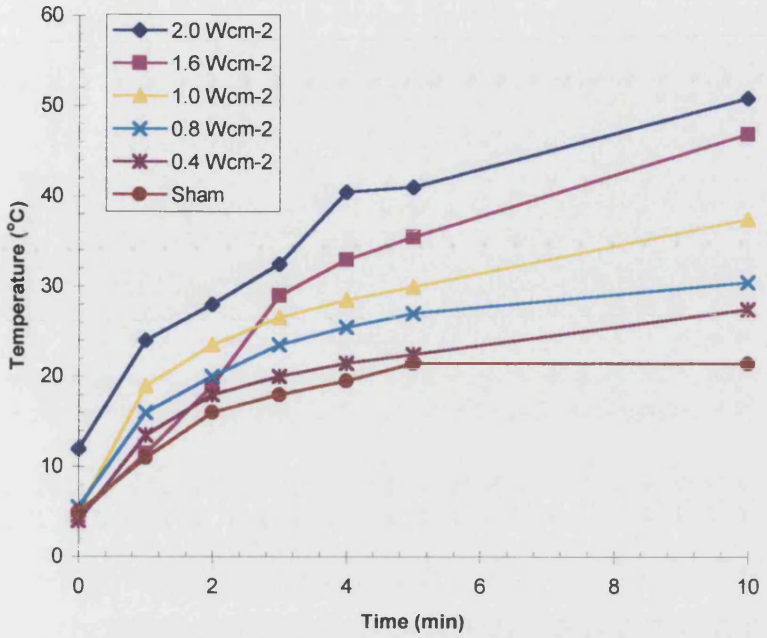

Figure 5.1(a): Temperature of bulk medium during insonation of L1210 cells at 3 MHz, CW at varying intensities.

The rise in temperature of the bulk medium as measured by thermometer during insonations of 3 MHz, CW at intensities of 2.0, 1.6, 1.0, 0.8, 0.4 Wcm^{-2} and sham insonated.

Figure 5.1(b) describes the total cell numbers during the same experiment. At the higher intensities of 2.0 and 1.6 Wcm^{-2} the total cell numbers fall as the insonation takes place, however in the case of the lower intensities 1.0, 0.8, 0.4 Wcm^{-2} and in the sham exposure the total number of cells remains constant (variation of +/- 16 %). This correlates well with the observed effect of insonation on cell permeability to trypan blue as depicted in Figure 5.1(c).

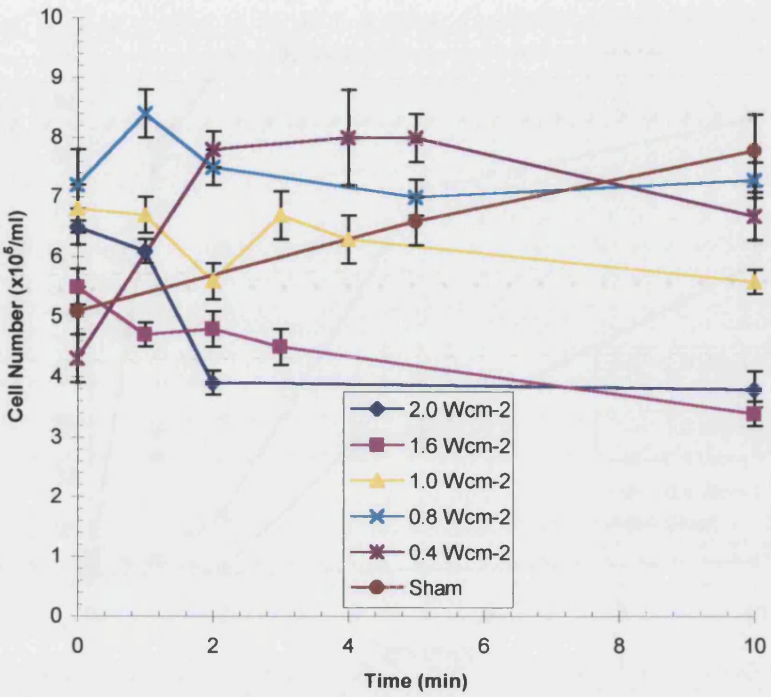

Figure 5.1(b): Cell numbers during insonation of L1210 cells at 3 MHz, CW at varying intensities.

Mean cell number/ml during insonations of 3 MHz, CW at intensities of 2.0, 1.6, 1.0, 0.8, 0.4 Wcm^{-2} and sham insonated. Error bars describe the standard error of the mean.

Cells exposed to 2.0, 1.6 or 1.0 Wcm^{-2} were all 100 % permeable to trypan blue (Figure 5.1(c)) by the end of the insonation period. However, in the case of 2.0 and 1.6 Wcm^{-2} ultrasound this occurred within the first 3 min. It would seem likely that after 3 min the cells exposed to these higher intensities begin to lyse leading to the observed fall in total cell number. At 0.8 and 0.4 Wcm^{-2} cells became progressively more permeable to trypan blue and after 10 min were 87.1 and 59.9 % permeable respectively. In the sham exposed sample the permeability to trypan blue remained below 5 % throughout.

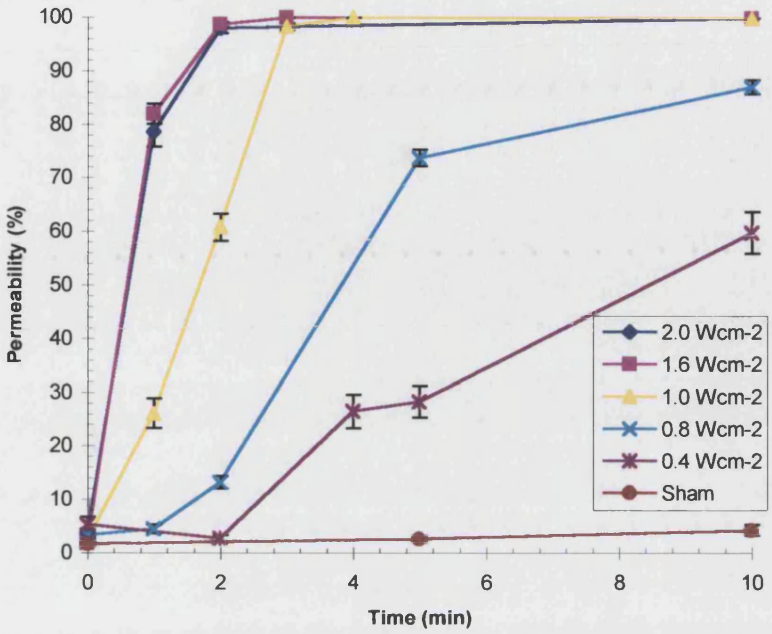

Figure 5.1(c): L1210 permeability to trypan blue during insonation at 3 MHz, CW at varying intensities.

Calculated mean percentage of cells permeable to trypan blue during insonations of 3 MHz, CW at intensities of 2.0, 1.6, 1.0, 0.8, 0.4 Wcm^{-2} and sham insonated. Error bars describe the standard error of the mean.

It is clear that 3 MHz, CW insonation of L1210 cells, within this experimental system, causes the bulk medium temperature to rise, cells to become increasingly permeable to trypan blue and is capable of inducing cell lysis. In all of these cases, increasing the intensity augments the observed effect. It is important to note that cell permeabilisation is not due to the increase in temperature as cells were 100 % permeable by 3 min of ultrasound treatment in the 2.0 and 1.6 Wcm^{-2} samples, where the temperatures were only 32.5 and 29.0 °C, respectively. Furthermore, in all other samples the temperature of the bulk medium remained below 37.5 °C, despite the occurrence of varying degrees of permeabilisation. However, it is possible that the

observed reduction in cell numbers in the 2.0 and 1.6 Wcm^{-2} samples was due to the increase in the temperature of the bulk medium.

5.4 Daily variation between experiments

In order to investigate the variation between experiments performed on different days the experiment described in section 5.3 was repeated at the lower intensities (1.0, 0.8, 0.4 Wcm^{-2} and sham insonated) and the results were compared by overlaying the graphs.

Figure 5.2(a) shows the observed temperature rises of the bulk medium in each flask on each day. It is clear that the results were similar on both occasions, although at each intensity the experiment performed in section 5.3 appeared to produce slightly higher temperatures. This is probably due to the fact that the bulk medium in these flasks was slightly warmer initially, possibly due to a higher room temperature as the sham exposed sample also produced a greater rise in temperature. However, it is important to note that this difference is negligible.

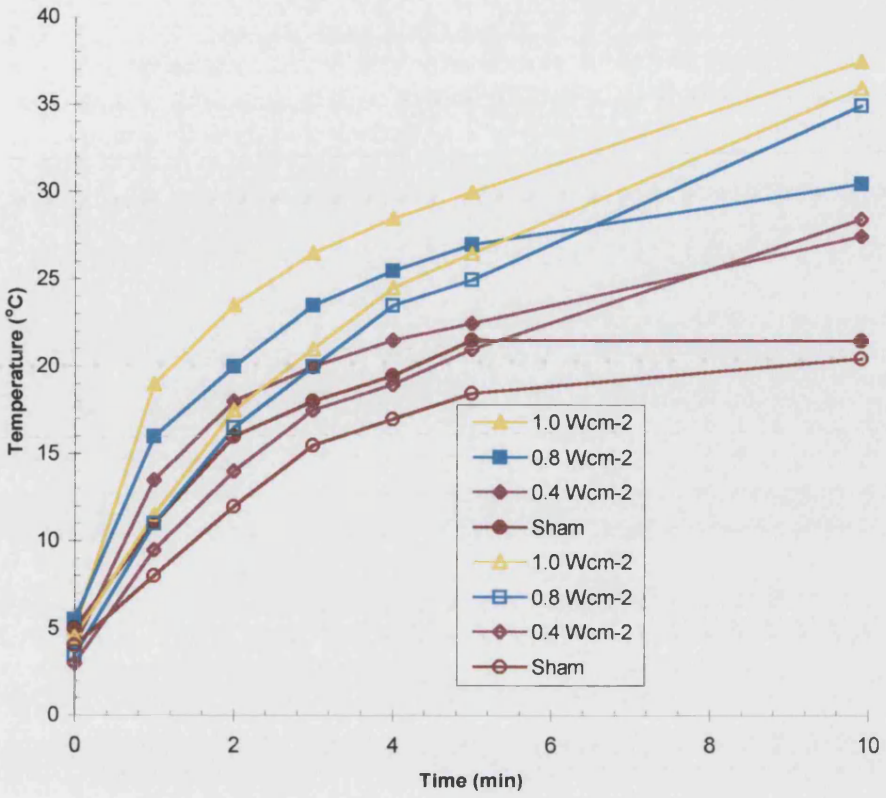

Figure 5.2(a): Comparison of temperature in bulk medium during insonation of L1210 cells at 3 MHz, CW at varying intensities as measured on different days.

L1210 cells were exposed to ultrasound at 3 MHz, CW at intensities of 1.0, 0.8, 0.4 Wcm^{-2} or sham exposed on two separate occasions. In both instances the temperature of the bulk medium was measured by thermometer. The shaded shapes represent the samples exposed in the experiment described in section 5.3 and the open shapes represent the repeat experiment.

Figure 5.2(b) shows the cell number/ml throughout the insonations on both days. In all cases the cell numbers remained constant (less than +/- 16 % variation with the exception of the 0.4 Wcm^{-2} repeat sample which showed +/- 30 % variation) during insonation.

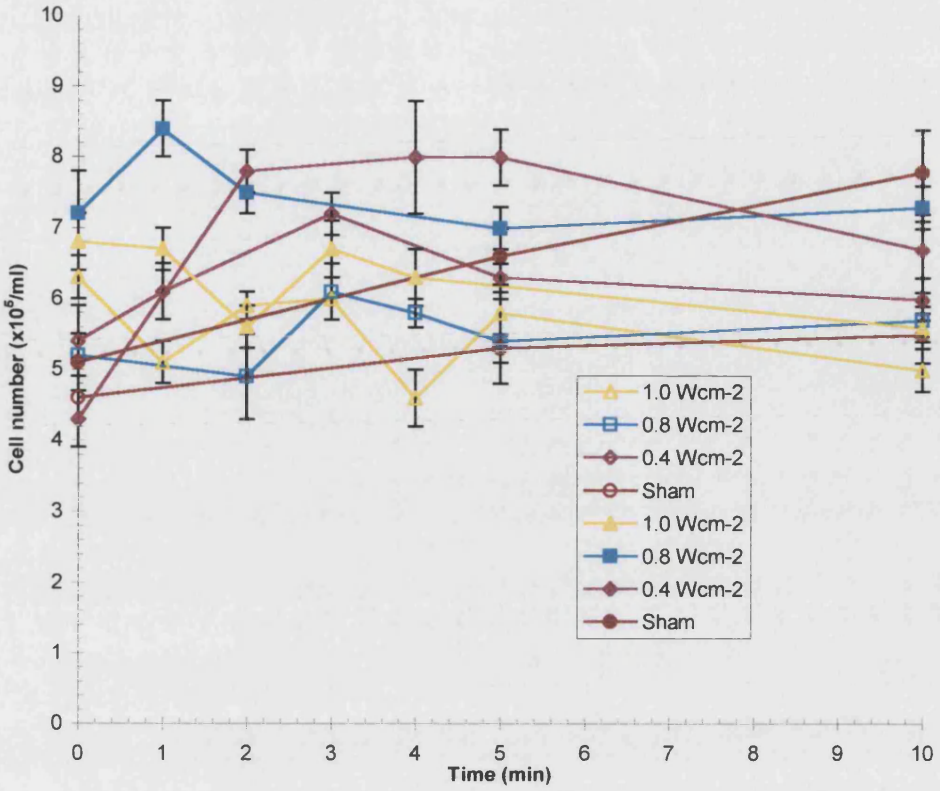

Figure 5.2(b): Comparison of cell numbers during insonation of L1210 cells at 3 MHz, CW at varying intensities, as measured on different days.

L1210 cells were exposed to ultrasound at 3 MHz, CW at intensities of 1.0, 0.8, 0.4 Wcm^{-2} or sham exposed on two separate occasions. Mean cell numbers/ml were calculated and the error bars represent the standard error of the mean. The shaded shapes represent the samples exposed in the experiment described in section 5.3 and the open shapes represent the repeat experiment.

Finally, figure 5.2(c) illustrates the percentage of cells permeable to trypan blue under the same ultrasonic conditions but on different days. The trends are undoubtedly the same, in that increasing the intensity increases the observed permeability to trypan blue, on both occasions. The differences observed between the results at 0.8 and 0.4 Wcm^{-2} are reasonable considering the experimental constraints, such as variations in cell growth. The magnitude of the difference observed in percentage of cells which became permeable increases as the exposure intensity decreases. This is due to the fact that cells which have only just lost their cell membrane integrity tend to stain very lightly with trypan blue and prove much harder to count accurately. In view of this

experiment it was decided that results could be compared from one day to the next, certainly with regard to the ranking of the samples.

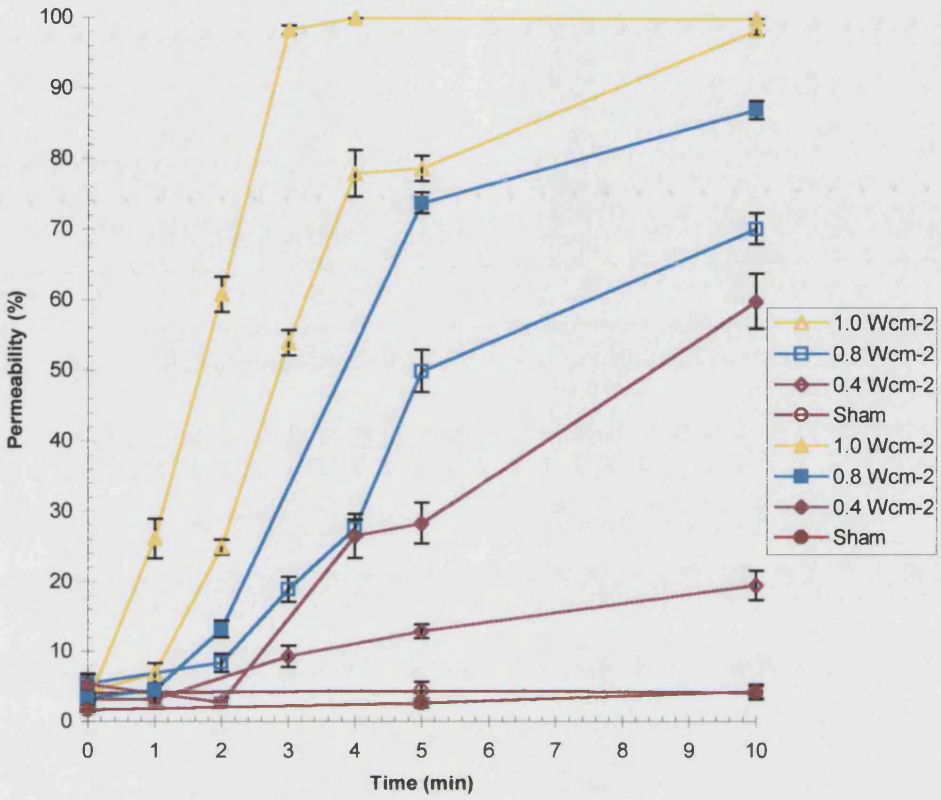

Figure 5.2(c): Comparison of L1210 permeability to trypan blue during insonation at 3 MHz, CW at varying intensities, as measured on different days.

Calculated mean percentage of cells permeable to trypan blue during insonations of 3 MHz, CW at intensities of 1.0, 0.8, 0.4 Wcm^{-2} or sham exposed on two separate occasions. Error bars represent the standard error of the mean. The shaded shapes represent the samples exposed in the experiment described in section 5.3 and the open shapes represent the repeat experiment

5.5 Effect of frequency during L1210 cell exposure to 1.0, 0.8 and 0.4 Wcm^{-2}, CW ultrasound

Cells were exposed to 1.0, 0.8 and 0.4 Wcm^{-2}, CW ultrasound at either 3 MHz or 1 MHz using the same protocol as previous experiments. Figure 5.3(a) shows the observed rise in temperature of the bulk medium. At 3 MHz the results were as

observed in section 5.3 and 5.4, where the temperature rise increased with increasing intensity, although the 1.0 and 0.8 Wcm^{-2} exposures gave a very similar rise in temperature on this occasion. This intensity dependent effect was also demonstrated for those samples exposed to 1 MHz ultrasound. At any given intensity the temperature rise in the 3 MHz sample was seen to be greater than in the 1 MHz sample. This effect is inline with the well documented observation that absorption of higher frequency ultrasound leads to greater heating. In fact at any given temperature the absorption is proportional to the square of the applied frequency in simple medium (Williams, 1983). There was no instance of the temperature rising above 37.5 °C during this experiment.

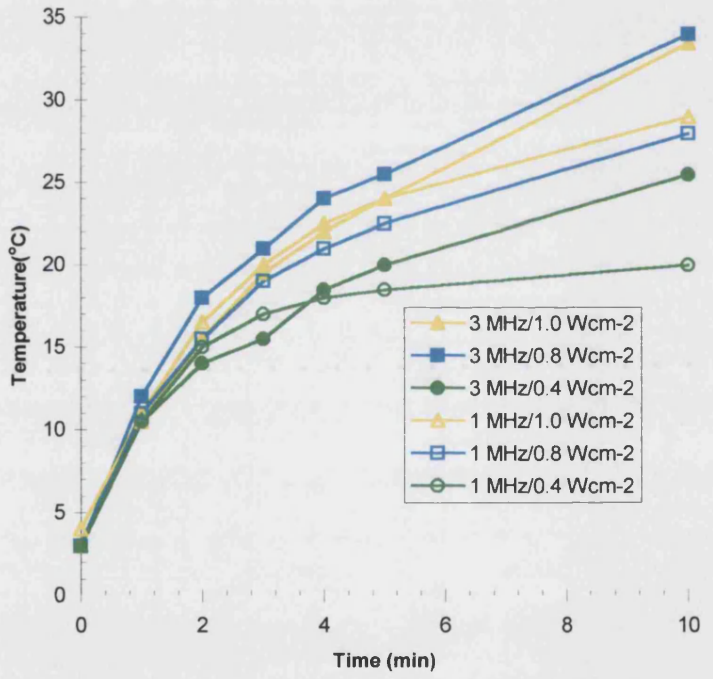

Figure 5.3(a):Temperature rise of bulk medium during insonation of L1210 cells at 3 MHz and 1 MHz, CW at varying intensities.

Cells were exposed to either 3 MHz or 1 MHz ultrasound at intensities of 1.0, 0.8 and 0.4 Wcm^{-2} and the temperature of the bulk medium was observed by thermometer. Shaded shapes represent insonations at 3 MHz while open shapes represent insonations at 1 MHz.

The effect of each frequency at the same range of intensities on the total cell number are shown in figure 5.3(b). At 3 MHz, cell numbers stay constant (variation of +/-16 % or less) at this range of intensities just as has been previously observed. However, at 1 MHz the total cell numbers fall dramatically over the insonation period. This effect seems to be intensity dependent and correlates well with the results observed for the exclusion of trypan blue represented in figure 5.3(c).

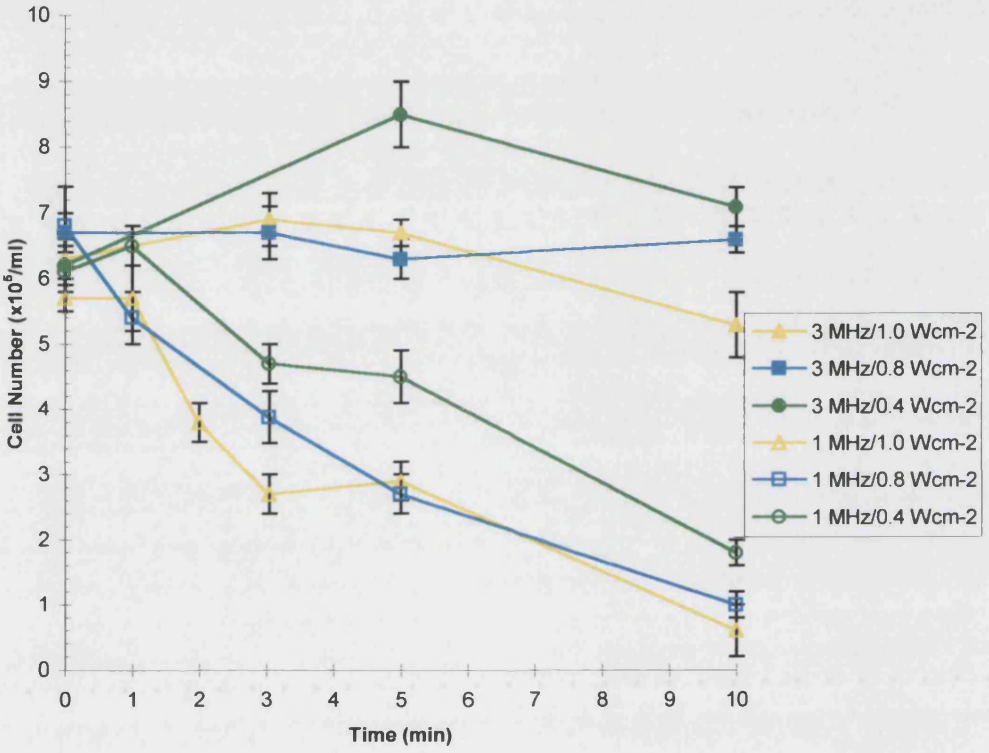

Figure 5.3(b): Cell numbers during insonation of L1210 cells at 3 MHz and 1 MHz, CW at varying intensities.

Cells were exposed to either 3 MHz or 1 MHz ultrasound at intensities of 1.0, 0.8 and 0.4 Wcm^{-2} and the mean cell number/ml were calculated. The error bars describe the standard error of the mean. Shaded shapes represent insonations at 3 MHz while open shapes represent insonations at 1 MHz.

In the 3 MHz samples trypan blue exclusion (Figure 5.3(c)) showed the same trends as previously observed, whereby the cells became increasing more permeable during the insonation and the magnitude of this effect was increased with increasing intensity.

This intensity dependent effect was also observed in the 1 MHz samples, however at a given intensity cells were far more permeable to trypan blue when insonated at 1 MHz than at 3 MHz. In fact, cells exposed to 1 MHz ultrasound became permeable to trypan blue very quickly, within 3 min of exposure cells were greater than 90 % permeable at all intensities. The huge loss of cells observed in these samples (Figure 5.3(b)) was associated with the high degree of permeability observed. It would appear that cells initially become permeable and that further insonation results in cell lysis. The cell loss observed in the 1 MHz samples is marked and occurs around the time when cells are observed to be 100 % permeable to trypan blue.

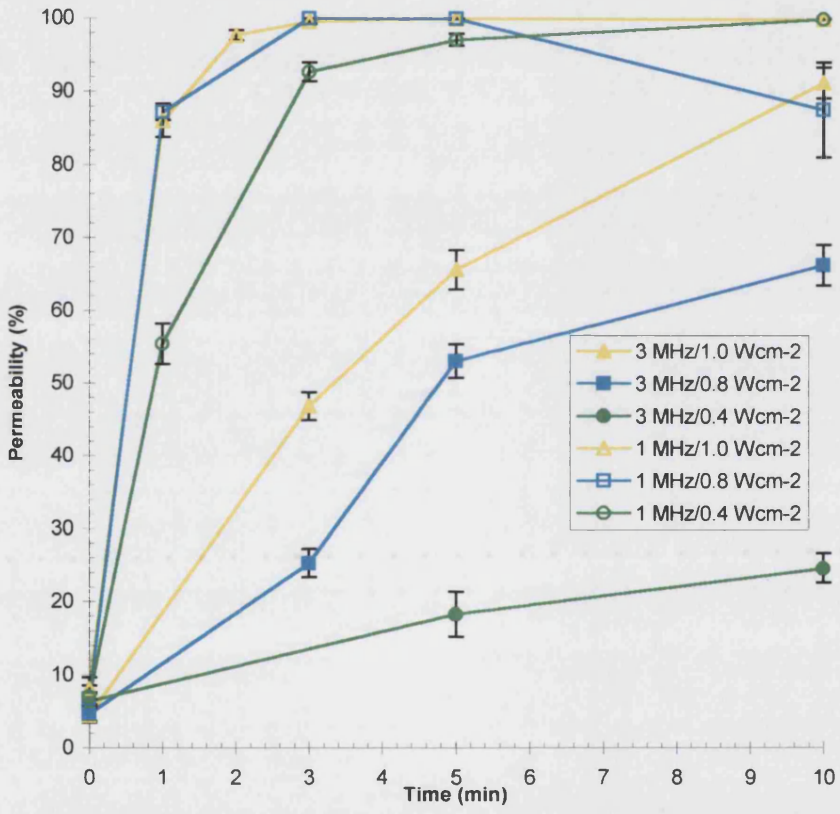

Figure 5.3(c): L1210 permeability to trypan blue during insonation at 3 MHz and 1 MHz, CW at varying intensities.

Cells were exposed to either 3 MHz or 1 MHz ultrasound at intensities of 1.0, 0.8 and 0.4 Wcm^{-2} and the mean percentage of cells permeable to trypan blue was calculated. The error bars describe the standard error of the mean. Shaded shapes represent insonations at 3 MHz while open shapes represent insonations at 1 MHz.

It is clear that the observed increase in cell permeability to trypan blue and the associated cell lysis is not a thermal effect as cell permeability is far more marked in the 1 MHz rather than in the 3 MHz samples. However, the rise in bulk medium temperature is greater in the 3 MHz samples. It is not likely that the localised intracellular temperatures are sufficiently elevated, in suspension cells where the temperature is controlled, to cause these effects (Love and Kremkau, 1980). The most likely mechanisms responsible for the observed effects of insonation on L1210 cells are either mechanical or cavitational. Certainly, it can be observed by the naked eye that the degree to which the cell suspension is perturbed and the number of bubbles produced, can be related to both the frequency and the intensity of the insonation. Disruption of the medium is increased with decreasing frequency and increasing intensity. However, it is somewhat more difficult to differentiate which of these mechanisms is responsible for the observed perturbations.

5.6 Effect of cell density during L1210 exposure to 3 MHz, 1.0 Wcm^{-2}, CW ultrasound

In section 5.1, the proposed possibility that increasing the cell density may provide protection from damage was summarised. In order to address this issue, within this experimental system, L1210 cells were insonated at 3 MHz, 1.0 Wcm^{-2}, CW at varying cell densities. Cells were counted and then serially diluted 1:1 with fresh medium to give the following cellular concentrations: $12x10^5$ cells/ml, $6x10^5$ cells/ml, $3.5x10^5$ cells/ml, $2.2x10^5$ cells/ml. Ultrasound exposures were carried out as described in section 5.2.

Figure 5.4(a) depicts the temperature rises in bulk medium observed in the presence of the various cell densities. It is clear that cell density does not alter the observed change in the temperature of the bulk medium under these experimental conditions.

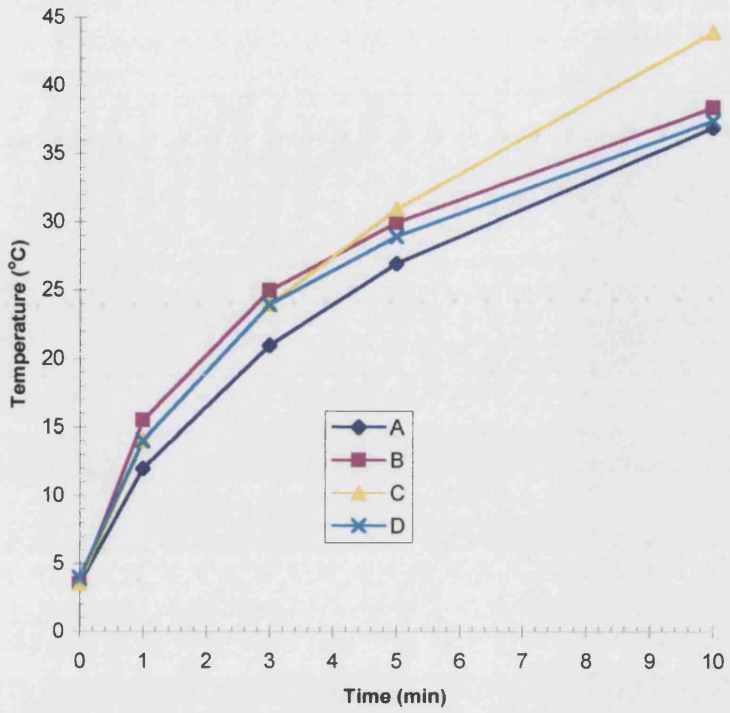

Figure 5.4(a): Temperature rise of bulk medium during insonation of L1210 cells at 3 MHz, 1.0 Wcm^{-2}, CW at varying cell densities.

Cells were exposed to 3 MHz ultrasound at cell densities of : A-$12x10^5$ cells/ml, B-$6x10^5$ cells/ml, C-$3.5x10^5$ cells/ml and D-$2.2x10^5$ cells/ml. Temperature of the bulk medium was observed by thermometer.

The effect of cell density on cell numbers during insonation are shown in figure 5.4(b). There is no cell loss at the highest density of $12x10^5$ cells/ml. However, there is some observed loss in the $6x10^5$ cells/ml, $3.5x10^5$ cells/ml and $2.2x10^5$ cells/ml samples, the calculated rates of this cell loss over the 10 min duration is $0.29x10^5$ cells/ml/min, $0.14x10^5$ cells/ml/min and $0.08x10^5$ cell/ml/min respectively. Interestingly, the percentage of the total cells lost is 41 %, 39 % and 35 %, respectively. It is apparent that at a density of $12x10^5$ cells/ml there is a protective effect, and although there is cell loss at lower densities the proportion of this loss remains similar regardless of the cellular concentration. However, the absolute number of cells lost is greater at greater densities.

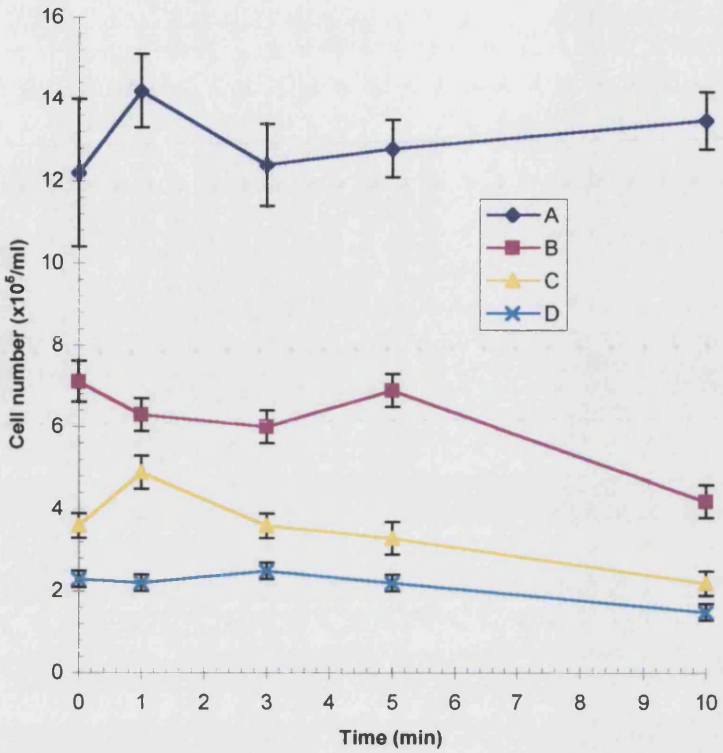

Figure 5.4(b): Cell numbers during insonation of L1210 cells at 3 MHz, 1.0 Wcm^{-2}, CW at varying cell densities.

Cells were exposed to 3 MHz ultrasound at cell densities of : A-12x10^5 cells/ml, B-6x10^5 cells/ml, C-3.5x10^5 cells/ml and D-2.2x10^5 cells/ml. The error bars describe the standard error of the mean.

Figure 5.4(c) describes the effect of cell density on the observed ultrasound induced permeability to trypan blue. No clear trend can be observed, although it is arguable that at higher densities cells may take longer to become permeable.

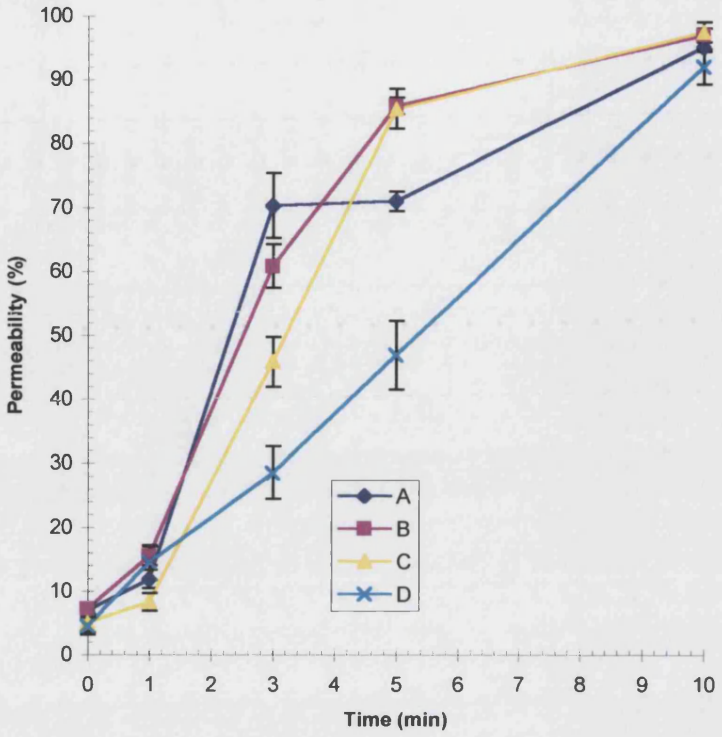

Figure 5.4(c): L1210 permeability to trypan blue during insonation at 3 MHz, 1.0 Wcm^{-2}, CW at varying cell densities.

Cells were exposed to 3 MHz ultrasound at cell densities of : A-12x10^5 cells/ml, B-6x10^5 cells/ml, C-3.5x10^5 cells/ml and D-2.2x10^5 cells/ml and the mean percentage of cells permeable to trypan blue was calculated. The error bars describe the standard error of the mean.

5.7 Effect of cell density during L1210 exposure to 1 MHz, 0.4 Wcm^{-2}, CW ultrasound

The previous experiment (5.6) was repeated using 1 MHz ultrasound. However, as at an intensity of 1.0 Wcm^{-2} cells are very quickly damaged using this frequency a lower intensity beam of 0.4 Wcm^{-2} was employed. Cells were counted and then serially diluted 1:1 with fresh medium to give the following cellular concentrations: 15x10^5 cells/ml, 7.8x10^5 cells/ml, 3.8x10^5 cells/ml, 2.0x10^5 cells/ml. Ultrasound exposures were carried out as described in section 5.2.

Figure 5.5(a) clearly shows that cell density has no effect on the observed rise in temperature when L1210 cells are exposed under these conditions.

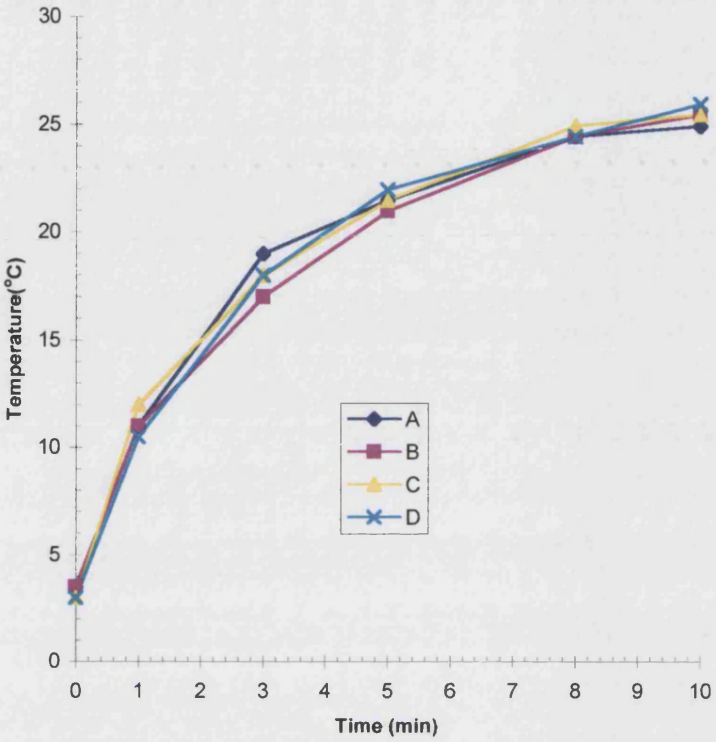

Figure 5.5(a): Temperature rise of bulk medium during insonation of L1210 cells at 1 MHz, 0.4 Wcm^{-2}, CW at varying cell densities.

Cells were exposed to 1 MHz ultrasound at cell densities of : A-$15x10^5$ cells/ml, B-$7.8x10^5$ cells/ml, C-$3.8x10^5$ cells/ml and D-$2.0x10^5$ cells/ml. Temperature of the bulk medium was observed by thermometer.

Figure 5.5(b) describes the cell number/ml with progression through the experiment. It is apparent that cells are lost regardless of the cell density. The rate of cell loss over the 10 min period in the $15x10^5$ cells/ml, $7.8x10^5$ cells/ml, $3.8x10^5$ cells/ml and $2.0x10^5$ cells/ml samples is $0.64x10^5$cells cells/ml/min, $0.42x10^5$cells cells/ml/min, $0.3x10^5$cells/ml/min and $0.16x10^5$cells/ml/min respectively, while the percentage of the total cells lost is 43 %, 54 %, 79 % and 80 % respectively. Therefore under these conditions the rate of cell loss increases with increasing density while the proportion

of cells lost decreases with increasing density, while the absolute number of cells lost is still greater in the higher density samples.

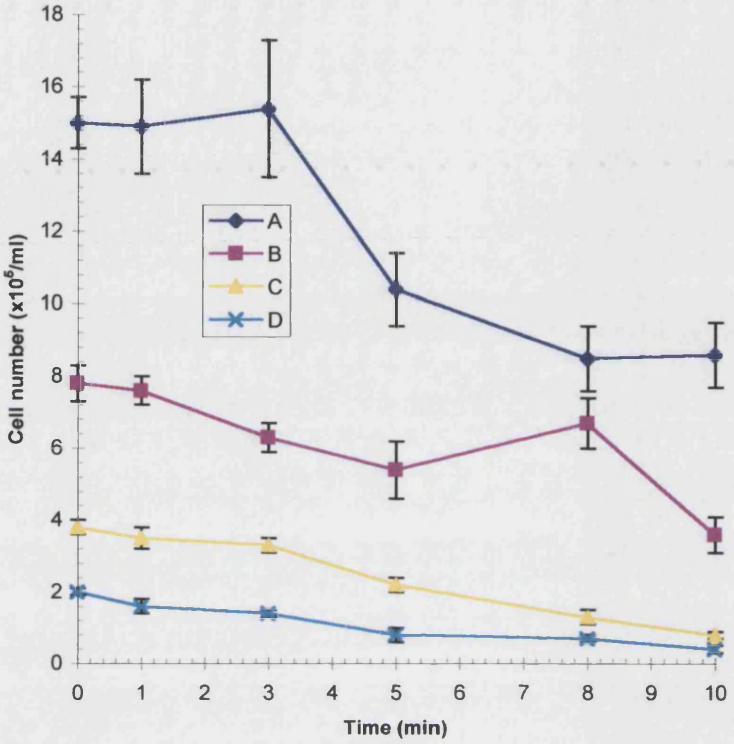

Figure 5.5(b): Cell numbers during insonation of L1210 cells at 1 MHz, 0.4 Wcm^{-2}, CW at varying cell densities.

Cells were exposed to 1 MHz ultrasound at cell densities of: A-15x10^5 cells/ml, B-7.8x10^5 cells/ml, C-3.8x10^5 cells/ml and D-2.0x10^5 cells/ml. The error bars describe the standard error of the mean.

Finally, figure 5.5(c) depicts the effect of changes in cell density on the ultrasonically induced permeability to trypan blue. Cell density clearly does not have any effect on the progression of permeability of L1210 cells during this insonation.

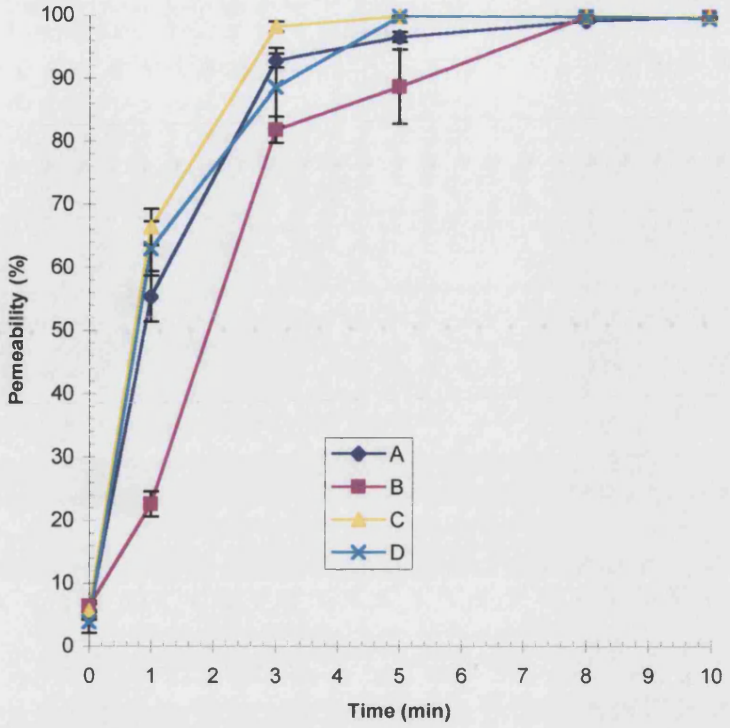

Figure 5.5(c): L1210 permeability to trypan blue during insonation at 1 MHz, 0.4 Wcm^{-2}, CW at varying cell densities.

Cells were exposed to 1 MHz ultrasound at cell densities of: A-15x10^5 cells/ml, B-7.8x10^5 cells/ml, C-3.8x10^5 cells/ml and D-2.0x10^5 cells/ml and the mean percentage of cells permeable to trypan blue was calculated. The error bars describe the standard error of the mean.

Results from both this section and the one previous (5.6) show that altering the cell density within the range and system described has no effect on the rise in temperature of bulk medium and no discernible effect on the percentage of cells which become permeable to trypan blue. However, there is some effect on cell lysis. At higher densities the rate of cell loss is greater, presumably due to the greater total number of cells within the ultrasonic field. In section 5.6 the percentage of total cell loss remained constant at the three lower densities, while in this section the percentage loss increased as the density decreased. Despite this, the absolute number of cells lost increased with increasing cellular concentration, with the exception of the highest density sample in section 5.6. These observations correlate well with the work of Brayman, Church and Miller (1996), although the cell densities which they employed

were far greater. The fact that the changes in bulk temperature during ultrasound exposure are the same regardless of the cell density indicates that the sonolytic effect is non-thermal. The proportion of the remaining cells which become permeable remains similar regardless of the cell density. The mechanism of this sonolyic effect remains unclear, although cavitational and mechanical bioeffects are likely to be important. Brayman, Church and Miller (1996) have proposed a theory which explains the observed protective effects of high cell densities. It implicates the inactivation of active cavitation bubbles as the key factor by using both theoretical and experimental data. Active cavitation bubbles can be inactivated by either a number of encounters with cells, the critical number of which is dependent on both cell and bubble size, or the aggregation of a group of cells around one bubble. The cell density is clearly crucial in how quickly either of these events can take place and may therefore account for the observed protective effects of a high cell density. It follows that sonolysis should reach a plateau with increased cell concentration and presumably this should be the case *in vivo* where cellular concentrations are in the order of $5x10^9$ cells/ml or greater (whole blood).

Finally, it should be noted that due to the nature of the experimental protocol namely serial dilution of cells, the lower cell density samples had a higher proportion of 'fresh' medium and this may be important with regard to production of cavitation nuclei. It is, however, a difficult problem to address.

5.8 Comparison of PBS and medium as cellular suspension fluids during L1210 exposure to 3 or 1 MHz, 1.0 Wcm^{-2}, CW ultrasound

The sonodynamic properties of fluids may differ greatly due to the presence of inhomogeneities which serve as cavitation nuclei or organic compounds which can induce sonochemical reactions (Suslick, 1988). Other qualities which are important are viscosity, temperature prior to insonation and gas content itself (Carstensen *et al*, 1993; Miller, Miller and Brayman, 1996; Armour and Corry, 1982). These phenomena may lead to differences in the observed cellular damage when cells are suspended in PBS as opposed to growth medium. This possibility was investigated by spinning L1210 cells out of the medium in which they had been grown, in a benchtop

centrifuge at 1500 rpm for 3 min and resuspending them in either fresh medium or fresh PBS, which had been warmed to 37 °C, at a concentration of $6x10^5$ cells/ml. The ultrasonic exposures were then conducted as detailed in section 5.2.

Figure 5.6(a) shows that the rise seen in bulk temperature of the medium samples is similar to that which we have observed in previous experiments. Furthermore, the temperature curves for the PBS samples are almost identical indicating that the fluid used to suspended cells does not affect the increase in temperature induced by ultrasound.

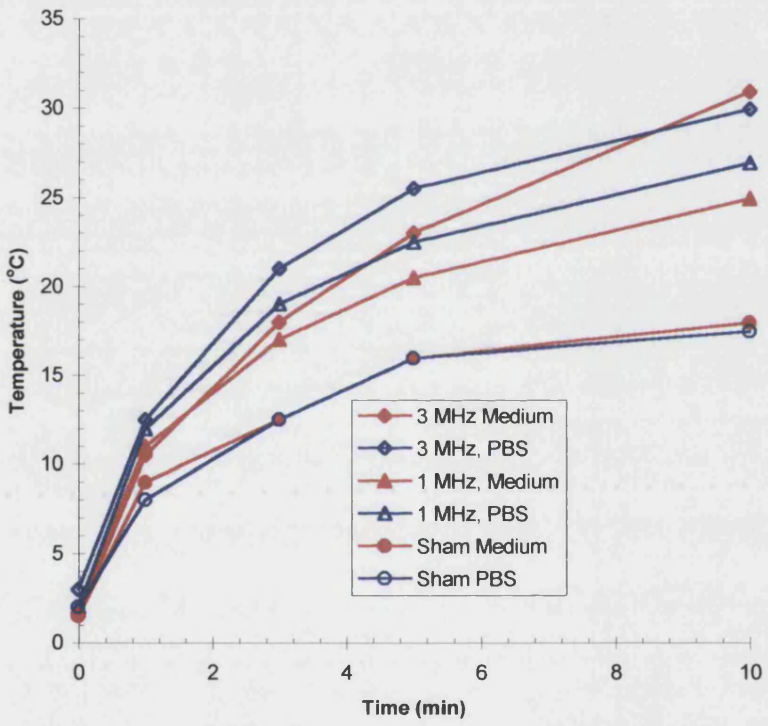

Figure 5.6(a): Temperature rise in bulk fluid during insonation of L1210 cells at 3 or 1 MHz, 1.0 Wcm^{-2}, CW in either medium or PBS.

The rise in bulk fluid as measured by thermometer during insonations 3 or 1 MHz at 1.0 Wcm^{-2} or sham exposure of L1210 cells suspended in either medium (shaded shapes) or PBS (open shapes).

The cell numbers observed during the experiment are shown in figure 5.6(b). In the samples resuspended in medium, the sham exposure and the sample insonated at 3 MHz showed no loss of cell number. However, as we have seen under similar conditions previously, the 1 MHz sample lost cells as the experiment proceeded. Unexpectedly, in the samples suspended in PBS, cell numbers were extremely low even before the experiment started. Infact, cells were approximately half as dense as they had been initially suspended in PBS, prior to their incubation on ice.

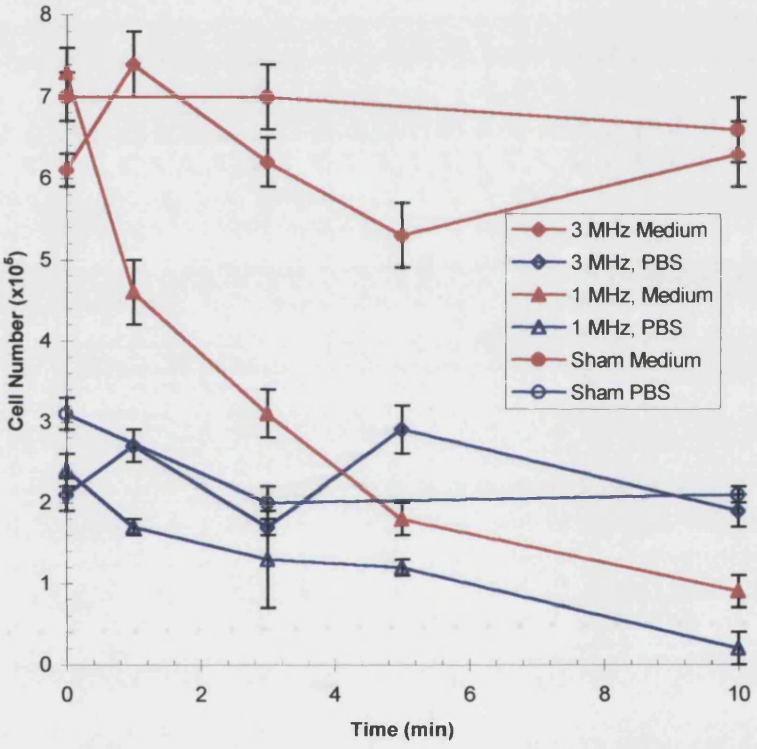

Figure 5.6(b): Cell numbers during insonation of L1210 cells at 3 or 1 MHz, 1.0 Wcm^{-2}, CW in either medium or PBS.

Cells were exposed to 3 or 1 MHz at 1.0 Wcm^{-2} or sham exposed while suspended in either medium (shaded shapes) or PBS (open shapes) and the mean cell number/ml was calculated. The error bars describe the standard error of the mean.

Figure 5.6(c) depicts the percentage of the total cells which were permeable to trypan blue during insonation. In the case of the samples resuspended in medium results were

as expected; sham exposed cells remained about 10 % permeable to trypan blue, while cells exposed to 1 MHz ultrasound became 85 % permeable within the first minute and cells exposed to 3 MHz were approximately 80 % permeable after 10 min. The results in the samples exposed to ultrasound while suspended in PBS were very different. Even before exposure cells were very permeable, almost 60 % permeable in the sham unexposed cells. In both the sham cells and the cells exposed to ultrasound the percentage of cells permeable to trypan blue increased to values greater than those seen in the corresponding medium samples throughout the experiment.

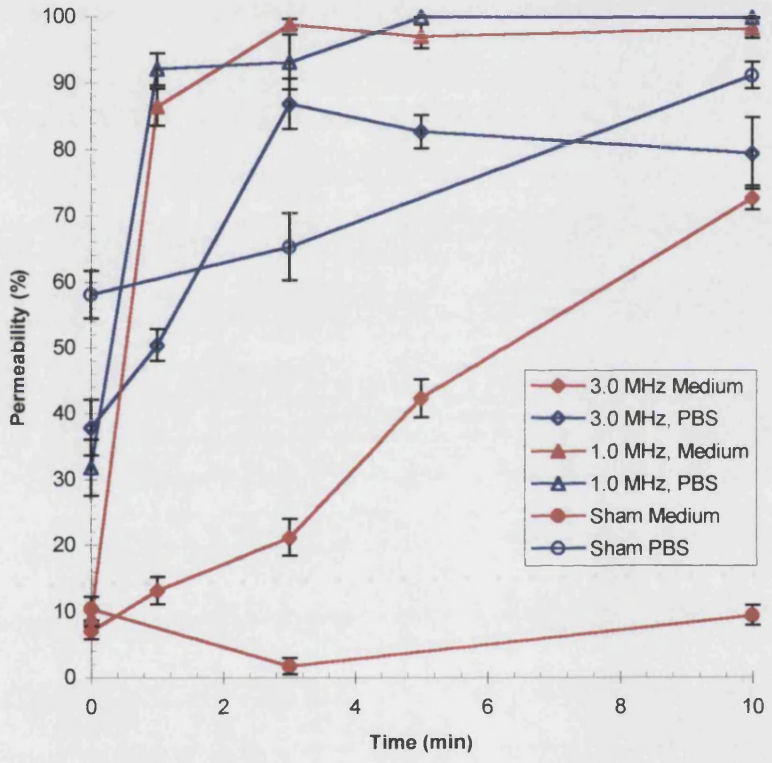

Figure 5.6(c): L1210 permeability to trypan blue during insonation at 3 or 1 MHz, 1.0 Wcm^{-2} ,CW in either medium or PBS.

Cells were exposed to 3 or 1 MHz at 1.0 Wcm^{-2} or sham exposed while suspended in either medium (shaded shapes) or PBS (open shapes) and the mean percentage of cells permeable to trypan blue was calculated. The error bars describe the standard error of the mean.

The experiment described above was carried out previously with the same results, thus it seems that cells resuspended in PBS and incubated on ice, lyse and become permeable even prior to ultrasonic exposure. In order to address this problem, L1210 cells were subjected to the experimental protocol described earlier, whereby cells were suspended in either fresh medium or fresh PBS at a concentration of approximately $6x10^5$ cells/ml, but were incubated on ice for a period of 4.5 hrs. Following this incubation cells were counted and the percentage of cells which were permeable to trypan blue was calculated. Results are shown below in table 5.1. It is clear that cells are lost, presumably by lysis, during incubation on ice in PBS. The cell counts observed in these samples were approximately half those observed in the samples suspended in medium. The percentage of cells permeable to trypan blue is also substantially higher in the PBS samples.

	PBS Sample1	PBS Sample 2	Medium Sample 1	Medium Sample 2
Cell count/ml	2.5 +/- 0.3 x 10^5	2.8 +/- 0.2 x 10^5	4.7 +/- 0.2 x 10^5	5.5 +/- 0.5 x 10^5
Permeability to trypan blue (%)	8.8 +/- 3.6	10.4 +/- 5.4	2.7 +/-1.0	0 +/-0

Table 5.1: L1210 cell numbers and permeability following 4.5 hrs incubation in either PBS or medium on ice.

Cells were resuspended in either PBS or medium at a concentration of $6x10^5$ cells/ml and were then incubated on ice for a period of 4.5 hrs. Cells were then counted and the percentage of the total number permeable to trypan blue was calculated.

It is apparent that cell health is substantially impaired when L1210 cells are allowed to stand on ice in PBS and thus the effects of medium versus PBS during insonation cannot be compared within this system. The cell lysis observed in table 5.1 can be seen to occur after much shorter periods of incubation by light microscopy, although exact cell numbers have not been counted. In fact, the lytic action of PBS under 'ice-cold' conditions appears to be almost instant. It is interesting that the PBS had been warmed prior to the resuspension of L1210 cells and that lysis occurred during the cooling of the bulk volume.

This PBS induced lysis is not consistent with work carried out by Miller's group on Chinese hamster ovary cells where samples were stored on ice to prevent repair of ultrasonically induced single strand breaks in DNA (Miller, Thomas and Frazier, 1991a). There is no mention of cell lysis due to PBS exposure at low temperature, although in a later paper by the same group (Miller, Thomas and Buschbom, 1995) 10 % foetal bovine serum was added to PBS in order to reduce the effects of cold shock following insonation. Cold shock has been previously described by Kruman *et al* (1992) as an apoptotic response to sudden temperature reduction using murine BW 5147 thymoma cells. It is possible that a similar mechanism has produced the effect observed here as the medium was supplemented by 15 % FCS while the PBS was not, furthermore cell lysis was almost instant. Unfortunately, the addition of FCS to PBS would, defeat the initial aim of the experiment which was to compare the sonodynamic properties of the solutions and the resultant effect on cells.

5.9 Effect of 100 IU/ml catalase during L1210 cell exposure to 3 or 1 MHz, 1.0 Wcm^{-2}, CW ultrasound

In order to attempt to elucidate or indeed eliminate mechanisms by which cell integrity was being compromised the effects of certain sonochemicals cavitationally produced were investigated. In chapter 1, the production of sonochemicals due to cavitation was described in detail (1.2.3), including the production of hydrogen peroxide (H_2O_2) which has a huge potential to induce cellular damage due to its oxidising properties. Catalase is a naturally occurring heme-containing enzyme found in peroxisomes and is responsible for the catalysis of H_2O_2 dismutation.

$$2\,H_2O_2 \longrightarrow 2\,H_2O + O_2$$

Catalase from *Aspergillus niger* was obtained from Sigma-Aldrich Co. Ltd. and was added to cell suspensions immediately prior to insonation at a concentration of 100 IU/ml. The unit definition for this enzyme being, one unit will decompose 1.0 μmole of H_2O_2 per min at pH 7.0 at 25 °C, while the H_2O_2 concentration falls from 10.3 to 9.2 mM. The concentration of catalase was determined by review of work from Miller's group (Miller, Thomas and Frazier, 1991b), in which catalase was employed

to eliminate H_2O_2 from PBS as part of a control experiment. Ultrasound exposures were carried out as described in section 5.2.

The effect of the addition of 100 IU/ml catalase on the temperature rise of bulk medium is shown in figure 5.7(a). In the presence of catalase the temperature rise was slightly higher. In general the temperature rises were greater than normally seen under these conditions as they were slightly warmer than usual prior to the experiment.

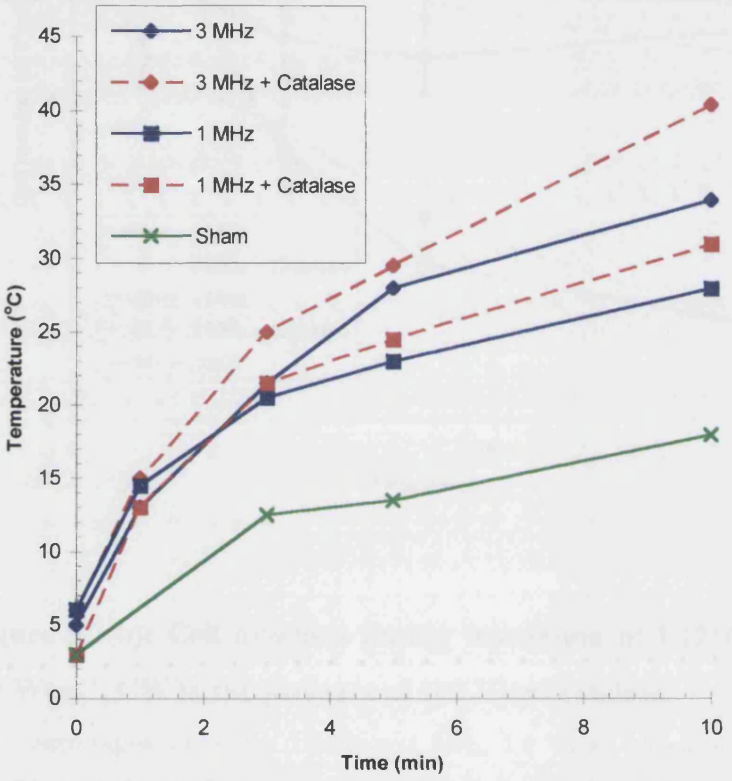

Figure 5.7(a):Temperature rise of bulk medium during insonation of L1210 cells at 3 or 1 MHz, 1.0 Wcm^{-2}, CW in the presence of 100 IU/ml catalase.

Cells were exposed to either 3 MHz or 1 MHz, 1.0 Wcm^{-2} ultrasound in the presence/absence of 100 IU/ml catalase and the temperature of the bulk medium was observed by thermometer. A sham exposure was also performed.

The presence of catalase did not affect the action of ultrasound on the cell number as is depicted in figure 5.7(b). There was no loss of cells in the sham sample and little

loss in the flasks exposed to 3 MHz. However, cell numbers did fall in the 1 MHz samples in a similar fashion to previous experiments in this chapter.

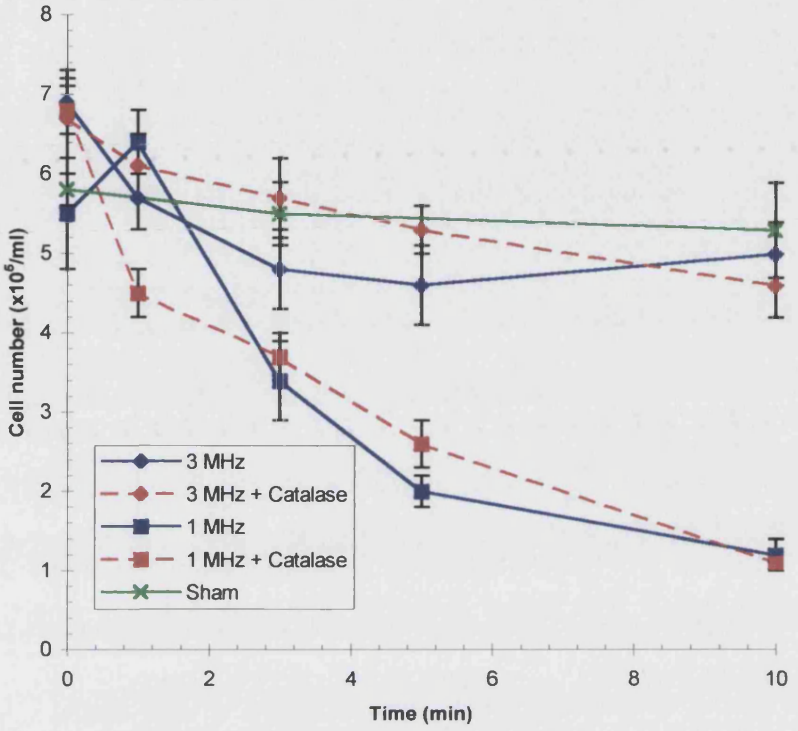

Figure 5.7(b): Cell numbers during insonation of L1210 cells at 3 or 1 MHz, 1.0 Wcm^{-2}, CW in the presence of 100 IU/ml catalase.

Cells were exposed to either 3 MHz or 1 MHz, 1.0 Wcm^{-2} ultrasound in the presence/absence of 100 IU/ml catalase and the mean cell number/ml was calculated. The error bars describe the standard error of the mean.

Figure 5.7(c) describes the percentage permeability to trypan blue during insonations in the presence and absence of catalase. It is clear that no protection from permeabilisation is provided by catalase at either 3 or 1 MHz. The results were again as previously observed under these conditions and there was no increase in permeability to trypan blue in the sham exposed sample.

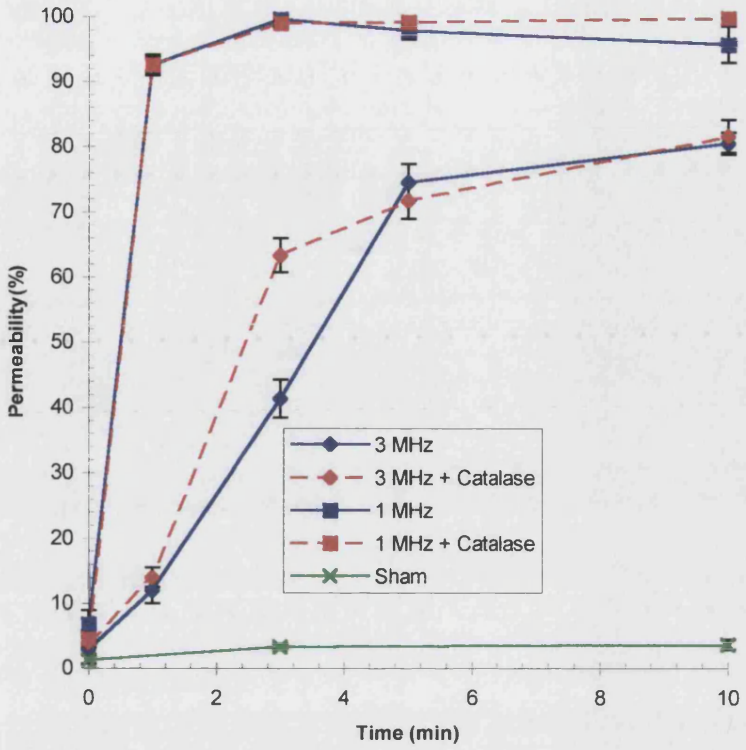

Figure 5.7(c): L1210 permeability to trypan blue during insonation at 3 or 1 MHz, 1.0 Wcm^{-2}, CW in the presence of 100 IU/ml catalase.

Cells were exposed to either 3 MHz or 1 MHz, 1.0 Wcm^{-2} ultrasound in the presence/absence of 100 IU/ml catalase and the mean percentage of cells permeable to trypan blue was calculated. The error bars describe the standard error of the mean.

It is clear that catalase at this concentration provides no protection from the damaging effects of insonation under these conditions. It is possible that there is so much H_2O_2 produced that catalase becomes saturated and in order to address this the concentration was elevated in section 5.10.

5.10 Effect of 1000 IU/ml catalase during L1210 cell exposure to 3 or 1 MHz, 1.0 Wcm^{-2}, CW ultrasound

The experimental method was as described in the previous section (5.9) with the exception that the concentration of catalase added prior to insonation was increased ten fold to 1000 IU/ml.

Figure 5.8(a) shows that the observed rises in temperature of the bulk medium are similar to those observed in 5.9, although the presence of catalase did not produce a greater temperature rise in the cells exposed to 1 MHz.

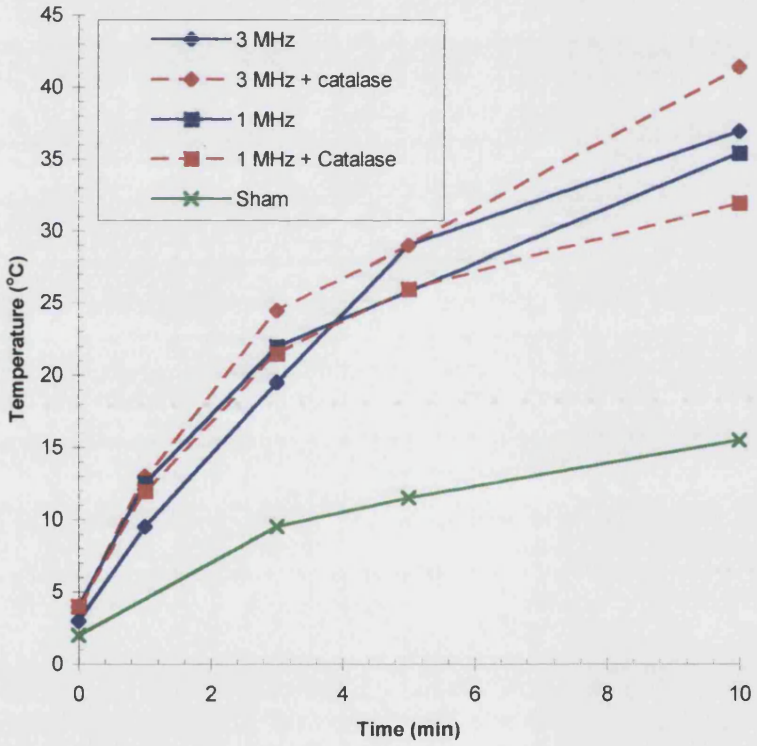

Figure 5.8(a):Temperature rise of bulk medium during insonation of L1210 cells at 3 or 1 MHz, 1.0 Wcm^{-2}, CW in the presence of 1000 IU/ml catalase.

Cells were exposed to either 3 MHz or 1 MHz, 1.0 Wcm^{-2} ultrasound in the presence/absence of 1000 IU/ml catalase and the temperature of the bulk medium was observed by thermometer. A sham exposure was also performed.

The ultrasonically induced effects on cell number (Figure 5.8(b)) are unchanged by the presence of 1000 IU/ml catalase and indeed the results are in agreement with those observed in response to insonation using these parameters previously.

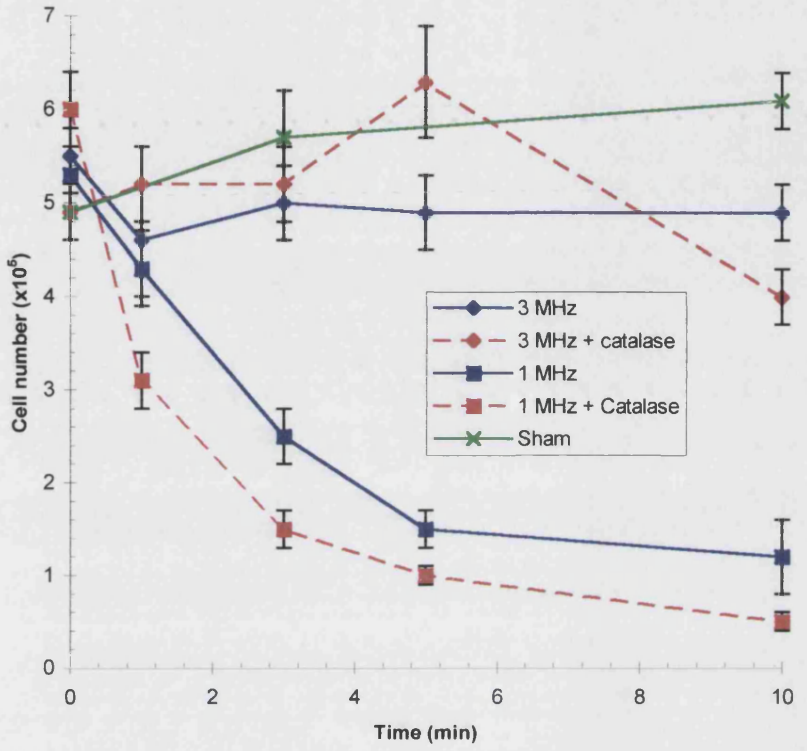

Figure 5.8(b): Cell numbers during insonation of L1210 cells at 3 or 1 MHz, 1.0 Wcm^{-2}, CW in the presence of 1000 IU/ml catalase.

Cells were exposed to either 3MHz or 1MHz, 1.0Wcm^{-2} ultrasound in the presence/absence of 1000IU/ml catalase and the mean cell number/ml was calculated. The error bars describe the standard error of the mean.

Figure 5.8(c) depicts the observed cell permeability to trypan blue in response to insonation, in the presence/absence of 1000 IU/ml catalase. At 1 MHz, catalase has no effect on the percentage of cells permeable to exclusion dye, while at 3 MHz catalase produces a slight increase in the percentage of L1210 cells permeable rather than providing the expected protective effect. However, as the sample exposed to a 3 MHz insonation in the absence of catalase produced lower than normal permeabilisation for

these conditions the observed catalase induced increase in the number of cells with reduced membrane integrity is likely to be marginal. The sham, unexposed sample remained approximately 10 % permeable throughout the experiment.

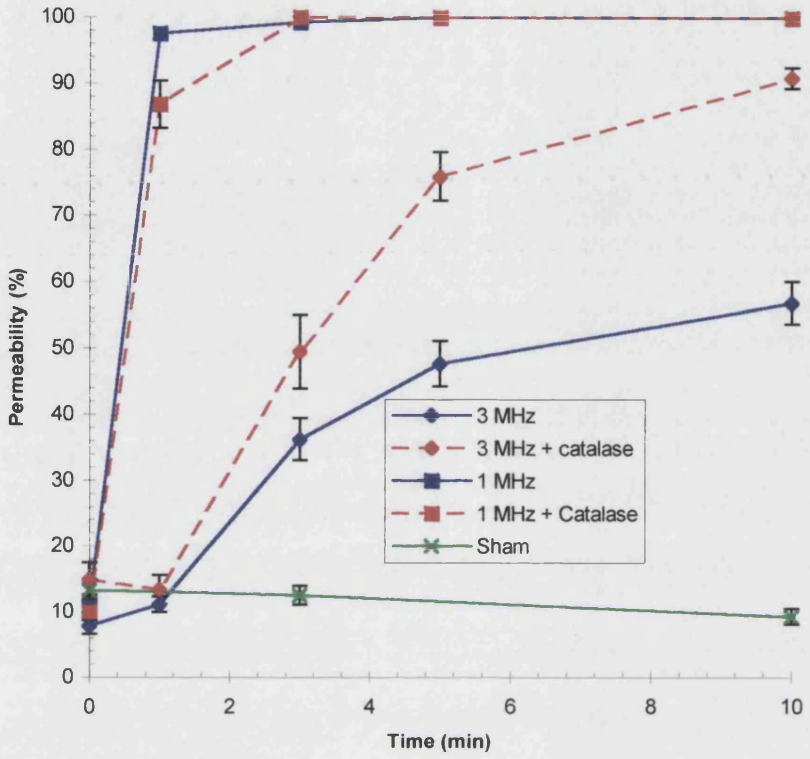

Figure 5.8(c): L1210 permeability to trypan blue during insonation at 3 or 1 MHz, 1.0 Wcm^{-2}, CW in the presence of 1000 IU/ml catalase.

Cells were exposed to either 3 MHz or 1 MHz, 1.0 Wcm^{-2} ultrasound in the presence/absence of 1000 IU/ml catalase and the mean percentage of cells permeable to trypan blue was calculated. The error bars describe the standard error of the mean.

It is clear that catalase either at 100 IU/ml (5.9) or 1000 IU/ml did not provide protection from the kind of cell damage observed within this chapter. This does not, however, rule out the effects of other sonochemicals or the much shorter lived free radicals produced by insonations as described in detail in 1.2.

5.11 Effect of 50 IU/ml SOD and/or 1000 IU/ml catalase during L1210 cell exposure to 3 or 1 MHz, 1.0 Wcm^{-2}, CW ultrasound

In 1.2.3 the production of the short lived, but highly reactive free radicals by insonation was described. This short life span makes them rather difficult to study. The superoxide dismutases (SOD) are a family of metalloenzymes which catalyse the dismutation of the superoxide free radical anion to hydrogen peroxide and oxygen.

$$2O_2^{-}\bullet + 2H^{+} \longrightarrow H_2O_2 + O_2$$

Three isoenzymes of SOD are known to occur in man, within cells copper-zinc SOD is found in the cytoplasm and manganese SOD is located in the cellular matrix, while the major extracellular isoenzyme is a copper and zinc containing enzyme.

In order to study the possibility that production of free radicals may be responsible for the ultrasound induced effects on cells described in the previous sections an excess of SOD (50 IU/ml) was added to the cell suspensions. SOD was investigated both alone and in the presence of 1000 IU/ml catalase. In the cases where both antioxidants were present, any superoxide present would be initially dismutated to H_2O_2 and then to water and oxygen. Ultrasound exposures were carried out as described in section 5.2 and SOD from bovine erythrocytes was obtained from Sigma-Aldrich Co. Ltd. and diluted in growth medium.

Figure 5.9(a) illustrates the effect of both antioxidants on the rise in temperature of the bulk medium during insonation. It is clear from these results that the addition of both SOD and catalase either individually or simultaneously did not have an effect on the ultrasonically induced temperatures at either frequency.

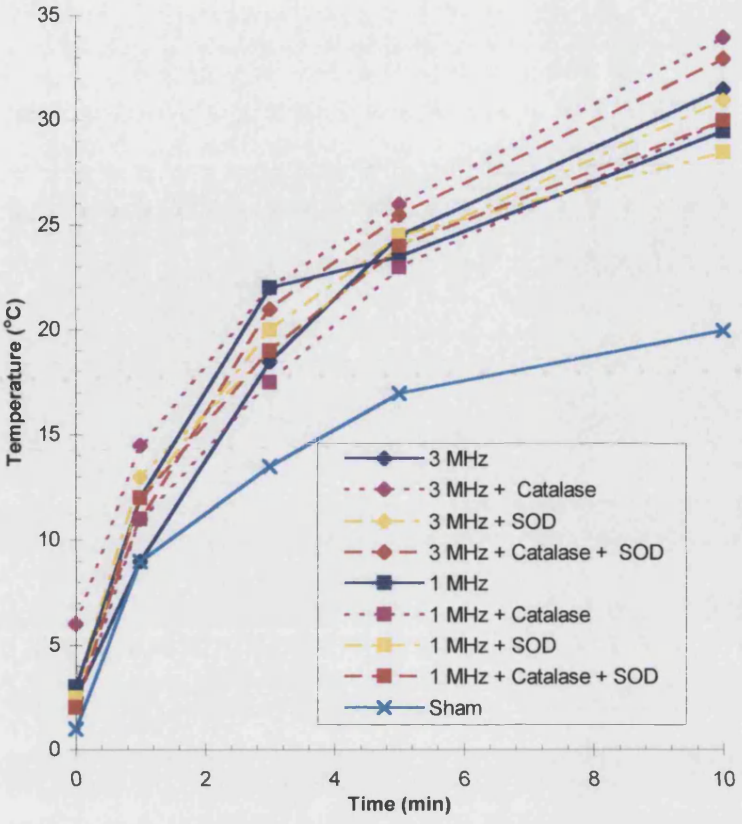

Figure 5.9(a):Temperature rise of bulk medium during insonation of L1210 cells at 3 or 1 MHz, 1.0 Wcm^{-2}, CW in the presence of 50 IU/ml SOD and/or 1000 IU/ml catalase.

Cells were exposed to either 3 MHz or 1 MHz, 1.0 Wcm^{-2} ultrasound in the presence/absence of 50 IU/ml SOD and/or 1000 IU/ml catalase and the temperature of the bulk medium was observed by thermometer. A sham exposure was also performed.

The cell number/ml was also unaffected by the addition of SOD and catalase as is clearly depicted in figure 5.9(b).

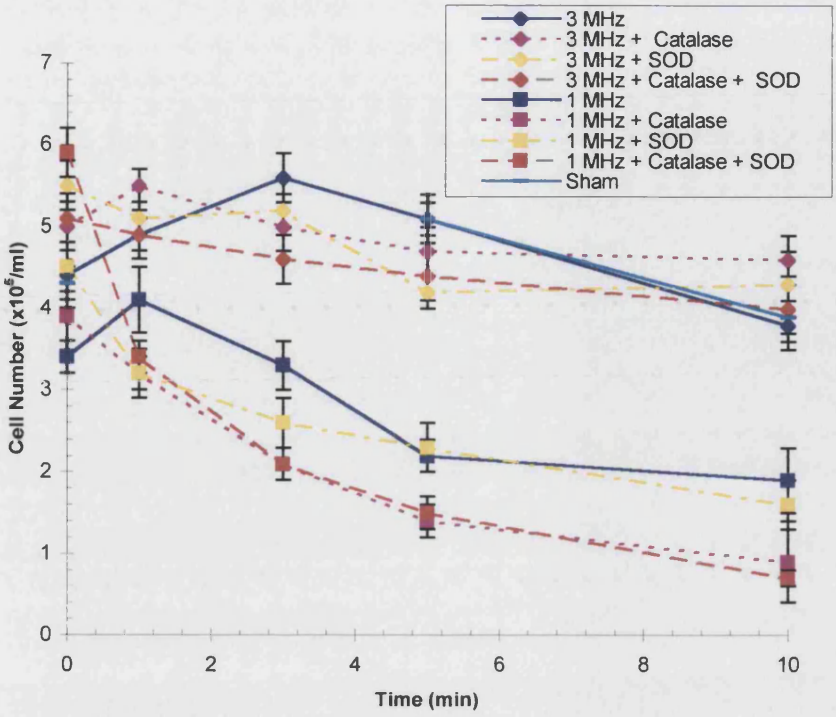

Figure 5.9(b): Cell numbers during insonation of L1210 cells at 3 or 1 MHz, 1.0 Wcm^{-2}, CW in the presence of 50 IU/ml SOD and/or 1000 IU/ml catalase.

Cells were exposed to either 3 MHz or 1 MHz, 1.0 Wcm^{-2} ultrasound in the presence/absence of 50 IU/ml SOD and/or 1000 IU/ml catalase and the mean cell number/ml was calculated. The error bars describe the standard error of the mean.

The determination of the percentage of cells permeable to trypan blue during ultrasonic exposure produced slightly higher proportions of permeable cells than usually observed (Figure 5.9(c)), as the incubation in the presence of the vital stain was somewhat lengthier than normal. This is clear when looking at the sham exposed cells, which were approximately 20 % permeable in this experiment as compared with 10-12 % permeabilities normally witnessed. The initial values prior to insonation in the remaining samples were also slightly higher than usual. Despite this, it is apparent that neither SOD nor catalase alone or in combination produced any cellular protection from the ultrasonically produced loss of membrane integrity.

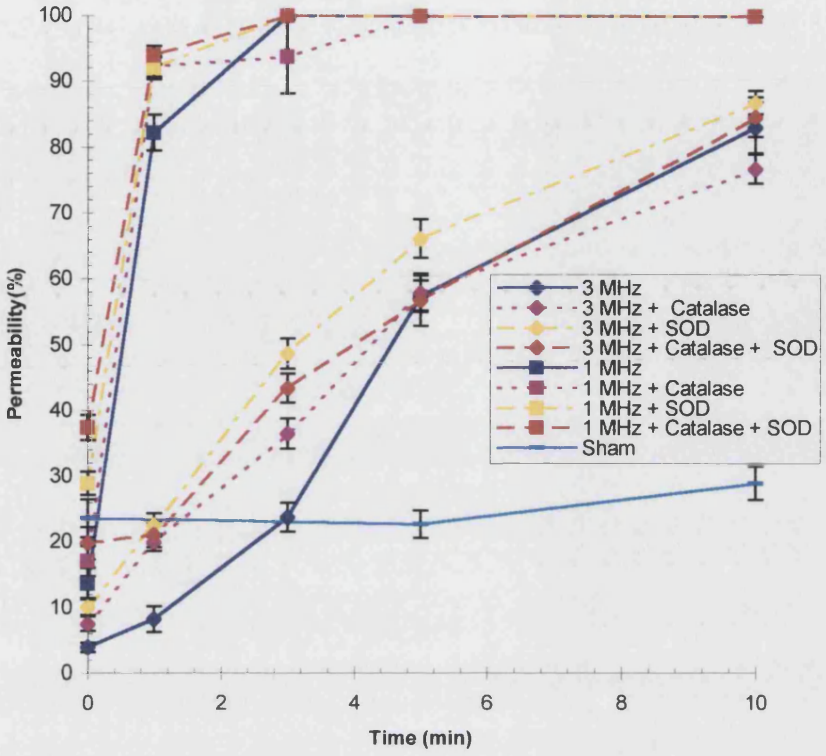

Figure 5.9(c): L1210 permeability to trypan blue during insonation at 3 or 1 MHz, 1.0 Wcm^{-2}, CW in the presence of 50 IU/ml SOD and/or 1000 IU/ml catalase.

Cells were exposed to either 3 MHz or 1 MHz, 1.0 Wcm^{-2} ultrasound in the presence/absence of 50 IU/ml and/or 1000 IU/ml catalase and the mean percentage of cells permeable to trypan blue was calculated. The error bars describe the standard error of the mean.

5.12 Capability of L1210 cells to reseal following insonation at 1 MHz, 1.0 Wcm^{-2}, CW for various durations

Previously, in this chapter, we have observed cellular damage in the form of both cell lysis and increased permeability of the plasma membrane to trypan blue, in response to ultrasonic exposure. Regarding the latter, it was of interest to ascertain whether L1210 cells were capable of resealing and thus regaining their membrane integrity to trypan blue.

Cells were set at a concentration of 5.5 +/- $0.4x10^5$ cells/ml and were 4.2 +/- 0.8 % permeable to trypan blue. The ultrasonic exposures were then conducted as detailed in section 5.2 at 1 MHz, 1.0 Wcm^{-2}, CW for 0, 15, 30 and 60 secs. Two flasks were exposed to each insonation. Cells were counted just prior to exposure at t=0 hrs and as soon as possible post-insonation at t=0.05 hrs, following which they were returned to the incubator and recounted at various intervals over a total period of 48 hrs.

Figure 5.10(a) depicts the total cell numbers as observed within the first six hours, where the most interesting results were likely to occur. Those samples which were not exposed to ultrasound, showed some cell growth after about 1 hr which remained relatively steady until 6 hrs. This was also the case for the samples insonated for 15 sec, while in the 30 sec sample results were harder to elucidate, but it seemed that by 6 hrs the cell numbers had picked up a little. Samples which had been insonated for 60 sec showed no growth after 6 hrs.

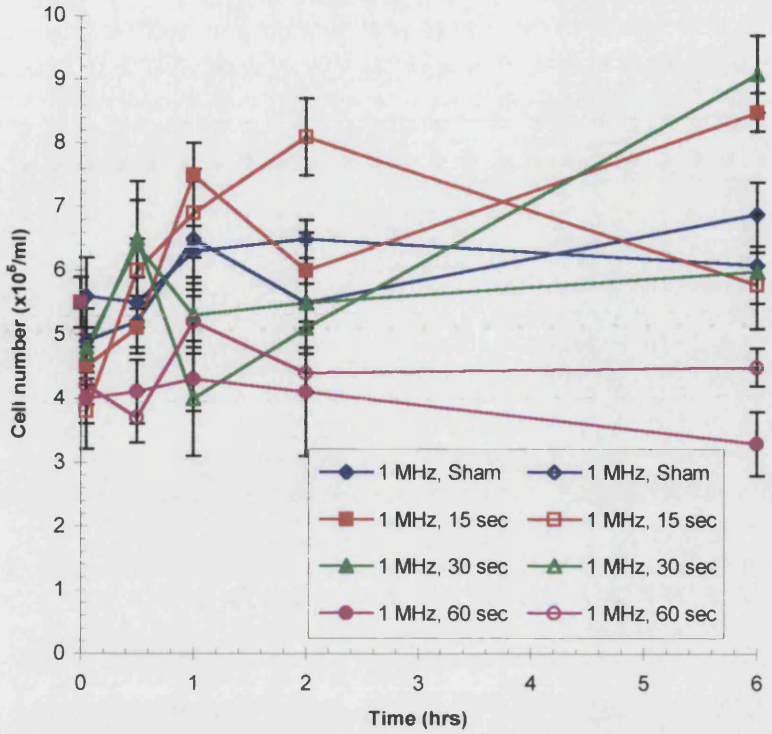

Figure 5.10(a): Cell numbers as counted post-insonation of L1210 at 1 MHz, 1.0 Wcm^{-2}, CW for various durations.

Cells were exposed to 1 MHz, 1.0 Wcm^{-2}, CW ultrasound for 15, 30, 60 sec or were sham insonated and subsequently returned to incubator conditions. The mean cell number/ml was calculated and error bars describe the standard error of the mean. Shaded shapes represent one flask exposed to a certain duration while open shapes represent a replicate. Samples up until 30 min were counted on 16 squares of a haemocytometer and 8 squares thereafter.

The permeability to trypan blue (Figure 5.10(b)) correlated well with the observed increases in cell numbers. In the sham exposed cells there was no change in the 6 % permeability of cells to trypan blue. The samples insonated for 15 sec showed a decrease in permeability after 30 min to 1 hr, around the time when cell numbers started to rise. However, in flasks which were insonated for 30 and 60 sec there was no decrease in permeability to trypan blue within the initial 6 hr period, despite an increase in cell numbers observed in the 30 sec samples.

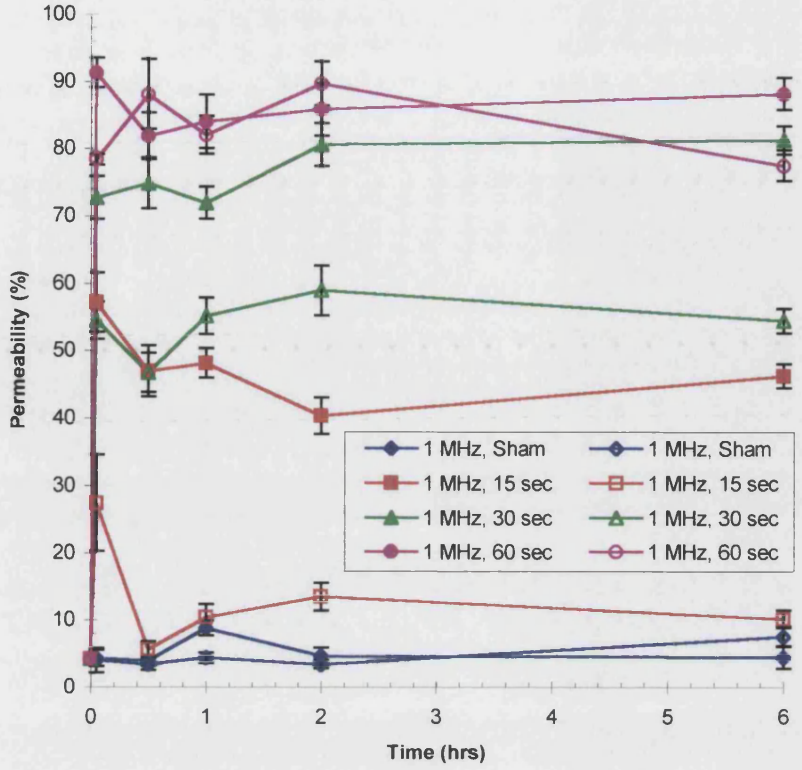

Figure 5.10(b): L1210 permeability to trypan blue post-insonation at 1 MHz, 1.0Wcm^{-2}, CW for various durations.

Cells were exposed to 1 MHz, 1.0 Wcm^{-2}, CW ultrasound for 15, 30, 60 sec or were sham insonated and subsequently returned to incubator conditions. The mean percentage of cells permeable to trypan blue was calculated and error bars describe the standard error of the mean. Shaded shapes represent one flask exposed to a certain duration while open shapes represent a replicate. Samples up until 30 min were counted on 16 squares of a haemocytometer and 8 squares thereafter.

The more long term rates of growth and permeability to trypan blue are shown in figures 5.11(a) and 5.11(b), respectively. It is clear that in all cases after 24 hrs cells were much less permeable to trypan blue and also growth started to take off.

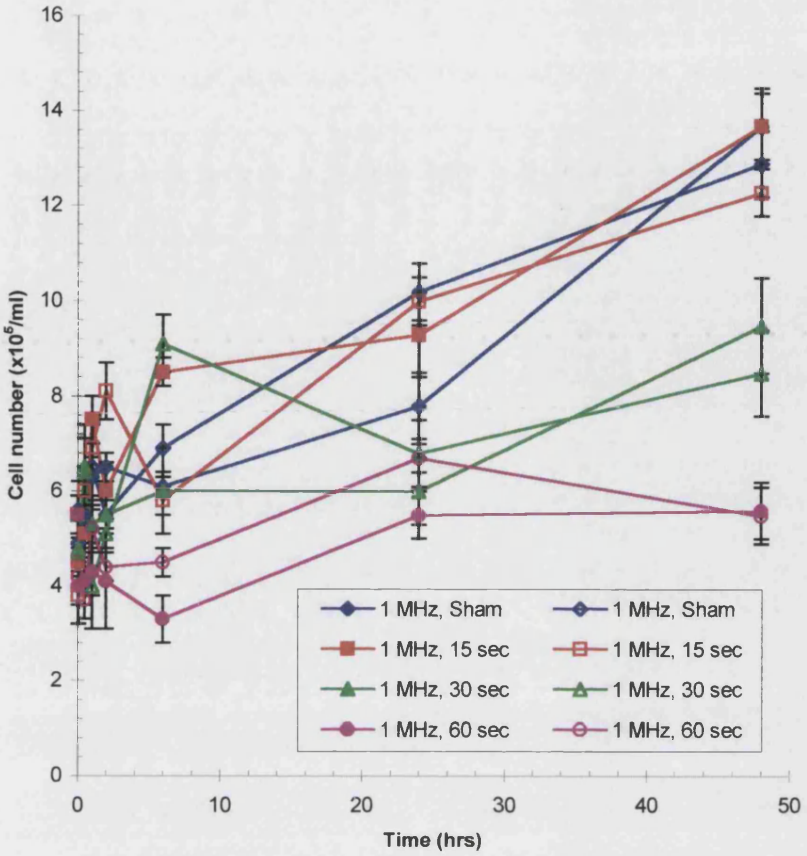

Figure 5.11(a): Cell numbers as counted post-insonation of L1210 at 1 MHz, 1.0 Wcm^{-2}, CW for various durations.

Cells were exposed to 1 MHz, 1.0 Wcm^{-2}, CW ultrasound for 15, 30, 60 sec or were sham insonated and subsequently returned to incubator conditions. The mean cell number/ml was calculated and error bars describe the standard error of the mean. Shaded shapes represent one flask exposed to a certain duration while open shapes represent a replicate. Samples up until 30 min were counted on 16 squares of a haemocytometer and 8 squares thereafter.

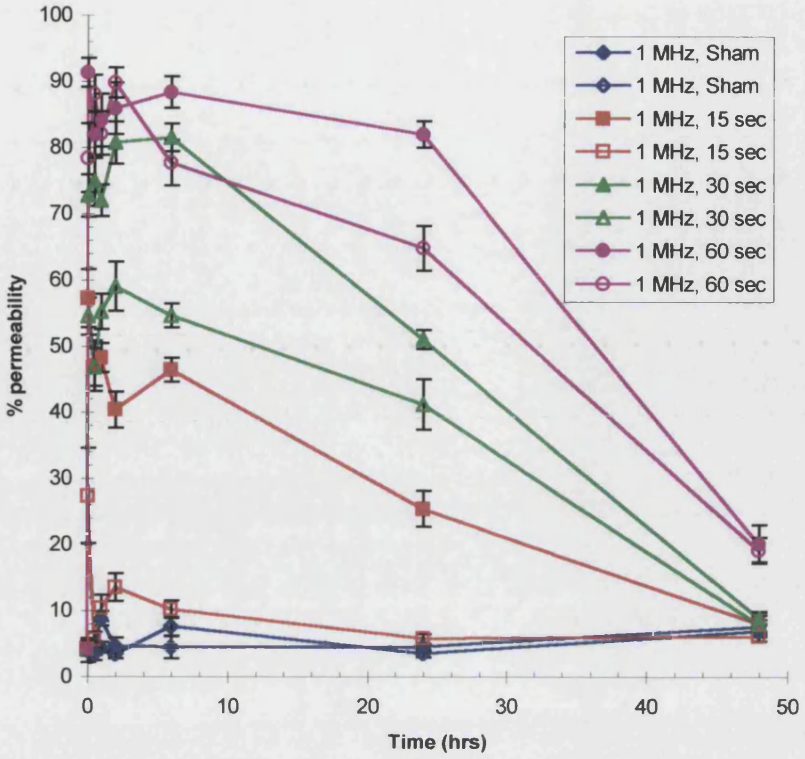

Figure 5.11(b): L1210 permeability to trypan blue post-insonation at 1 MHz, 1.0 Wcm^{-2}, CW for various durations.

Cells were exposed to 1 MHz, 1.0 Wcm^{-2}, CW ultrasound for 15, 30, 60 sec or were sham insonated and subsequently returned to incubator conditions. The mean percentage of cells permeable to trypan blue was calculated and error bars describe the standard error of the mean. Shaded shapes represent one flask exposed to a certain duration while open shapes represent a replicate. Samples up until 30 min were counted on 16 squares of a haemocytometer and 8 squares thereafter.

It was almost impossible to decipher if resealing is occurring or rather the viable cells are merely growing out and producing similar results. The likelihood is that healthy cells were taking over the culture, certainly after 24 hrs incubation. However, what was happening within the initial period following insonation is not so clear. It is plausible that a minority of cells were capable of resealing. Cells exposed to insonation were frequently returned to the incubator and counted after 12-24 hrs throughout this project, but there was never any clear evidence that resealing occurred. Despite the question of resealing being inconclusive, this experiment did

provide clear evidence that cells which appear viable following ultrasonic exposure can proliferate. This observation consolidates the work of other groups such as Kaufman and Miller (1978).

5.13 Discussion

Clearly insonation causes loss of membrane integrity within this exposure system. It has been shown that a number of parameters are important in the magnitude of this cellular damage including duration of exposure, intensity, frequency and to a lesser extent cell density. However, the mechanism by which ultrasound causes this cellular damage remains unclear. Observation of a sample under exposure leaves no doubt that cavitation is occurring and indeed the perturbations witnessed ensure that mechanical bioeffects must be taking place. It is apparent that the mechanism of damage is not thermal as the temperature rises induced by ultrasonic exposure did not exceed 37.5 °C. The likelihood is that a cavitational mechanism is involved since total damage is increased at lower frequency and higher intensity, both of which are known to reduce the cavitation threshold. Cavitation has been proposed as a mechanism for damage by a number of other groups using different cell and ultrasound models, as described in 5.1.

Results from sections 5.9, 5.10, 5.11 suggest that perturbations of the cellular plasma membrane seen here were unlikely to be the result of sonochemical or free radical induced effects. Infact, although most reports of membrane damage suggest cavitation as a mechanism of cell lysis, there are relatively few where sonochemicals are implicated, in the literature. Miller and Thomas (1993) described ways in which experimental systems can be altered to encourage either haemolytic or sonochemical effects of cavitation, but did not suggest that sonochemicals were responsible for the observed lysis. Indeed, under conditions where 100 % lysis occurred within 1 min only 10μM concentrations of H_2O_2 were produced even after 30 min exposure. For comparison, H_2O_2 is required in concentrations in the order 1 mM to produce cell killing and this is thought to be a result of DNA damage, not direct membrane disruption (Prise, Davis and Michael, 1989). Matthews *et al* (1993) did elucidate that inactivation of the erythrocyte ATPase pump was due to the production of free

radicals and sonochemicals following detection of H_2O_2 by fluorescence assay and abolition of the enzymatic inactivation in the presence of free radical scavengers. However, relatively low frequency ultrasound was used (36 kHz) and the results conflict with those of Fahnestock *et al* (1989) who examined neuroblastoma cell membranes in a physiologically viable state (5.1). In a later paper by Al-Karmi *et al* (1994), where calcium ions where shown to augment the ultrasonically induced increase in conductance in frog skin, it was suggested that calcium ions potentiate the effects of oxygen free radicals on the mitochondria and lipid peroxidation, although this was thought to occur in addition to membrane damage. The bulk of the literature describes either streaming effects which are distinct from cavitation or microstreaming during gas body activation as the mechanism for cell membrane damage or lysis (Dinno, Dyson and Young *et al*, 1989; Dinno, Crum and Wu, 1989; Salz, Rosenfield and Wussling, 1997; Young and Dyson, 1990; Brayman, Church and Miller, 1996; Pohl, Antonenko, and Rosenfeld, 1993; Pohl *et al*, 1995 and Mortimer and Dyson, 1988), the results described within this chapter are consistent with this. The hypothesis proposed here is that lysis itself is produced by mechanical mechanisms or by the physical effects of inertial cavitation, while increased membrane permeability is caused by acoustic streaming, gas body activational microstreaming or alterations in the thickness of the unstirred layer close to the cell plasma membrane.

CHAPTER SIX

INVESTIGATION OF PLASMA MEMBRANE INTEGRITY FOLLOWING INSONATION USING TRANSFECTION AS AN ANALYTICAL PROBE

6.1 Introduction

In recent years, there have been reports that ultrasound facilitates gene transfection both in plant (Joersbo and Brunstedt, 1990; 1992) and mammalian cell lines (Kim *et al*, 1996; Bao, Thrall and Miller, 1997), although in plant cells very low frequencies were employed. This documented enhancement of cellular transfection implies that plasma membranes can indeed be perturbed ultrasonically as clearly DNA must traverse the cell membrane in order to reach the nucleus. This phenomenon has the potential to provide a very elegant marker for the occurrence of membrane alterations under differing ultrasonic and experimental conditions and was therefore further investigated.

In the first instance, it was not terribly important either which cell line was transfected or indeed which piece of DNA was used to perform that transfection. However, it was important that those cells which had been transfected could be quickly and accurately identified. With this in mind, three leukemic cell lines were used. K562 and U937 are human in origin, while 32Dp210 is murine, further details of the cellular characteristics are provided in section 6.2. The plasmid employed during the transfections was pTR-UF/UF1/UF2 which included a region coding for green fluorescent protein (GFP), enabling easy detection of transiently transfected cells by their fluorescence using a fluorescence-activated cell-sorting (FACS) machine. The plasmid also conferred resistance to geneticin (G418) and allowed stable transfections

to be detected by selection with this antibiotic, with the exception of 32Dp210 cells which were resistant to geneticin.

6.2 Methods

6.2.1 Cell Lines

K562 cells

This is a human caucasian chronic myelogenous leukaemia cell line (Andersson, Nilsson and Gahmberg, 1979). It is a continuous line and was established from pleural effusion of a 53 year old female with chronic myeloid leukaemia in terminal blast crisis. The cell population is highly undifferentiated and granulocytic. Cells have the morphology of lymphoblasts and were grown in the same media as the L1210 cell line (2.1.2).

U937 cells

This is a human caucasian histiocytic lymphoma cell line which was isolated from pleural effusion of a 37 year old caucasian male with diffuse histiocytic lymphoma (Sundstrom and Nilsson, 1976). These cells are unusual in that they still express many of the monocytic like characteristics of the original histiocytic cells. They are also grown in the same media as the L1210 cell line (2.1.2).

32Dp210 cells

This is a murine myeloid leukemic cell line which was derived from a non-leukemic myeloid cell line, 32Dc, by transformation with the chimaeric BCR/ABL oncogene (Matulonis, 1995), which can be detected in virtually all cases of chronic myelogenous leukaemia. Again the growth media was as used for L1210 cells (2.1.2).

6.2.2 Plasmid

The plasmid pTR-UF/UF1/UF2 was used in the transfection experiments and was obtained as a gift (Dr Towner, Guy's Medical School, London). This plasmid provided two important reporter genes; the first of these was green fluorescent

protein (GFP), a chemically synthesised version of the *A. victoria* cDNA and the second coded for resistance to the antibiotic geneticin (G418), an analogue of neomycin.

6.2.3 Insonation method

Experimental design was based on the work of Kim *et al* (1996) in which primary fibroblasts and chrondocytes were exposed to ultrasonic treatment in a 6 well tray format in the presence of plasmids containg *lac* Z and *neo* genes. Their findings were considered regarding such things as cell density (not important), temperature (no transfection occurred at room temperature) and plasmid degradation (occurred at approximately 1.5 Wcm^{-2}) in the experimental protocol.

For all cell lines, a total volume of 2 ml of cells at a concentration of 5 x 10^5 cells/ml were seeded per well in a six well plate (Corning-Costar Corp.) format. Cells were then allowed to settle in the incubator. Forty five min prior to the addition of plasmid DNA, the medium was removed and replaced with fresh serum free medium. Fifteen μg of plasmid was added to each well just before treatment with ultrasound commenced. The $5cm^2$ ultrasound probe was applied to the bottom of each well and a seal was formed using 'Aquasonic®' gel (4.2.2). Ultrasonic treatment was applied as a 1:4 pulse wave at 1 Wcm^{-2} and 1 MHz. In all of the cell lines one well was used to perform each of the following conditions :-

(i) No DNA, Sham.

(ii)DNA, Sham.

(iii)DNA, 5 sec of ultrasound treatment.

(iv)DNA, 10 sec of ultrasound treatment.

(v)DNA, 15 sec of ultrasound treatment.

6.2.4 Detection of transfected cells.

Following insonation, cultures were returned to the incubator. Medium was replaced with that which contained FCS the following day, although it may have been more beneficial if this had been done 2 hrs after insonation.

Transient transfection

At 24 hours post-insonation, a sample of cells was washed, pelleted and resuspended in Hank's balanced salt solution (Sigma-Aldrich, Ltd.) and analysed using a FACS machine, for the presence of GFP. This process was repeated at 48 hrs.

Stable transfection

In order to observe the number of stable transfections cells were selected over a period of 3 weeks in 500 μg/ml active geneticin (Life Technologies Inc.) and compared to control unselected non-transfected cells by FACS analysis. The selection procedure was only employed in the case of the K562 cell line.

6.3 Results

The results of FACS analysis at 24 hours post ultrasound application are shown in figure 6.1. In all cell lines, wild-type cells show a fluorescence of less than ten units with an approximate intensity of 20-30 units. Figure 6.1(d) shows an example of a successful transformation where there has been a population shift of the cells to the right due to the fluorescence produced by the presence of GFP. In the 32Dp210 cell line (Figure 6.1(a)), following a 15 sec ultrasound exposure, some fluorescent activity was observed in the region above 10 units, although this was of relatively low intensity. The proportion of cells in this region was around 3 % of the total population, indicating that some low-level transfection had occurred. Indeed looking at figure 6.1(a), it can be seen that there are small traces of fluorescence even after 5 sec of ultrasound treatment. U937 cells are notoriously difficult to transfect with this plasmid (personal communication with Dr D Darling, King's College Medical School, London.) and even after 15 sec of ultrasound treatment few or no transfections were observed on FACS analysis (Figure 6.1(b)). In K562 cells (Figure 6.1(c)), transfection began to occur after 5 sec treatment with ultrasound and by 15 sec about 5 % of the population showed fluorescence above 10 units.

(a) 32Dp210

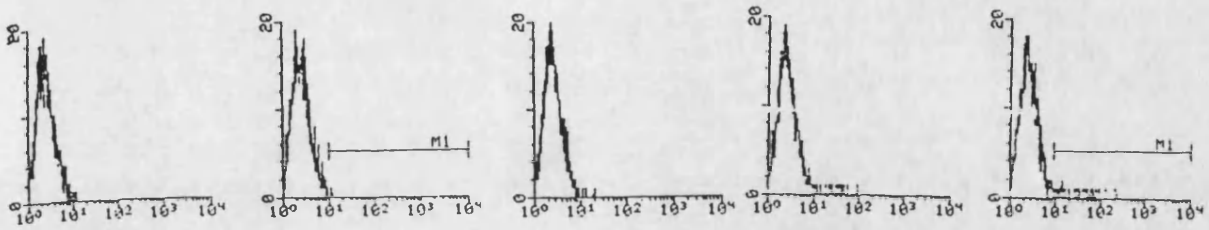

(i) No DNA/Sham (ii) DNA/Sham (iii) DNA/5sec (iv) DNA/10sec (v) DNA/15sec

(b) U937

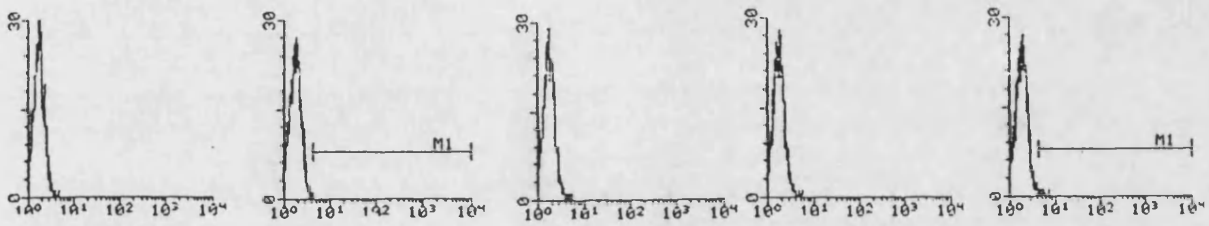

(i) No DNA/Sham (ii) DNA/Sham (iii) DNA/5sec (iv) DNA/10sec (v) DNA/15sec

(c) K562

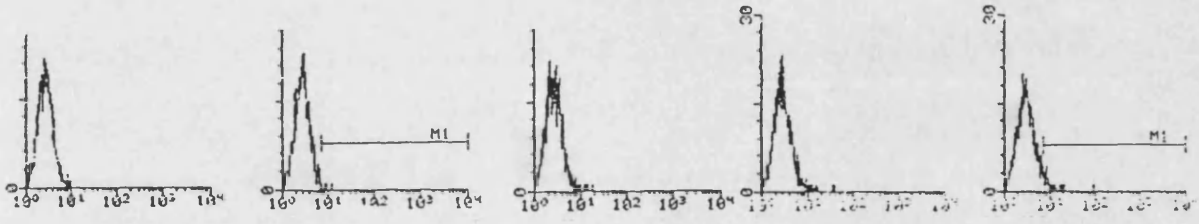

(i) No DNA/Sham (ii) DNA/Sham (iii) DNA/5sec (iv) DNA/10sec (v) DNA/15sec

(d) Example of good transfection

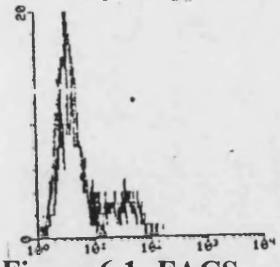

Figure 6.1: FACS analysis of cell populations 24 hrs post-insonation.

All cell lines (a)32Dp210, (b) U937, (c) K562 were observed by FACS in order to detect the presence of fluorescence due to GFP. In each line, cells had been subjected to the following conditions:- (i) No DNA/Sham, (ii) DNA/Sham, (iii) DNA/5 sec , (iv) DNA/10 sec, (v) DNA/15 sec. Ultrasound parameters were 1 MHz, 1 Wcm^{-2}, 1:4 pulsed wave using the 5 cm^2 transducer. 15 μg of plasmid DNA added to the well where appropriate. The percentage of the cell population in the areas marked as M1 was calculated using the FACS machine statistics package and the results are given in the text. An example of the FACS analysis of a successful transfection is given in (d).

Figure 6.2 depicts the results of FACS analysis 48 hrs after ultrasound exposure in 32Dp210 and K562. In 32Dp210 (Figure 6.2(a)), the sample exposed to 15 sec of ultrasound treatment produced a proportion of 5 % of the total population with fluorescence greater than 10 units. This value was slightly higher than that observed after 24 hrs. However, there appeared to be a 3-4 % background of control cells (no DNA, sham exposed or DNA but no ultrasound treatment). K562 (Figure 6.2(b)) cells exposed to ultrasound for 15 sec produced a 7 % proportion of the population with a fluorescence of greater than 10 units, which again was higher than that observed after 24 hrs. There was a background of 2-3 % of all cells in this region of the graph according to the negative controls.

(a) 32Dp210

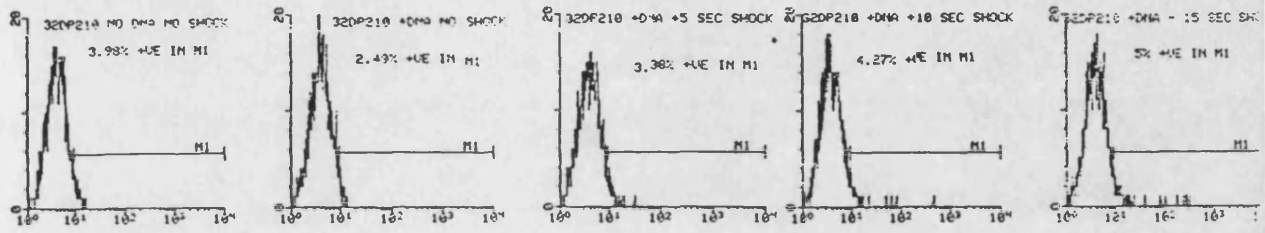

(i) No DNA/Sham (ii) DNA/Sham (iii) DNA/5sec (iv) DNA/10sec (v) DNA/15sec

(b) K562

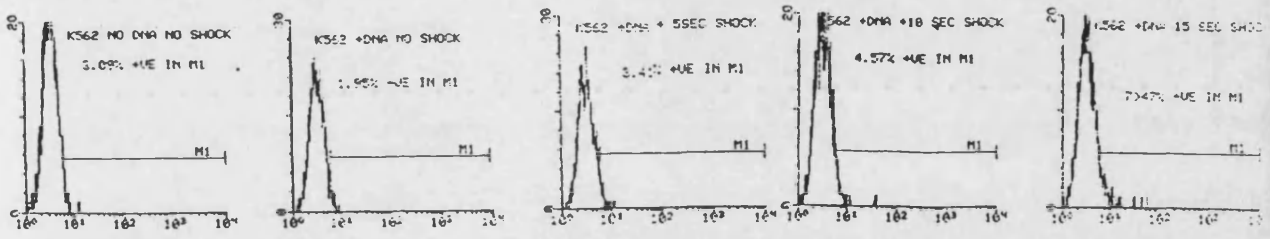

(i) No DNA/Sham (ii) DNA/Sham (iii) DNA/5sec (iv) DNA/10sec (v) DNA/15sec

Figure 6.2: FACS analysis of cell populations 48 hrs post-insonation.

The cells lines (a) 32Dp210 and (b) K562 in which there had been evidence of transfection 24 hours post-insonation were observed after 48 hours. In each line, cells had been subjected to the following conditions:- (i) No DNA/Sham, (ii) DNA/Sham, (iii) DNA/5 sec, (iv) DNA/10 sec, (v) DNA/15 sec. Ultrasound parameters were 1 MHz, 1 Wcm^{-2}, 1:4 pulsed wave using the 5 cm^2 transducer. 15 μg of plasmid DNA added to the well where appropriate. The percentage of the cell population in the areas marked as M1 was calculated using the FACS machine statistics package and the results are given in the text.

Insonation under these conditions produced transient transfection in both 32Dp210 and K562 which began to occur even after only 5 sec of ultrasound treatment. U937 were not transiently transfected using this method. The observed background of apparently transfected cells in the negative controls could be explained in those samples where plasmid DNA was present, but no ultrasound exposure was applied as, in each cell line, all samples were treated in the same 6 well plate and it is therefore possible that ultrasonic shock waves from neighbouring wells caused the observed transfections. Where there was neither DNA nor ultrasonic exposure the observed increase in fluorescence could not be explained.

K562 cells showed the highest rate of transient transfection and it was therefore decided they undergo selection with geneticin. Following three weeks of selection the cells which had been exposed to 15 sec of ultrasound, were again observed by FACS and compared to a control sample of un-selected, non-transfected K562 (Figure 6.3) The control sample consisted almost entirely of a population with a fluorescence of less than 10 units, while in the selected cells a 40 % proportion of cells that exhibited fluorescence of greater than 10 units. The lower panel shows an overlay of the control sample and the ultrasonically exposed sample, making the shift of the general population of cells to the right clearer. It is evident that exposure to ultrasound has produced stable transfection in these cells. It is, however, unclear why in a population of cells completely resistant to geneticin only 40 % expressed enough GFP to be positive on the FACS machine.

During selection it appeared that the resistant population took over the culture much more quickly than would be expected during electroporation using the same plasmid (un-controlled experiment, personal communication with Dr D. Darling, King's College Medical School, London.) This would suggest that the rate of integration is higher than that which would have been estimated from the FACS data.

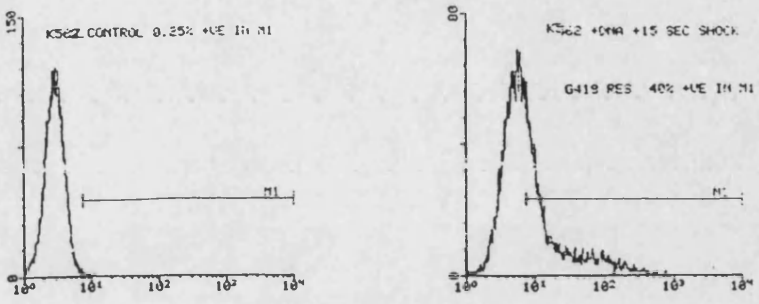

(a) Control un-selected, non-transfected K562 (b) Selected K562

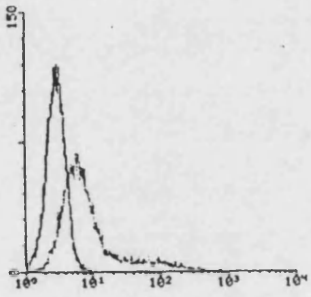

(c) Overlay of (a) + (b).

Figure 6.3: FACS analysis of K562 population following 3 weeks selection in geneticin.

K562 cells which had been exposed to 15 sec of ultrasound in the presence of plasmid DNA were selected in geneticin for 3 weeks and then analysed by FACS for the presence of GFP. Panel (a) shows a FACS scan of a population of un-selected, non-transfected K562, panel (b) shows a FACS scan of transfected and selected K562 and panel (c) shows a scan of (a) and (b) overlayed

6.4 Discussion

Clearly, ultrasound can induce stable transfection under these conditions, indicating that the cell membrane is at least transiently perturbed. Furthermore, ultrasonic transfections appear to be as efficient, if not more efficient, than those we would expect to see using electroporation.

Since the completion of this work, a number of other groups have published similar findings, which despite using wide-ranging conditions and set-ups are nonetheless useful in elucidating the mechanisms by which ultrasonic energy can be used to induce cellular transfection. Indeed, recently experimental modifications have shown ultrasound to be a highly efficient method of cellular transfection (Greenleaf *et al*, 1998).

In the system used within this project, U937 cells did not become transfected, which was not an unexpected result in view of the fact that they are known to be difficult to transfect by other mechanisms. However, it has been suggested that ultrasound may greatly enhance gene expression in 'hard-to-transfect' cells (Unger, M^{c}Creery and Sweitzer, 1997). It is possible, therefore, that optimisation of the system may lead to successful transfection in U937 cells.

During the transient transfections of both K562 and 32Dp210 cells, the control cells which were not exposed to either ultrasound treatment or plasmid produced a 2-3 % background fluorescence which could not be explained. A similar phenomenon was observed by Miller's group (Miller, Bao and Morris, 1999) during sonoporation of Chinese hamster ovary cells in the presence of fluorescent dextran, whereby a low background fluorescence was observed by FACS but not by haemocytometer in conjunction with a fluorescent microscope, in sham exposed cells. They speculated that a low incidence of multiple-cell droplets may have lead to an 'autofluorescence' of greater than the cut-off. It is elucidated that such a mechanism could be responsible for the background fluorescence observed here.

Bao, Thrall and Miller (1997) observed that transfection was improved in the presence of serum in the exposure media during insonation of Chinese hamster ovary cells. Indeed a number of other groups have included serum in the media during insonation (Unger, M^{c}Creery and Sweitzer, 1997; Tata, Dunn and Tindall, 1997; Miller, Bao and Morris, 1999). The increased rate of transfection is probably due, at least in part, to the protection that serum provides from cell lysis, despite the increased likelihood of free radical production (Edmonds and Sancier, 1983; 4.1). The addition of serum to the exposure media during insonation in the exposure system used in this chapter may therefore have improved transfection efficiency.

The amount of plasmid DNA added prior to sonication is also implicated in the efficiency of the transfection (Kim *et al*, 1996; Greenleaf *et al*, 1998). The relationship is linearly proportional initially but reaches a plateau. This implies that DNA reaches a saturation point thus transfection is dependent on ultrasound induced membrane permeabilisation (Greenleaf *et al*, 1998).

In all of the literature published within this area the proposed mechanism of action of ultrasound-mediated transfections is cavitation induced sonoporation and it is by encouraging such phenomena that the efficiency of transfection has been increased. Sonoporation has been observed to occur at intensities lower than those required to produce H_2O_2 (Bao, Thrall and Miller, 1997) implying that sonoporation, at least, is a product of the mechanical effects of cavitation such as microstreaming around bubbles and not sonochemical production. Initial reports of ultrasound induced transfection gave low transient transfection rates of 2.4 % (Kim *et al*, 1996) and 7 % (6.3) but, recently up to 50 % transfection has been described (Greenleaf *et al*, 1998).

Rotation of the exposure chamber is one way in which caviational activity and transfection efficiency have been increased (Bao, Thrall and Miller, 1997; Miller, Bao and Morris, 1999), but the addition of Albunex® microbubbles (Mallinckrodt Medical Inc., St Louis, U.S.A.) has been predominant (Bao, Thrall, Miller, 1997; Greenleaf *et al*, 1998, Miller, Bao and Morris, 1999). Albunex® is a commercially available ultrasound contrast agent consisting of human albumin that has been sonicated to produce a microbubble of gas encapsulated by an albumin shell. Albunex®

microbubbles have been shown to provide stable gas bodies that nucleate cavitation events (Miller and Thomas, 1995). Greenleaf's group used Albunex® (Greenleaf *et al*, 1998) to enhance ultrasound mediated gene transfection efficiency to a level twenty times greater than their previous work (Kim *et al*, 1996), on which the experimentation in the chapter is based. However, the use of GFP as a more sensitive marker system than the counting of β-galactosidase positive cells was at least in part responsible for this increased efficiency. Indeed, using the same experimental parameters but a different cell line produced a 15 % transfection rate when GFP was used as compared with only 2.4 % when β-galactosidase was employed as a detection method. It is interesting to note that the transient transfection rate seen in K562 cells in this chapter using GFP as the marker was 7 %. Sequential one second bursts of ultrasound in combination with fresh Albunex® microbubbles was most successful as a protocol for transfection during Greenleaf's work. This means that transfection, or at the very least, sonoporation is triggered by the destructive presence of the microbubbles. The generally accepted interpretation of such results is that at higher intensities microbubbles burst violently enough to cause cell permeabilisation and subsequent transfection while at lower intensities microbubbles rupture sedately and have a much lesser effect on the cell. Indeed, when Albunex® microbubbles were fluorescently tagged albumin protein from the shells was observed embedded in the cell membrane (Greenleaf *et al*, 1998).

The recent breakthroughs in the techniques used to transfect cells employing ultrasonic energy have far reaching implications. Modifications like those described above have meant that acoustically induced transfection has as high a performance as techniques such as lipofection. This, when coupled with the fact that the protocol is quick and easy since it can be performed through a cell culture flask or dishes, makes ultrasound mediated transfection a highly useful technique for *in vitro* cellular manipulations. The only drawback to the use of this technique is the relatively large amounts of DNA which are required due to its dispersal throughout the exposure media. This should not present a problem as DNA is relatively inexpensive.

Genetic therapy generally requires alteration of cells by transfection either *in vivo* or *ex vivo*. *Ex vivo* techniques usually involve harvesting a patients cells, culturing them,

transfecting them and then reimplanting them in the patient's body and hence techniques which cannot be performed *in vivo* are not generally employed. However, many malignant cells *in vivo* are extremely difficult to specifically target and this has provided a stumbling block for quick, easy and effective treatment to date. Greenleaf *et al* (1998) suggested that further enhancement of ultrasonic transfection methods could be achieved by the attachment of DNA to microbubbles which would allow effective transfection *in vivo* by the injection of these microbubble-DNA constructs into the blood stream and their subsequent activation by ultrasonic energy. However, similar techniques are already being employed by another group (Unger, M^{c}Creery and Sweitzer, 1997; ImaRx Pharmaceutrical Corp., 1997; M^{c}Creery *et al* 1998a+b).

Liposomes are synthetic lipid gene delivery particles which have been used to mediate transfection (Felgner and Ringbold, 1989) as they are relatively easy to manufacture and of lower toxicity than viruses. Unfortunately, gene expression using liposomes is usually less efficient than using viral vectors, however, ultrasound has been shown to enhance gene expression during conventional liposomal transfection in mammalian derived cell lines (Unger, M^{c}Creery and Sweitzer, 1997). Interestingly, the most effective time for the application of ultrasound was observed to be 60 min after the addition of the liposomes to the culture. Recently, ultrasound contrast-agents based on gas-filled phosolipid liposomes have been developed (Unger, M^{c}Creery and Sweitzer, 1997). Aerosomes® (ImaRx Pharmaceutical Corp. Tucson, U.S.A.) have similar properties to liposomes in that they can deliver foreign DNA, but are also ultrasonically active in the same way as microbubbles. They have the potential to be injected directly into the blood stream and allow DNA to be delivered directly to the target site by the application of ultrasound. They can also be tracked by ultrasound as they have contrast-agent properties. Aerosomes® have been used to successfully perform transfections in fish and mice and fluorinated compounds used for the gaseous core have been found to be particularly effective (ImaRx Pharmaceutrical Corp. 1997; M^{c}Creery *et al* 1998a). During investigative experimentation of these techniques it has also been observed that at 4 hrs incubation post-ultrasound treatment there is an upregulation of the expression of DNA repair genes as compared with control cells *in vitro*, despite an initial suppression of expression directly after insonation (M^{c}Creery *et al* 1998b). This upregulation continued at least as far as 48

hrs and may account for the high rates of integration that were seen in K562 cells here.

In conclusion, it is apparent that ultrasound mediated transfection has the potential to provide a very powerful non-invasive method of gene therapy. The results described within this chapter have clearly shown that membrane damage occurs during insonation under these conditions. It is without a doubt that, by optimising this technique, greater transfection efficiencies could have been achieved, though this was not pursued as cellular damage is the major focus of the project. It should be noted that the work within this chapter is one of the only clear descriptions of stable transfection by insonation in the literature.

CHAPTER SEVEN

POLY(ADP-RIBOSE) POLYMERASE ACTIVITY AS A METHOD OF ASSESSMENT OF DNA DAMAGE DUE TO INSONATION

7.1 Introduction

The literature on ultrasound-induced DNA damage provides disparate results (Miller, Miller and Brayman, 1996) making any clear conclusions difficult. However, amongst other contradictory work, a number of groups have reported detrimental ultrasonic effects on cellular DNA. Elevated sister chromatid exchanges have been observed in lymphocyte and lymphoblastoid cells (Martin *et al*, 1991), increased chromosomal aberrations and a loss of mitotic spindles have been seen in fibroblasts (De Deyne and Kirsch-Volders, 1995), while DNA in solution has been described to suffer base damage in response to ultrasound (Fuciarelli *et al*, 1995).

The most elegant work in this area has been produced by Miller's group during investigations of ultrasound-induced damage in Chinese hamster ovary cells. DNA strand breaks have been observed, primarily in nonviable cells (Miller, Thomas and Frazier, 1991a) following ultrasonic exposure. Strand breaks were also shown to be produced in viable cells by exposing them to medium which had been insonated for a prolonged period of time, without actually exposing the cells themselves (indirect exposure). This appeared to be an H_2O_2 mediated effect (Miller, Thomas and Frazier, 1991b). Later, using a very sensitive method of detection for single strand breaks, known as the comet assay (a single-cell electrophoresis technique), the same effect was observed in the few remaining viable cells, which survived direct insonation (Miller, Thomas and Buschbom, 1995). These cells were capable of repairing some of the strand breaks, an indication of their viability. This effect was associated with the

production of H_2O_2, but was not eliminated by catalase and hence the DNA damage was not due to H_2O_2 alone.

There have been a number of reports of increased rates of mutation in Chinese hamster V79 cells in response to ultrasound exposure (Kaufman, 1985; Doida *et al*, 1990; Doida, Brayman and Miller, 1992; Doida *et al*, 1998). Sonochemicals were confirmed as being responsible for this effect by Doida *et al* (1998) following indirect insonation of V79 cells. Increased mutation rates were also observed in mouse L5178Y cells (Doida *et al*, 1990).

It should be noted that many groups purposely induced cavitation by various methods to achieve these results, for example, by tube rotation (Fuciarelli *et al*, 1995; Miller, Thomas and Frazier, 1991a; Miller, Thomas and Frazier, 1991b; Doida *et al*, 1990; Doida, Brayman and Miller, 1992; Doida *et al*, 1998), the use of gaseous bubbling (Miller, Thomas and Buschbom, 1995) or the addition of Albunex® (Doida *et al*, 1998). Nonetheless, these observations are important and it was decided that possible DNA damage within our systems should be further investigated as such damage could lead to alterations of cellular properties in biofermentation and could have serious implications if they occur *in vivo*.

In most eukaryotes, one of the earliest cellular responses to DNA strand interruptions generated by DNA-damaging agents, is the induction of poly(adenosine diphosphate ribose) or poly(ADP-ribose) synthesis from nicotinamide adenine dinucleotide (NAD) in the cell nucleus (Figure 7.1). Poly(ADP-ribose) is a homopolymer which is made up of repeating units linked by (1"2') ribosyl ribose glycosidic bonds and is bound by covalent bonds to nuclear acceptor proteins. ADP-ribose polymers vary in complexity, chain lengths can range from 2-300 residues and several branching points are found within larger polymers (Althaus and Richer, 1987). The enzyme poly(ADP-ribose) polymerase (PARP) is responsible for the catalysis of the transfer of the ADP-ribose moiety from NAD to acceptor proteins such as topisomerase, histones or PARP itself and the subsequent elongation and branching reaction (Figure 7.1). Activation of PARP requires DNA containing either single- or double-strand breaks,

whereas covalently closed circular DNA or single-stranded DNA are ineffective (Benjamin and Gill, 1980).

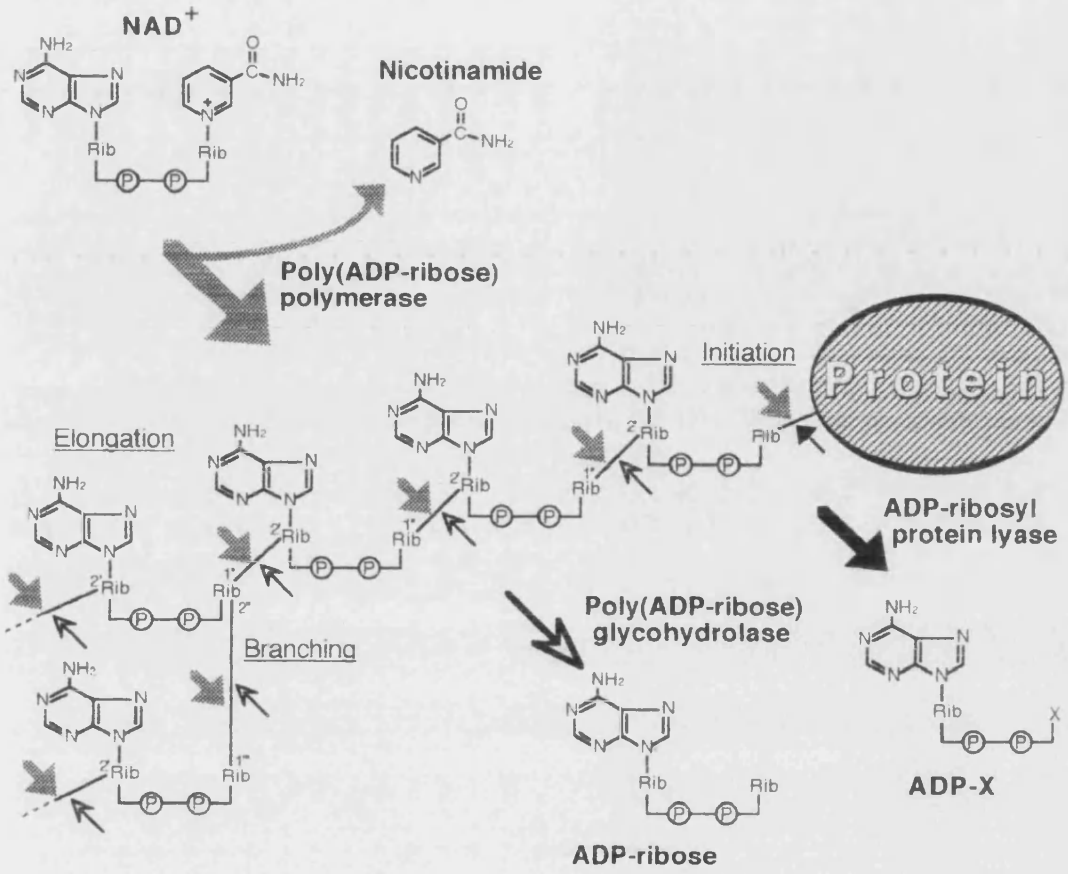

Figure 7.1: Structure of protein-bound poly(ADP-ribose).

Biosynthesis and degradation of poly(ADP-ribose): Poly(ADP) is synthesised from NAD by the enzyme poly(ADP-ribose) polymerase (PARP). Polymer degradation is catalysed *in vivo* by poly(ADP-ribose) glycohydrolase and protein lyase [adapted from Kappus (1997)].

Most acceptor proteins modified by ADP-ribose polymers transiently lose their normal function due to a large increase in their negative charge and PARP, which is the main acceptor protein, is no exception to this. Dramatic automodification means that PARP loses its ability to bind DNA strand breaks due to the electrostatic repulsion between poly(ADP-ribose) and DNA, exposing the damaged DNA to proteins involved in the repair process (Figure 7.2) (Le Rhun, Kirkland and Shah,

1998). Poly(ADP-ribose) is a short-lived polymer *in vivo* and chains synthesised in response to DNA damage are largely degraded within the space of 1-2 minutes (Alvarez-Gonzalez and Jacobson, 1987; Alvarez-Gonzalez and Althaus, 1989). This is due to the action of poly(ADP-ribose) glycohydrolase which is responsible for the degradation of the polymer (Figure 7.1), with the exception of the ADP-ribosyl residue most proximal to the protein which is removed by ribosyl protein lyase (Figure 7.1). The glycohydrolase acts slowly on short poly(ADP-ribose) chains (Hatakeyama *et al*, 1989) allowing some time during which repair can occur at DNA strand breaks before PARP is ready to re-attach to the lesion. Strand breaks induced by γ-ray irradiation produce long poly(ADP-ribose) chains. However, their degradation occurs well before DNA joining takes place. Lindahl *et al* (1995) have proposed that under normal conditions, poly(ADP-ribose) synthesis leads to rapid release of automodified PARP molecules from strand breaks allowing DNA repair enzymes to rejoin the break (Figure 7.2). However, if poly(ADP-ribosyl)ation is prevented, the release mechanism is abolished and persistently bound PARP prevents the repair enzymes from reaching the strand breaks.

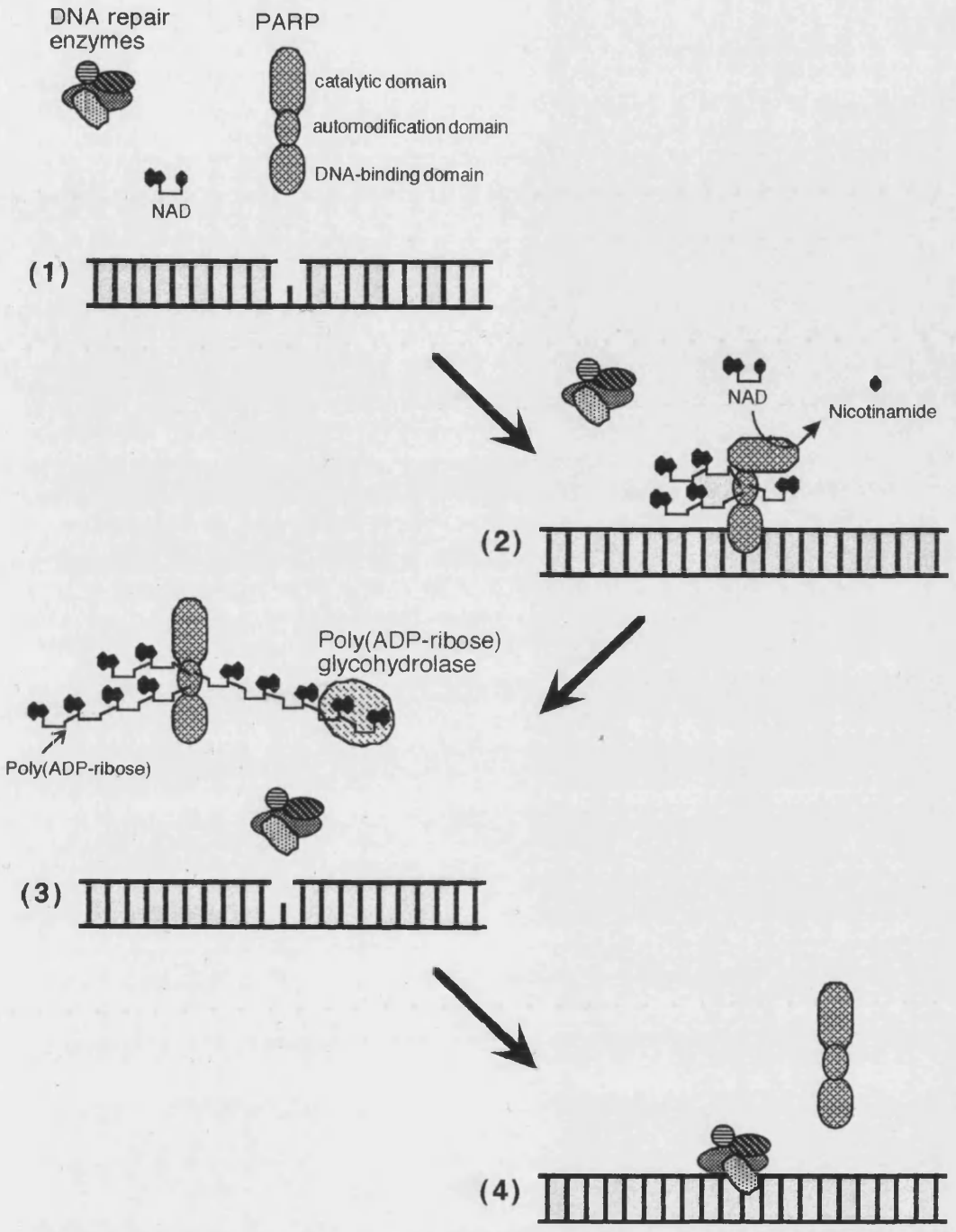

Figure 7.2: Model for the involvement of poly(ADP-ribose) formation in DNA repair.

(1) PARP competes with DNA repair enzymes for binding to DNA strand breaks. (2) Binding of PARP to DNA strand breaks inhibits DNA repair but activates the enzyme. (3) The automodified PARP has reduced affinity for DNA and is released. (4) DNA repair enzymes can complete DNA strand rejoining. (3+4) Degradation of poly(ADP-ribose) glycohydrolase returns PARP to its original form [Adapted from Kappus (1997)].

The structural and enzymatic properties of PARP are fairly well understood. It is a monomeric enzyme with a calculated molecular weight of 113.3 kDa (de Murcia, Menissier-de Murcia and Schreiber, 1991). The enzyme is found in all eukaryotic cells so far studied, except yeast, (Scovassi *et al*, 1986) and there are approximately one million copies present in the mammalian cell nucleus (Yamanaka *et al*, 1988). Following limited proteolysis three functional domains have been identified in the enzyme molecule (Kameshita *et al*, 1984): a 46 kDa amino-terminal fragment including the DNA binding domain; a central 22 kDa polypeptide containing the automodification sites; and a carboxy-terminal fragment of 54 kDa bearing the NAD-binding domain (Figure 7.2). At the amino acid level, PARP is a highly conserved protein; the overall conservation is 62 % when only the vertebrate sequence is considered or 32 % when the *Drosophila* sequence is included (De-Murcia *et al*, 1994).

PARP produces poly(ADP-ribose) by employing NAD as a precursor and liberating the nicotinamide moiety in this unusual reaction (Figure 7.1). Nicotinamide itself has been shown to be an inhibitor of this reaction (Preiss, Schlaeger and Hilz, 1971). Infact, the most frequently employed competitive inhibitors of PARP are structural analogues of nicotinamide, such as benzamide and its derivatives (Althaus and Richter, 1987). These inhibitors of PARP have been used to study the biological function of poly(ADP-ribosylation) (Lindahl *et al*, 1995). Indeed, nicotinamide will be utilised within this chapter.

Over the past twenty years, PARP has been implicated in a number of different cellular responses to genotoxic damage, including cell survival, DNA transformation and cell death, although its exact contribution remains ill-defined (Le Rhun, Kirkland and Shan, 1998). A variety of experimental approaches have been used to understand the physiological role of poly(ADP-ribose) synthesis in response to DNA damage. These include, chemical inhibition of the catalytic activity of PARP, transdominant inhibition of PARP by over expression of its DNA binding domain, anti-sense PARP expression and cell lines with reduced or increased expression of PARP. This work has produced strong arguments in favour of PARP participating in a variety of DNA-related functions, including gene amplification, gene expression, cell-division,

differentiation, transformation and most interestingly DNA excision-repair (Le Rhun, Kirkland and Shan, 1998). More recently, the production of PARP knock out mice has clearly established the role of PARP in the maintenance of genomic integrity, but has produced other ambivalent results confirming that the precise role of PARP in the response to DNA cell damage remains elusive and requires further study (Le Rhun, Kirkland and Shan, 1998).

A full understanding of the exact role of PARP in the DNA repair process is not of vital importance for its utilisation as a tool to measure the extent of DNA damage produced in response to ultrasonic exposure. The fact that PARP activation precedes many other stress-responses such as DNA repair itself, activation of DNA-dependent protein kinase and induction of p53 (Le Rhun, Kirkland and Shan, 1998) married with the fact that its main structural features have been largely retained during evolution, despite the high energy cost of its metabolism (De-Murcia *et al*, 1994) imply that it has an very important function in the DNA repair process. Moreover, PARP's most important characteristic with regard to this work is the correlation between its activity and the number of strand breaks observed in a given piece of DNA (Ohgushi, Yoshihara and Kamiya, 1980; Benjamin, R.C. and Gill, 1980). It is, therefore, proposed that by following the activity of PARP using radio-labelled NAD the extent of DNA damage induced by insonation can be further investigated.

7.2 Hypotonic permeabilisation of L1210 cells

7.2.1 Background

The system employed to conduct the insonations in the first part of this chapter is shown in section 4.2.1. This set-up is relatively 'kind' to cells and does not produce cellular permeabilisation even after prolonged periods of exposure (data not shown). However, since intact cells are impermeable to NAD and PARP is a nuclear enzyme this means that cells must be gently permeabilised to allow PARP activity to be measured by the incorporation of radio-labelled NAD. Permeabilisation of cells following insonation was therefore carried out using a hypotonic shock method (Durkacz *et al*, 1980; Halldorsson, Gray and Shall, 1978), whereby there is a rapid influx of fluid into the cell through the plasma membrane causing it to loose its integrity.

7.2.2 Buffers

All chemicals were obtained from Sigma-Aldrich Ltd. (Irvine, U.K.).

Pucks Saline pH 7.4

5.4 mM KH_2PO_4, 4.2 mM $NaHCO_3$, 137 mM NaCl, 5.5 mM glucose.

Hypotonic Buffer pH 7.8

9 mM hepes (N-(2-hydroxyethyl)piperazine-N'-(2-ethanesulfonic acid)), 4.5 %(w/v) dextran (approximate MWt 150,000), 1 mM EGTA (ethylene glycol-bis(oxyethylenenitrilo)tetraacetic acid), 4.5 mM $MgCl_2$, 5 mM DTT (dithiotreitol).

Isotonic Buffer pH 8

40 mM hepes, 130 mM KCl, 4.0 %(w/v) dextran, 225 mM sucrose, 2 mM EGTA, 2.3 mM $MgCl_2$, 2.5 mM DTT.

DTT was added to buffers just prior to use from a 100 mM stock stored at -20 °C.

7.2.3 Method

A 10 ml sample of L1210 cells, at a density of approximately $2x10^6$ cells/ml, was dispensed into a round bottom corex tube and allowed to cool on ice. Cells were then spun in a benchtop centrifuge at 1500 rpm for 3 min. The supernatant was discarded and the cells were gently resuspended in 10 ml of Pucks saline, before being respun as previously described. The supernatant was again discarded and the cells were resuspended in 1 ml of hypotonic buffer for 30 min. This was determined as the optimal incubation time in hypotonic buffer by prior experimentation (7.2.4). Finally, 9 ml of isotonic buffer was added and the cells were counted in the presence of trypan blue in order to ascertain the percentage of cells permeabilised.

7.2.4 Optimisation of procedure

The protocol described (7.2.3) was optimised from the original (Durkacz *et al*, 1980; Halldorsson, Gray and Shall, 1978). To achieve this, three experiments were conducted where the behaviour of cells over a prolonged period of time in hypotonic buffer was observed. At ten minute intervals the cell number was counted and the percentage of cells which had become permeable was assessed by trypan blue exclusion (Figure 7.3). Control cells experienced the same experimental protocol, but were treated with PBS only. The upper panel in figure 7.3 shows that control cells were consistently less than 15 % permeable, while the sample cells were significantly permeabilised (at least 55 %) even after the first 10 min of exposure to hypotonic buffer. Maximal permeabilisation had taken place after 20 min and thereafter the graphs plateau. It is of note, that the levels of maximal permeabilisation varied depending on the experiment. Indeed, permeabilisations cannot be compared between one experiment and another. The lower panel in figure 7.3 shows that total cell numbers remained relatively stable throughout the experiment, although they began to tail off towards the end of the time course. In view of these results, it was decided

that a 30 min exposure to hypotonic buffer should be employed since this allowed maximal permeabilisation, but did not produce a reduction in total cell number.

The dextran content of the hypotonic buffer was also investigated. At 3 %(w/v) and below cells became faint and undefined, therefore it was concluded that 4.5 %(w/v) dextran was appropriate in this procedure.

This permeabilisation procedure is perceived as a relatively gentle method and has been specially selected to avoid inducing PARP activity, although inevitably some is induced. It has also been designed to prevent resealing as this would interfere with the PARP assay. Cell resealing did not occur within the duration of a PARP assay, indeed even if permeabilised cells were replaced in medium and returned to the incubator they did not reseal.

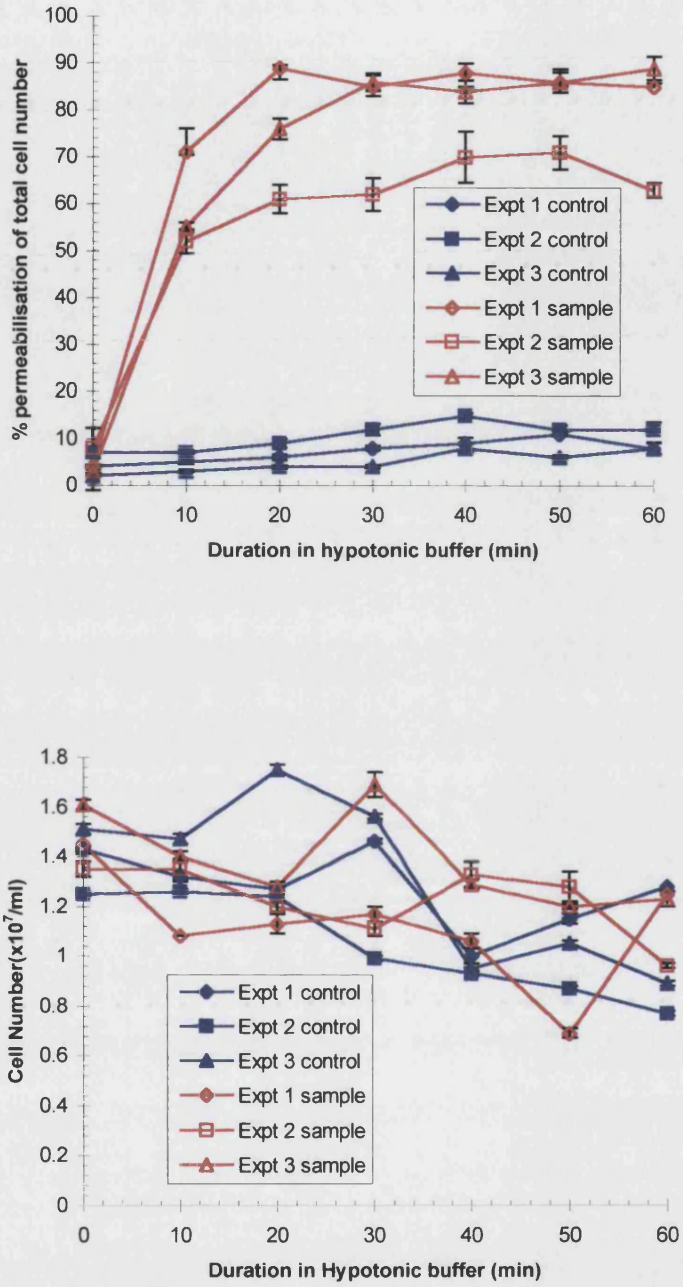

Figure 7.3: Investigation of cell permeability (upper panel) and total cell number (lower panel) with duration in hypotonic buffer.

Sample cells were allowed to cool on ice and then spun in a bench top centrifuge at 1500 rpm and resuspended in hypotonic buffer. At ten minutely intervals, cells were counted and assessed for permeability using trypan blue exclusion. Control cells were treated in an identical manner with the exception that they were resuspended in PBS. This was repeated on three occasions. The error bars describe the standard error of the mean.

7.2.5 Effect of insonation on permeabilisation procedure

There was a possibility that ultrasonic exposure could alter the sensitivity of the L1210 cells to the hypotonic procedure. In order to address this problem three experiments were carried out where a sample (10 ml of L1210 cells at $2.0x10^6$ cells/ml) was exposed to an insonation of 3 MHz, 1 Wcm^{-2} for a period of 30 min and then subjected to the permeabilisation protocol. The insonation apparatus was as depicted in 4.2.1, with the exception that it was suspended in a beaker at room temperature. A control which had not been exposed to ultrasound (sham) was also permeabilised in each experiment. In the final experiment, a further control was placed in the water bath at 37 °C. The total cell number and the percentage permeabilisation were observed during exposure to hypotonic buffer. Figure 7.4 depicts the results. The upper panel clearly shows that the total cell number remains steady in all samples throughout their time in hypotonic buffer. The lower panel shows the percentage permeabilisation of the samples. It appears that samples exposed to ultrasound may be slightly more susceptible to permeabilisation than the control samples. However, this effect is marginal even if it is real. The control sample exposed to hypotonic buffer following 30 min at 37 °C gave the most successful permeabilisation. In view of the overall results, that ultrasonic exposure does not hugely affect permeabilisation, although, the process is more efficient at 37 °C, it was decided that all insonations would be carried out in the water bath as described in 4.2.1. This had the added advantage that cells would remain in, close to, physiological conditions during ultrasound exposure.

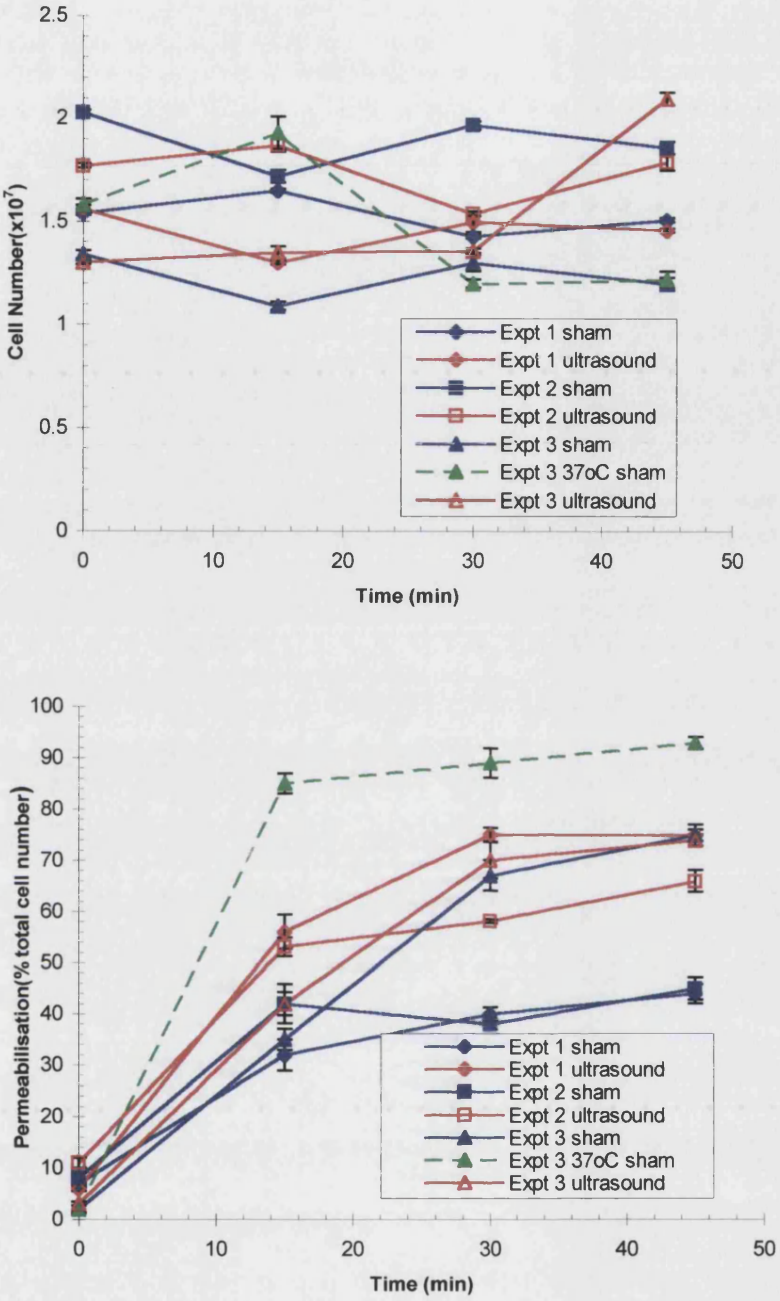

Figure 7.4: The effect of ultrasonic exposure of L1210 cells on subsequent hypotonic shock permeabilisation.

Ultrasound samples were exposed to 3 MHz, 1 Wcm^{-2}, CW insonation for 30 min before being subjected to the permeabilisation procedure. Control (sham) samples were not insonated. All samples were treated at 25 °C with the exception of one control sample which was placed in a water bath for 30 min at 37 °C. The upper panel depicts the total cell numbers in each sample with their duration in hypotonic buffer while the lower panel shows the progression of cell permeabilisation with time in hypotonic buffer. The error bars represent the standard error of the mean.

7.3 Poly(ADP-ribose) polymerase activity assay

7.3.1 Adenosine-[^{3}H]NAD

Adenosine-[^{3}H]NAD (1 mCi/μmol) was synthesised by Dr W.J.D. Whish of the University of Bath using [^{3}H]ATP (Amersham International, Buckinghamshire, UK.) and employing the method of Ohtsu and Nishizuka (1971). This stock solution was diluted 1:10 in 95 %(v/v) ethanol. The stock solution was prepared in June 1989 and the calculated activity of the diluted solution at the time when this experimentation was conducted was 66-68 μCi/ml or 16 mCi/μmole.
In later assays, commercial [^{3}H]NAD (ICN, Oxfordshire,UK.) was used. The stock solution had an activity of 1000 μCi/ml, 30 mCi/μmole which was diluted 1:10 in 50%(v/v) ethanol to give a final activity of 100 μCi/ml, 30 mCi/μmole.

7.3.2 Nicotinamide

A stock solution of 1 M nicotinamide (BDH, Poole, UK.) was stored at 4 °C and used as a competitive inhibitor of PARP.

7.3.3 PARP assay buffer

Isotonic Buffer
Permeabilised cells were simply assayed in the isotonic buffer described in the cell permeabilisation protocol (7.2.2).

7.3.4 PARP assay method

Each PARP assay was carried out in a water bath at 26 °C. Samples were incubated for 5 min to allow them to reach 26 °C. [^{3}H]NAD was added at time zero to start the reaction. At various time points (depending on the experiment) after the addition of [^{3}H]NAD, 50 μl of sample was removed and precipitated in 2 ml of 20 %(w/v)

trichloroacetic acid (TCA), on ice, overnight in the cold room. Normally, each assay involved seven time points and had a final volume of 400 µl, of which 8 µl was [^{3}H]NAD (6 µl were used to reduce cost when commercial [^{3}H]NAD was employed). In most cases the assay contained either 2.4 x10^5 cells or nuclei. In all cases the final radioactivity counts were given as CPM(counts per minute)/10^5 cells. The procedure was standardised using 3 x10^5 to 6 x10^5 cells in a final volume of 400 µl. The time-course of the [^{3}H] incorporation reaction was initially linear and depended on cell number.

It should be noted that during incubation in isotonic buffer the DNA of permeabilised cells can become further degraded and hence increase PARP activity (Halldorsson, Gray and Shall, 1978). However, in the experimentation described any increase in PARP activity due to incubation will be uniform between samples and will not therefore influence the final results.

In assays where nicotinamide was used as a PARP inhibitor, it was added five minutes prior to the addition of [^{3}H]NAD at a final concentration of 100 mM.

7.3.5 Evaluation of acid-insoluble radioactivity

Eighteen hours after the PARP assay was completed, each sample was deposited on a GF/C filter (Whatman, Maidstone, UK.) prewashed with 5 ml of cold 5 %(w/v) TCA. The filter was then washed three times with cold 5 %(w/v) TCA and then 6 ml of 95 %(v/v) ethanol and transferred to a scintillation vial (Packard Instrument Co., Meriden, CT., U.S.A.,). Filters were then dried at 80 °C for 30 min, allowed to cool and finally counted in 2ml of Optiphase (Fisons Chemicals Ltd., Loughborough, U.K.).

7.4 Poly(ADP-ribose) polymerase activity produced in response to 3 MHz, 1.0 Wcm^{-2}, CW ultrasound for 30 min

The nature of investigations into PARP activity dictated that although activities within an experiment were comparable it was impossible to compare data between experiments. This is illustrated in figure 7.5 and is largely due to differences in the cells themselves and the degree to which they were permeabilised. Figure 7.5 shows the results of two experiments which were performed in exactly the same manner, but on two separate occasions. The experimental procedure consisted of an insonation carried out at 3 MHz, 1.0 Wcm^{-2}, CW for 30 min at 37 °C in the case of the ultrasound sample and the same incubation but in the absence of ultrasound in the case of the sham sample. This was followed by permeabilisation by hypotonic shock (7.2) and a PARP activity assay (7.3). The only difference between the two protocols was the time points at which PARP activity was assessed by [^{3}H]NAD incorporation. Although both of these experiments show relatively similar trends, in that it is very difficult to differentiate between the sample exposed to ultrasound and the sample which was not as regards the PARP activity, the scales of the CPM/10^5 permeable cells are very different indicating that the total PARP activity varies greatly between experiments.

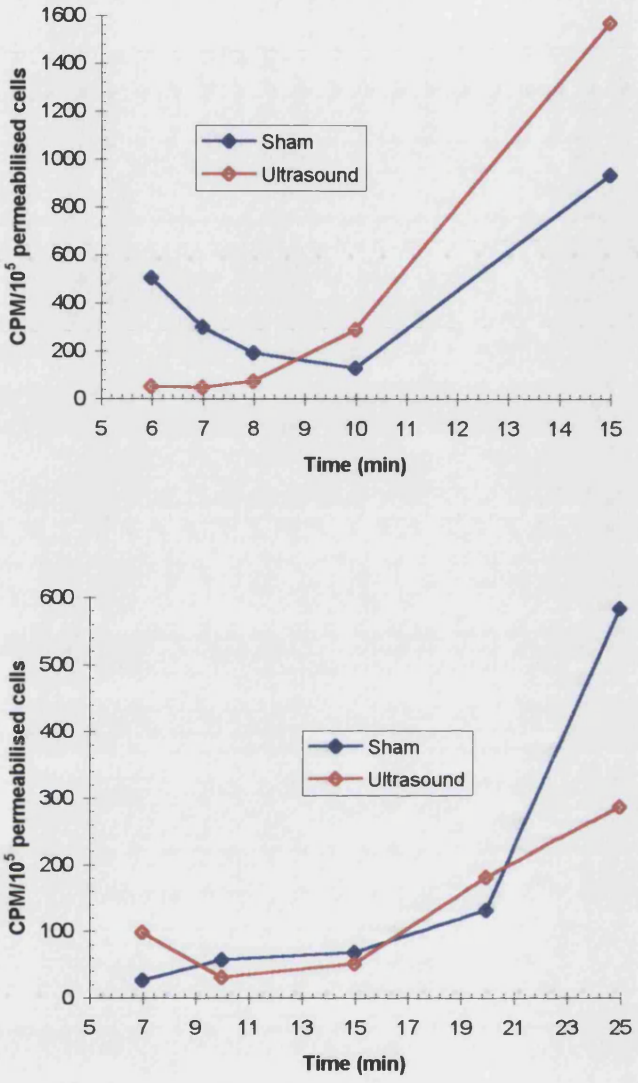

Figure 7.5: PARP activity as determined by [^{3}H]NAD incorporation in response to ultrasound exposure at 3 MHz, 1.0 Wcm^{-2}, CW for 30 min.

The panels depict the same experimental procedure carried out on two separate occasions. Both samples were placed in a water bath at 37 °C for 30 min. However, the sham sample was not exposed to ultrasound. Samples were then permeabilised using hypotonic shock and PARP activity was measured by following the incorporation of [^{3}H]NAD at 26 °C. The incorporation was assessed at 6, 7, 8, 9, 10 and 15 min in the upper panel and at 7, 10, 15, 20 and 25 min in the lower panel. Attention should be drawn to the differences in scale in this figure.

7.5 Extracted cell nuclei as a positive control for PARP activity in response to severe DNA damage

7.5.1 Background

The results described by figure 7.5 show that within this experimental system ultrasound exposure has little effect on PARP activity. However, it was considered prudent to confirm that detection of high PARP activity was possible using the assays described. In the past, extracted cell nuclei have been employed to assess PARP activity in response to DNA damage. However, the extraction process (7.5.2) itself causes a high background activity. In addition, sonication (ultrasonic waves at much lower frequency and higher intensity than insonation) is a well-known way to cause cellular DNA damage which in turn serves to increase PARP activity. It was therefore decided that extracted nuclei should be subjected to sonication in order to confirm that the experimental methods used here could detect high degrees of PARP activity.

7.5.2 Extraction of cell nuclei

All chemicals were obtained from Sigma-Aldrich Ltd. (Irvine, U.K.).

Buffer A (hypotonic cell wash buffer)
4 mM $MgCl_2$, 10 mM Tris-HCl pH 7.9, 0.3 mM EDTA (ethylendiamine tetraacetic acid), 0.02 %(v/v) β-mercaptoethanol, 1 mM $CaCl_2$.

Buffer B (homogenisation buffer)
0.32 M sucrose, 0.003 %(v/v) Triton N101, 1 mM $MgCl_2$, 10 mM Tris-HCl pH 6.8, 0.02 %(v/v) β-mercaptoethanol, 1 mM $CaCl_2$.

Buffer C (nuclei wash buffer)
4 mM KF, 60 mM KCl, 10 mM $MgCl_2$, 100 mM triethanolamine-HCl pH 8.2, 0.5 mM DTT.

In all cases $CaCl_2$, β-mercaptoethanol and DTT were added to the buffer just prior to its use.

Method

Cells were cooled on ice in 4 x 30 ml Corex tubes (approximately 2 $x10^6$ cells/ml) for 10-15 min and then centrifuged at 1500 rpm in a benchtop centrifuge. Each pellet was then gently resuspended in 5 ml of buffer A and the resultant cell solutions were transferred to two 15 ml Corex tubes. Cells were incubated on ice for 10 min and then respun at 1500 rpm for 10 min. Pellets were resuspended in 10 ml of buffer B and subjected to eight strokes of a teflon homogeniser, before another spin for 10 min at 1500 rpm. These pellets were resuspended in 10 ml of buffer C and respun for a final time at 1500 rpm for 10 min. The pelleted nuclei were then resuspended in a total volume of 200 µl of buffer C and counted using methylene blue.

7.5.3 Experimental Protocol

L1210 cells were either nuclei extracted (7.5.2) or were permeabilised by hypotonic shock (7.2). A sample of nuclei (200 µl) was then exposed to sonication on ice using a benchtop sonicator (Output Frequency 20 kHz, Amplitude 5 microns) for 10 sec. PARP activity assays were then carried out as in 7.3, which the exception that assay was carried out in the presence of 2x Assay Buffer (20 mM $MgCl_2$, 2 mM DTT, 200 mM TEA, pH 8.0) where nuclei were used. The number of nuclei used in each assay was exactly the same as the number of cells used (7.3).

7.5.4 Initial results

Figure 7.6 clearly depicts that PARP activity due to nuclear extraction alone is greater than that due to permeabilisation by hypotonic shock alone. Nuclei exposed to sonication showed a dramatic increase in PARP activity as measured by [^{3}H]NAD incorporation.

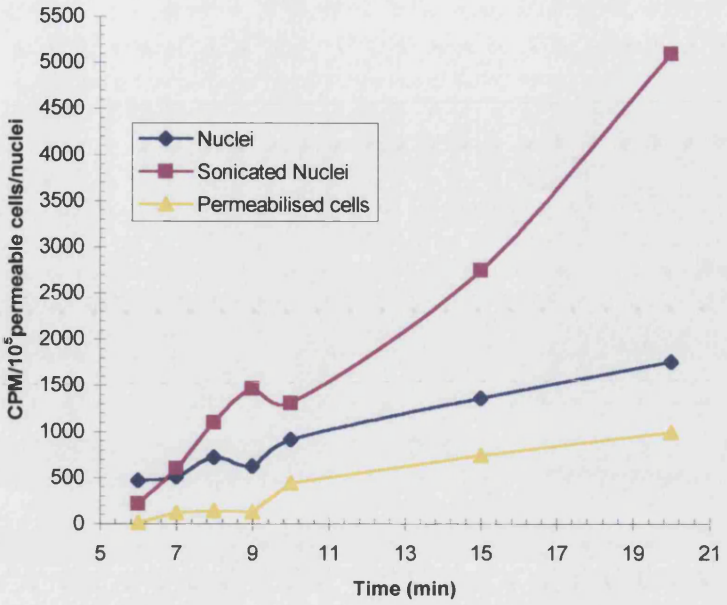

Figure 7.6: A comparison of PARP activity in untreated L1210 nuclei and permeabilised cells and nuclei exposed to sonication.

Nuclei were extracted from L1210 cells and the sample was divided into two parts. One part was exposed to sonication for 10 sec at an amplitude of 3 microns (sonicated nuclei), while the other part was left untreated (nuclei). L1210 cells from the same flask were permeabilised using hypotonic shock (permeabilised cells). [^{3}H]NAD incorporation assays were carried out to assay the PARP activity in all cases. Samples were taken at 6, 7, 8, 9, 10, 15 and 20 min.

7.5.5 Inhibition of induced PARP activity by nicotinamide

In order to ensure that the radioactivity detected in figure 7.6 was due to the incorporation of [^{3}H]NAD by PARP the experiment described in 7.5.3 was repeated, but 100 mM nicotinamide was added to each of the samples prior to the PARP assay (7.3). Figure 7.7 depicts the results of the addition of nicotinamide. It is clear that there was no detected radioactivity in the presence of PARP in any of the samples indicating that the observed activity was indeed due to the incorporation of [^{3}H]NAD by PARP. The ranking of the samples by PARP activity was identical to that seen in figure 7.6.

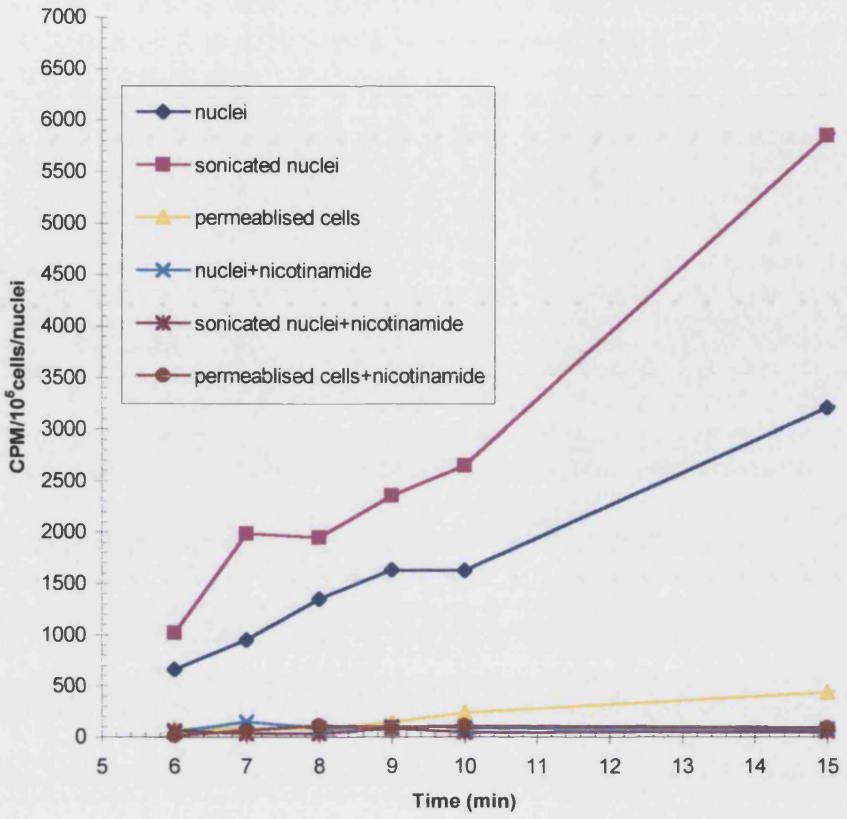

Figure 7.7: A comparison of PARP activity in untreated L1210 nuclei and permeabilised cells and nuclei exposed to sonication in the presence/absence of nicotinamide.

Nuclei were extracted from L1210 cells and the sample was divided into two parts. One part was exposed to sonication for ten sec at an amplitude of 3 microns (sonicated nuclei), while the other part was left untreated (nuclei). L1210 cells from the same flask were permeabilised using hypotonic shock (permeabilised cells). [^{3}H]NAD incorporation assays were carried out to assay the PARP activity in all cases. Samples were taken at 6, 7, 8, 9, 10, 15 and 20 min. PARP activity was also observed in all cases in the presence of 100 mM nicotinamide (nuclei + nicotinamide, sonicated nuclei + nicotinamide and permeabilised cells + nicotinamide).

7.6 Sonicated permeabilised cells as a positive control for PARP activity in response to severe DNA damage

7.6.1 Background

Nuclei, especially sonicated nuclei were indeed very useful as positive controls for PARP activity and the work depicted in Figure 7.7 proved this activity could be measured by [^{3}H]NAD incorporation assays. However, nuclei are not the ideal control for permeabilised cells. Permeabilised cells are not necessarily instantly assessable to [^{3}H]NAD in the same way that nuclei are due to the presence of the majority of the cell structure and contents. This means that the PARP activity, in response to the same number of strand breaks, is likely to produce higher CPMs in nuclei than in permeabilised cells over the same period of time. In view of these concerns, it was proposed that a more appropriate positive control, in the context of this experimentation, might be permeabilised cells which had been exposed to sonication.

7.6.2 Experimental protocol and results

Experiments conducted in exactly the same fashion but on different occasions produced conflicting results with regard to PARP activity induced by sonication of permeabilised cells. In figure 7.8 the data from two such experiments are shown. PARP assays were conducted on permeabilised cells which had been exposed to sonication (7.5.3), insonation (3 MHz, 2.0 Wcm^{-2}, CW at 37 °C) or were untreated (at 37 °C) in the presence and absence of nicotinamide. In the upper panel, sonication clearly produced a large increase in [^{3}H]NAD incorporation which was inhibited by the addition of 100 mM nicotinamide, although in the lower panel this [^{3}H]NAD incorporation was not observed despite the fact that the sonication was carried out under identical conditions.

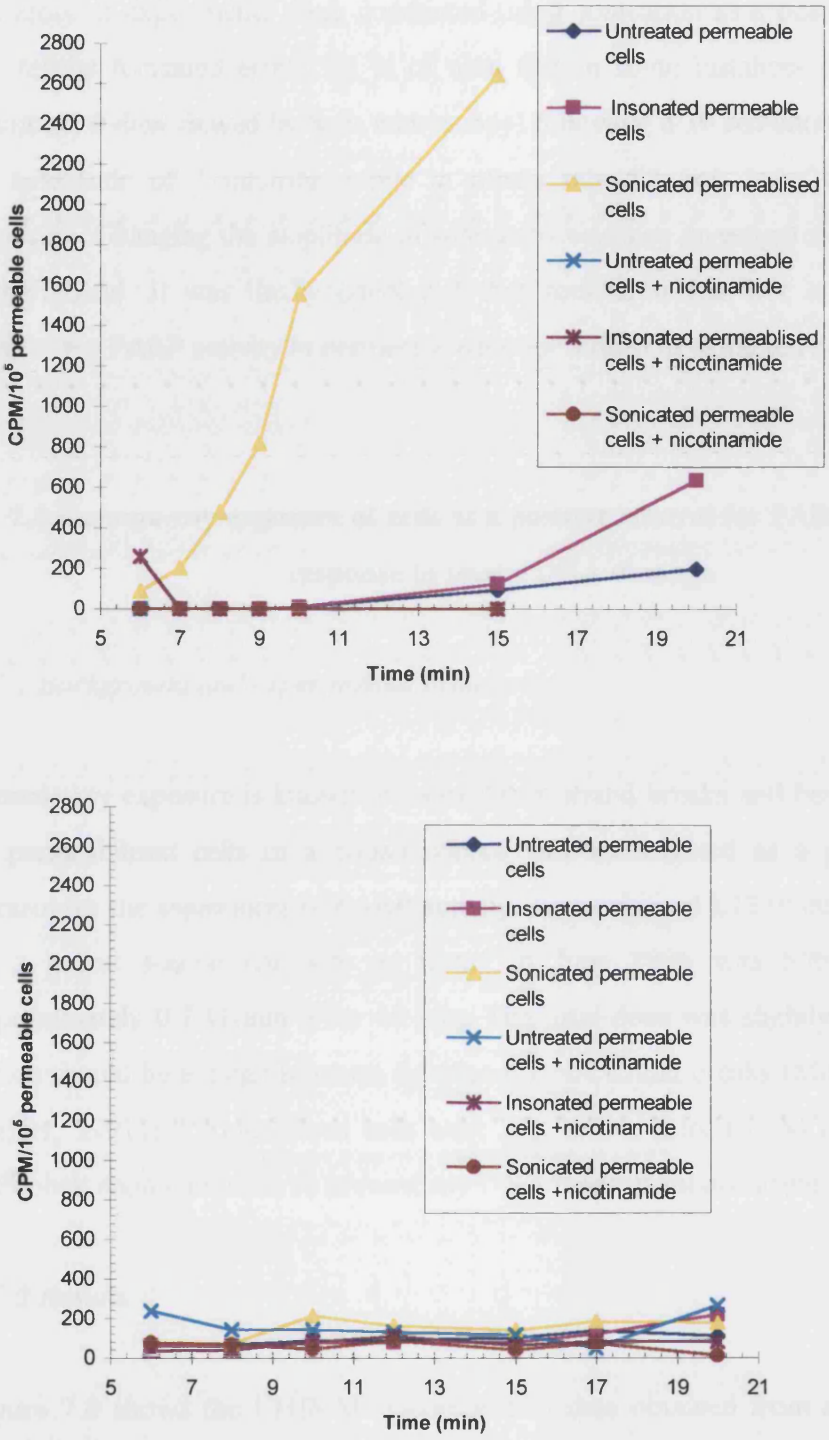

Figure 7.7: The use of sonication as a positive control for PARP activity in permeabilised L1210 cells.

Panels show data from experimentation conducted in exactly the same manner on different occasions. L1210 cells were either insonated at 37 °C at 3 MHz, 2.0 Wcm^{-2}, CW for 30 min (Insonated permeable cells) or were merely incubated at 37 °C for 30 min. Cells were then permeabilised and a portion of the untreated permeable cells were sonicated at amplitude 3 microns for 10 sec (Sonicated permeable cells) PARP assays were then conducted in the presence and absence of 100 mM nicotinamide in all cases.

An array of experiments were conducted using sonication as a positive control, but the results remained erratic. It is of note that in some instances the cells became disrupted (when viewed by light microscopy) following a 10 sec burst of sonication at an amplitude of 3 microns, while in others this did not occur despite repeated exposure. Changing the amplitude of sonication was also investigated, but this did not prove useful. It was finally concluded that sonication was not a reliable positive control for PARP activity in permeable cells nor indeed in extracted nuclei.

7.7 Gamma-ray exposure of cells as a positive control for PARP activity in response to severe DNA damage

7.7.1 Background and experimental protocol

Gamma-ray exposure is known to cause DNA strand breaks and hence the exposure of permeabilised cells to a cobalt source was investigated as a possible positive control for the assessment of PARP activity. Permeabilised L1210 cells were exposed to a cobalt source (Activity as tested in June 1996 was 500 GBq (13 Ci), approximately 0.7 $Gymin^{-1}$) for 10 min. The total dose was slightly less than 7 Gy, which should be enough to cause significant DNA strand breaks (Miller, Thomas and Frazier, 1991a). Permeabilised cells were kept on ice prior to and after exposure to the cobalt source in order to prevent any DNA repair from occurring.

7.7.2 Results

Figure 7.8 shows the [^{3}H]NAD incorporation data obtained from a cobalt exposed sample as compared with untreated permeabilised cells and insonated permeabilised cells. In the first 10 min of the PARP assay there was no difference between rates of incorporation in any of the samples. However after this time the rate of [^{3}H]NAD incorporation in the permeabilised cells exposed to the cobalt source was notably faster than either the insonated sample or the untreated sample. The rates [^{3}H]NAD incorporation in untreated and insonated cells were indistinguishable from each other. The increased rate of [^{3}H]NAD incorporation induced by exposure to gamma-rays

was reproducible and therefore provides a useful control. However, increasing the magnitude of this effect by a prolonged duration of exposure to the cobalt source is a technique employed later in this chapter.

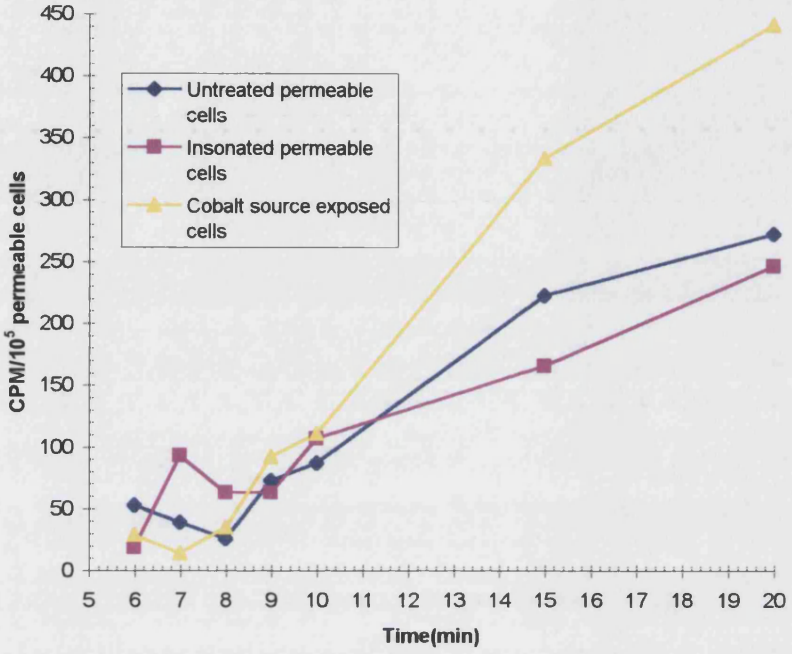

Figure 7.8: The use of gamma-rays as a positive control for PARP activity in permeabilised L1210 cells.

L1210 cells were either exposed to an insonation at 37 °C at 3 MHz, 2.0 Wcm^{-2}, CW for 30 min or were merely incubated at 37 °C for 30 min and then permeabilised. The latter untreated sample was divided into 2 parts, one of these was exposed to the cobalt source for 10 min (7 Gy) while the other remained on ice. [^{3}H]NAD incorporation assays were then performed to assess PARP activity at 6, 7, 8, 9, 10, 15 and 20 min.

7.8 Comparison of permeabilisation by hypotonic shock and by digitonin exposure

7.8.1 Background

Unfortunately, although permeabilisation by hypotonic shock was a relatively gentle method, the proportion of cells that were successfully permeabilised varied between

experiments. It was therefore proposed that exposure to digitonin might produce better and more effective results.

7.8.2 Permeabilisation by exposure to digitonin

Digitonin is a steroid glycoside which can selectively permeabilise the plasma membrane. Its action is believed to be due to selective binding to cholesterol and other β-hydroxysterols present in the plasma membrane. The molar ratio of cholesterol to phospholipid in eurkaryotic plasma membranes is several fold greater than in intracellular membranes and hence the selectivity of digitonin for the plasma membrane (Fiskum *et al*, 1980). This property has been used to study transport activities in the mitochondria and in endoplasmic reticulum (Fiskum *et al*, 1980). Digitonin also allows rapid and efficient cell permeabilisation which is the reason for its utilisation here.

Method

L1210 cells were cooled on ice (10 ml at 2.0 x10^6 cells/ml) and then spun in a benchtop centrifuge at 1500 rpm. Cells were then resuspended in 5 ml of isotonic buffer (7.2.2) and exposed to 0.01%(w/v) digitonin (Sigma-Aldrich Ltd. Irvine, U.K.) for 2 min. Cells were immediately re-spun and resuspended in fresh isotonic medium. This method was adapted from that of Fiskum *et al* (1980).

7.8.3 Comparison of PARP activity following permeabilisation by hypotonic shock or digitonin

L1210 cells were either exposed to permeabilisation by hypotonic shock (7.2) or digitonin (7.8.2) before undergoing a PARP assay (7.3). In each case, three procedures were executed. Using the hypotonic shock method samples were 54, 46 and 52 % permeable, while digitonin exposure meant that all samples were 100 % permeable by trypan blue exclusion. However, there was some degree of cell loss in the digitonin exposed cells. The results of the PARP assays are shown in figure 7.9. The incubation time in the presence of [^{3}H]NAD prior to sampling was prolonged in these assays, in order to try and improve its uptake by the permeabilised cells.

Digitonin exposed cells showed slightly more PARP activity than those subjected to hypotonic shock, this may be due to the extra centrifugation step that they experience following initial permeabilisation, which may also account for the observed slight loss in cell numbers. However, digitonin exposure provided an effective and reliable method of permeabilising all of the cells within a sample and the marginal elevation in PARP activity that the procedure caused was not considered to be as important as its efficiency and it is hence used later in this chapter.

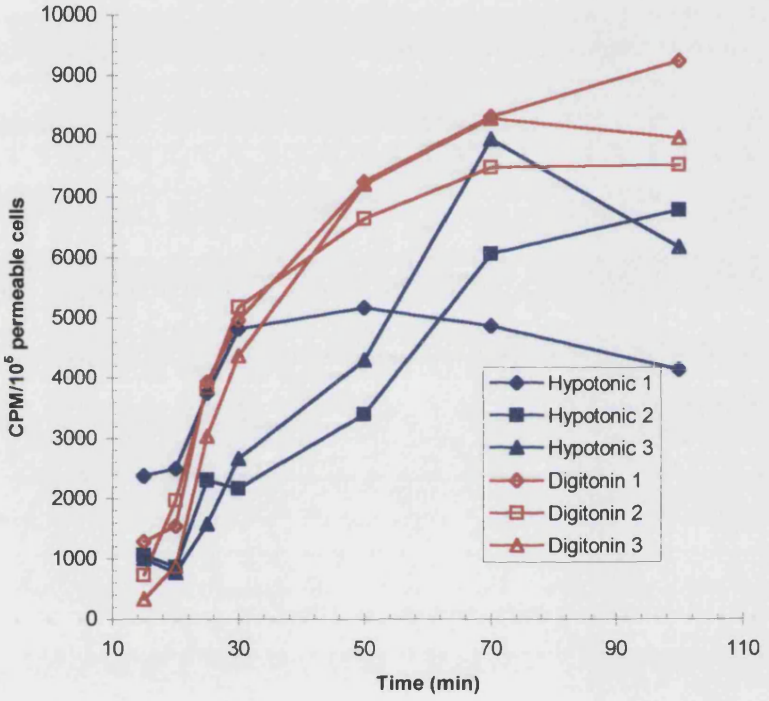

Figure 7.9: Comparison of PARP activation following permeabilisation with either hypotonic shock or digitonin exposure.

L1210 cells were subjected to either hypotonic shock or digitonin exposure before a PARP assay was conducted where samples were taken at 15, 20, 25, 30, 50, 70 and 100 min (n=3).

There was no re-sealing of cells regardless of the method of permeabilisation even when cells were resuspended in fresh media and returned to the incubator. Indeed, no resealing was ever observed in permeabilised cells despite repeated attempts

throughout the project to encourage them to do so. This is advantageous as any re-sealing could interfere with the PARP activity assays.

7.9 Gamma-ray exposure of cells as a positive control for PARP activity in response to severe DNA damage in digitonin permeabilised cells

7.9.1 Background and experimental protocol

In order to confirm that gamma-ray exposure of cells provided an adequate control in cells permeabilised using digitonin the following procedure was employed. L1210 cells were divided into 2 scintillation vials. The first was exposed to the cobalt source for 1 hr (exposed) and experienced approximately 42 Gy (7.7.1) while the other was placed on top of the cobalt source in order that it experienced similar thermal conditions, but not irradiation (control). Each sample was divided into three (control 1-3 and exposed 1-3) and all samples were permeabilised using the digitonin protocol (7.8.2). Interestingly the control cells were dark blue and looked intact upon trypan blue exclusion and observation by light microscopy, while the exposed cells stained a far lighter blue, were more diffuse and contained more cell debris. PARP assays were conducted on all the samples in the normal manner (7.3).

7.9.2 Results

The results of the PARP activity assays are shown in figure 7.10 which clearly depicts that those cells exposed to the cobalt source had a far greater PARP activity and therefore substantially more DNA damage than the control cells which had only experienced digitonin permeabilisation. Indeed, PARP activity is approximately 2.5 times greater in the exposed cells than the unexposed cells confirming that exposure of L1210 cells to the cobalt source is a useful positive control for PARP activity under these conditions.

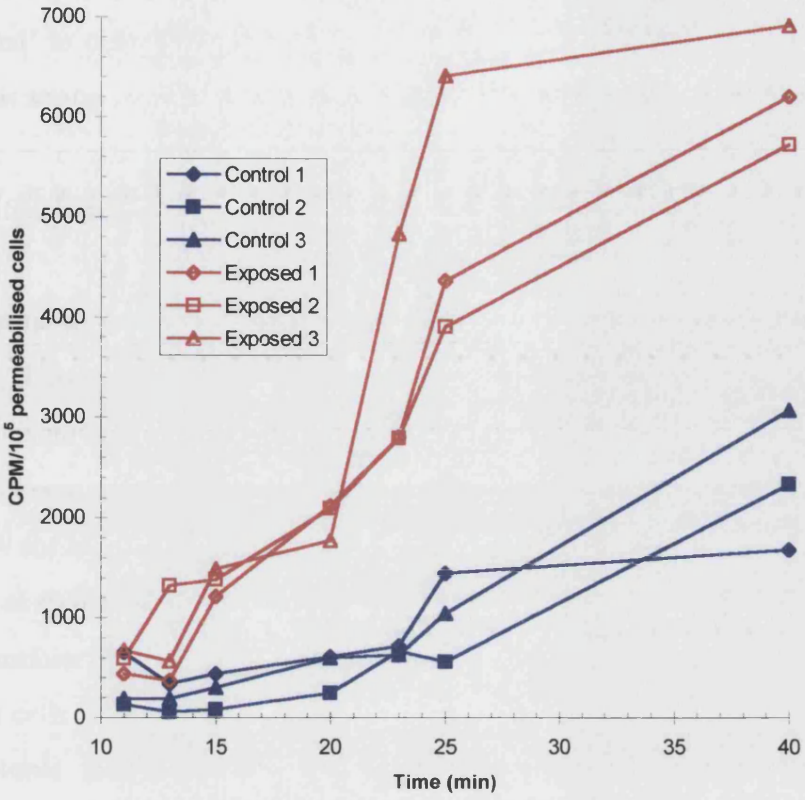

Figure 7.10: The use of gamma-rays as a positive control for PARP activity in digitonin permeabilised L1210 cells.

L1210 cells were either exposed to the cobalt source for 1 hr (exposed 1-3) or maintained under similar conditions but not exposed (control 1-3) before being subjected to digitonin induced permeabilisation. PARP activity assays were then conducted on all samples using 11, 13, 15, 20, 25 and 40 min as time points.

7.10 PARP activity in response to 3 MHz, 1.0 Wcm^{-2}, CW ultrasound using the tissue culture flask exposure system

7.10.1 Background

The ultrasound system used in the early part of this chapter is relatively 'kind' to cells experiencing insonation and unsurprisingly has not produced any significant increase in PARP activity as compared with control sham insonations. It was therefore decided that the exposure system described in 4.2.3 should be employed in order to further

investigate PARP activity induced by ultrasonic exposure. This system is far less 'kind' to cells and indeed caused significant membrane permeabilisation (Chapter 5). This set-up was used throughout the remainder of this chapter.

7.10.2 Experimental protocol and results

A total of seven 10 ml samples of L1210 cells set at $6x10^5$ cells/ml were cooled on ice. This cell density is somewhat lower than that used in the previously employed exposure system (4.2.1), but is comparable to the other occasions when this system has been utilised (Chapter 5). Three samples were insonated at 3 MHz, 1.0 Wcm^{-2}, CW for a period of 10 min during which time their temperatures rose to 39, 40 and 39 ^{o}C as measured by thermometer. Following insonation the cells became permeable and therefore 77, 84 and 95 % did not exclude trypan blue. Following re-cooling, on ice, the cells were spun at 1500 rpm and concentrated by being resuspended in 2.5 ml of isotonic buffer (7.2.2). Although some cells were lost during this process the percentage of permeable cells remained constant. The four remaining samples were exposed to digitonin permeabilisation (7.8.2) which was 100 % efficient in all cases.

PARP assays were conducted on all of the samples (7.3) and the results are shown in figure 7.11. Three of the digitonin permeabilised samples were assayed in the presence of 100 mM nicotinamide and one was used as a comparison for the insonated samples. It is clear that digitonin permeabilisation did cause an increase in PARP activity as this was abolished in the presence of nicotinamide. It is also apparent that insonation did not induce more activity than was seen in cells which had merely undergone digitonin exposure. Hence it remains unclear if PARP activity is significantly elevated by ultrasonic exposure, although some increased activity does occur.

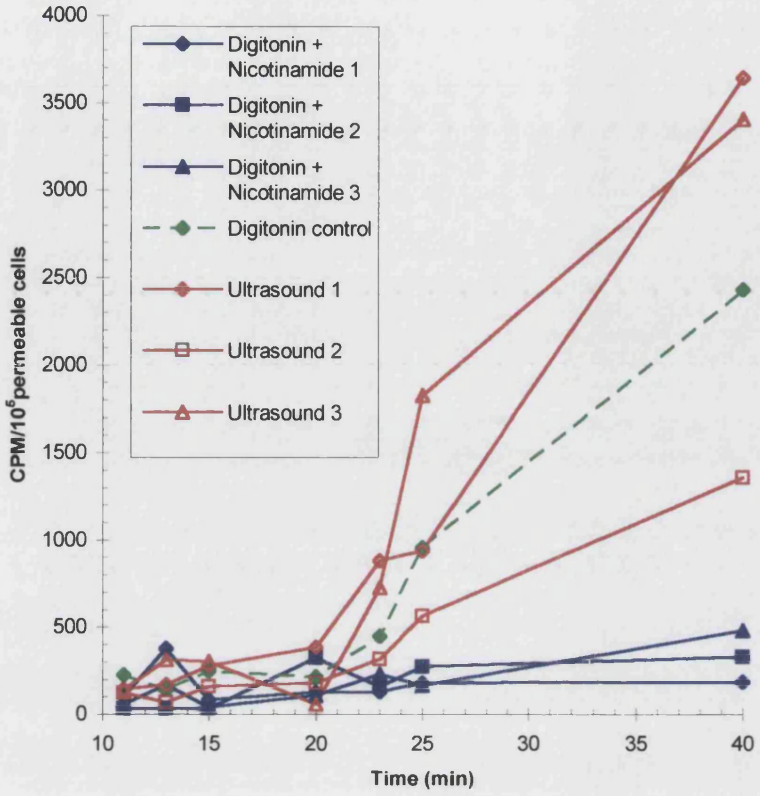

Figure 7.11: PARP activity in response to 3 MHz, 1.0 Wcm^{-2}, CW ultrasound exposure.

L1210 cells were exposed to either digitonin permeabilisation or insonation at 3 MHz, 1.0 Wcm^{-2}, CW and then PARP assays were carried out. 100 mM nicotinamide was present in three of the digitonin exposed samples. Assays were carried out at 11, 13, 15, 20, 23, 25 and 40 min time points.

7.11 The effect of duration of exposure, in L1210 cells exposed to 3 MHz, 1.0 Wcm^{-2}, CW ultrasound and then permeabilised by digitonin, on PARP activity

7.11.1 Background and experimental procedure

It was proposed that L1210 cells be exposed to ultrasound for different periods of time in order to investigate the effect on PARP activity. However, since insonated cells were only partially permeabilised using this exposure system they were treated

with digitonin following ultrasonic exposure, which meant that samples were 100 % permeable.

Cells were insonated at 3 MHz, 1.0 Wcm^{-2}, CW for 10, 5 or 2 min periods. For each duration, there were three samples and one control sample which was not insonated. Exposures were conducted at a cellular concentration of $7x10^5$ cells/ml. Following, insonation samples were spun at 1500 rpm for 3 min in Cortex tubes and then subjected to digitonin permeabilisation (7.8.2), including the control sample, before re-spinning and subsequent suspension in 2.5ml of isotonic buffer. All samples were then subjected to a PARP assay (7.3).

7.11.2 Results

Permeabilities of the cells following insonation, but prior to digitonin treatment were 50, 87 and 75 % in the samples exposed for 10 mins; 54, 57 and 60 % in the samples exposed for 5 min; 2, 18 and 22 % in the samples exposed for 2 min and 1 % in the unexposed sample. Following treatment with digitonin all samples were 100 % permeable to trypan blue. There was some cell loss (50 %) during the procedure, although loss of cell number was also observed in the experiment described in 7.10 where cells were not exposed to digitonin following insonation.

The results of the PARP activity assay are depicted in figure 7.12, but are rather difficult to decipher. The digitonin control produced similar results to that shown in figure 7.11. However, PARP activities in the insonated samples produced strange results. It is questionable that a difference between the samples exists, although if anything, the trend which occurred was that a shorter insonation produced greatest PARP activity and thus greater DNA damage. An explanation for this may be that cells were already damaged following insonation making them more susceptible to digitonin treatment, to the extent that after longer insonations cells were totally disrupted.

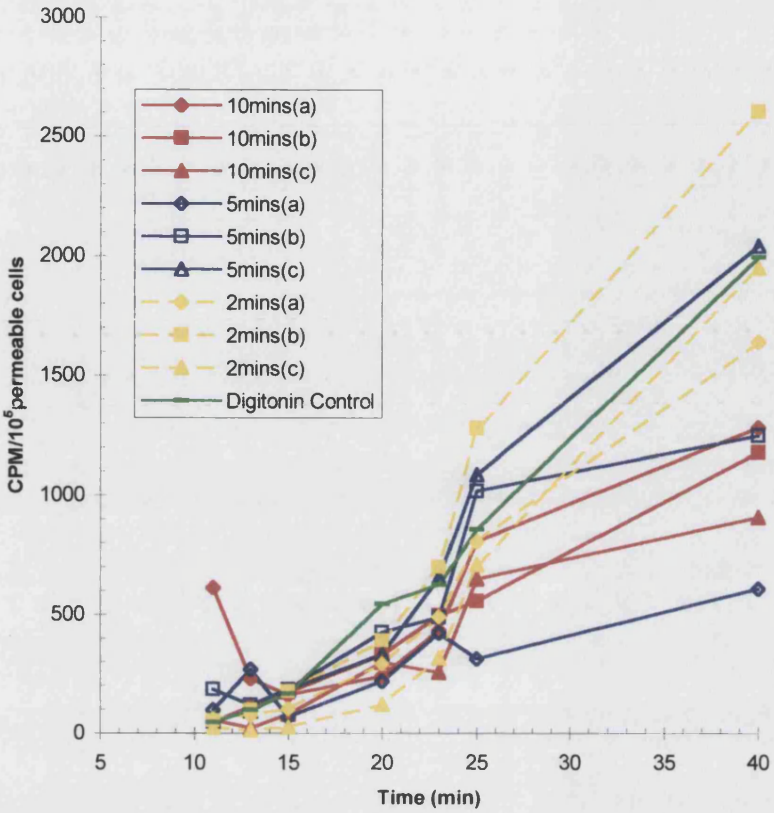

Figure 7.12: The effect of duration of exposure, in L1210 cells exposed to 3 MHz, 1.0 Wcm^{-2}, CW ultrasound and then permeabilised by digitonin, on PARP activity.

L1210 cells were insonated for 10 min (10(a), 10(b), 10(c)), 5 min (5(a), 5(b), 5(c)) or 2 min (2(a), 2(b), 2(c)) and were then completely permeabilised by exposure to digitonin. A control which was not insonated but was permeabilised by digitonin was also performed. All samples were then subjected to a PARP assay using 11, 13, 15, 20, 25, 40 min time points.

7.12 The effect of permeabilisation of L1210 cells with digitonin following insonation at 3 MHz, 1.0 Wcm^{-2}, CW for 5 min on PARP activity

7.12.1 Background and experimental protocol

In view of the results obtained in 7.11 it was necessary to investigate the effect of post-insonation digitonin treatment further. A 5 min insonation at 3 MHz, 1.0 Wcm^{-2} was carried out and a comparison was conducted whereby some cells were exposed

to digitonin prior to a PARP assay while others were not. A further sample was exposed to digitonin but had not been previously insonated.

7.12.2 Results

The temperature rises observed within all insonated flasks were as seen in similar exposures in chapter 5 and ranged from a final temperature of 30-33.5 °C. In response to the insonation alone, cells were 60, 80 and 61 % permeable in the group not digitonin treated and 63, 81 and 60 % permeable in group which were treated with digitonin. Following the digitonin procedure the untreated group were 66, 74 and 71 % permeable and treated group were all 100 % permeable. Finally the control sample which was digitonin exposed but not insonated was also 100 % permeable. The loss of total cell number ranged between 20-30 %, and was not increased by digitonin treatment.

Figure 7.13 shows the results of the PARP assays. Digitonin treatment following insonation clearly reduces the PARP activity which goes some way to explain the results depicted in figure 7.12. It may be that cells which were already damaged by insonation became drastically disrupted by further treatment and thus PARP activity was unmeasurable in most cells.

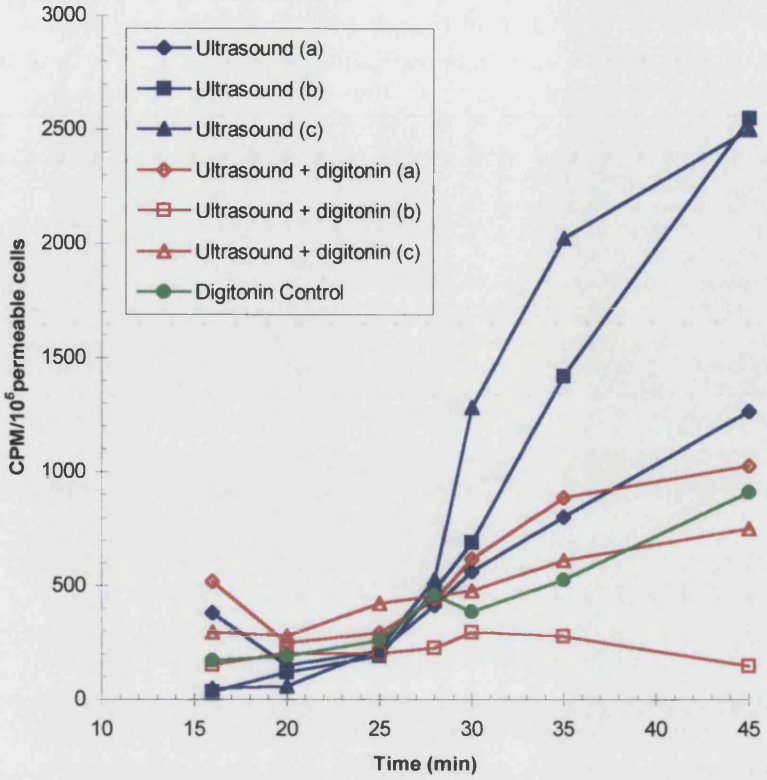

Figure 7.13: Comparison of PARP activity following insonation with or without subsequent digitonin permeabilisation.

L1210 cells were subjected to insonation at 3 MHz, 1.0 Wcm^{-2}, CW ultrasound for 5 min in triplicate. Cells were then either treated with digitonin (Ultrasound + digitonin) or not (Ultrasound). One control sample was also performed where cells were only subjected to digitonin treatment and not insonation. PARP assays were then conducted on all samples and time points were taken at 16, 20, 25, 28, 30, 35 and 40 min.

7.13 The effect of unpermeabilised cells present within the PARP activity assay

7.13.1 Background

It was clear from section 7.12 that insonation cannot be followed by digitonin treatment if the subsequent PARP assay was to give meaningful results. However, it was a concern that the plasma membrane of cells which were not permeable following insonation could be 'sticky' to [^{3}H]NAD. This would be important if it occurred as

variations in the parameters of insonation allow different numbers of cells to remain intact and hence the proportion of unpermeabilised cells within each PARP assay is not uniform.

7.13.2 Experimental protocol and results

L1210 cells were permeabilised by all of the methods used to date: hypotonic shock (7.2), digitonin exposure (7.8.2) and insonation (3 MHz, 1.0 Wcm^{-2}, CW for 5 min). These procedures resulted in 63, 100 and 42 % permeability to trypan blue respectively. A control sample was not permeabilised in any way and thus was only 9 % permeable to trypan blue. All samples underwent a PARP activity assay in the presence and absence of 100 mM nicotinamide, the results of which are reflected in figure 7.14. Interesting, hypotonic shock produced greater PARP activity than either insonation or digitonin, a result which is not in agreement with those described in section 7.8. The reason for this is not clear, but is perhaps due to experimental difference. The results in the presence of nicotinamide are interesting in that there was almost no activity until relatively late in the time course (30 min onwards) where a low level was observed. It is unlikely that this activity is due to [^{3}H]NAD sticking to the outside of cells as activity of this nature would have been uniform throughout the time course, instead it is more likely that this is merely the background activity which would be expected to rise with time. Comparisons can therefore be made between PARP assays resulting from different insonation conditions providing that the same number of permeabilised cells are present regardless of the presence of variable numbers of intact cells.

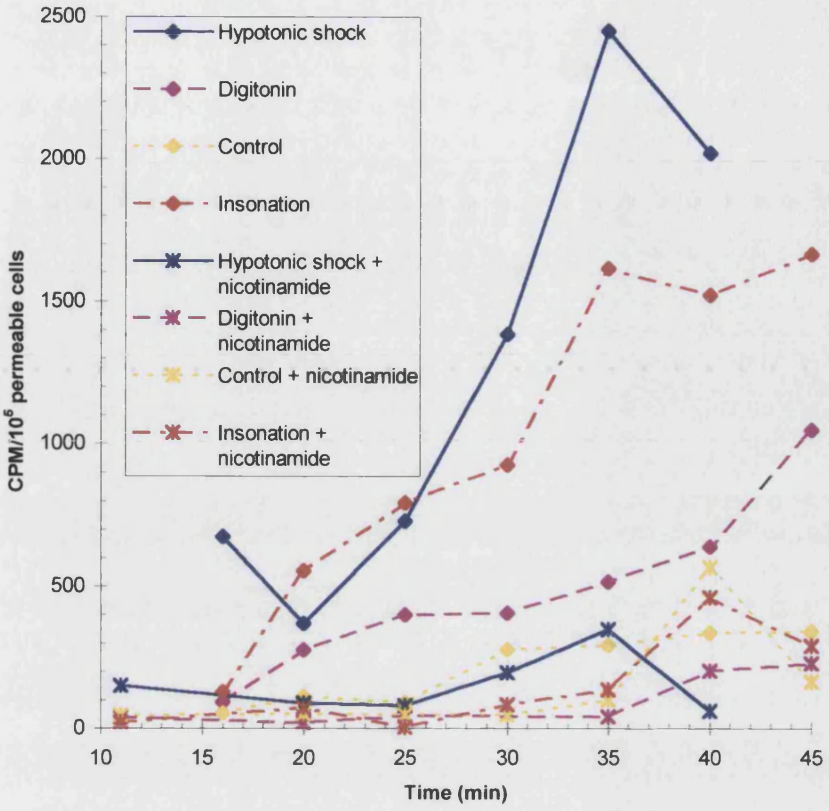

Figure 7.14: Comparison of PARP activity induced by various permeabilisation techniques in the presence and absence of nicotinamide.

L1210 cells were permeabilised by hypotonic shock, digitonin or insonation and in the case of the control cells were not permeabilised at all. All samples were the assayed for PARP activity in the presence and absence of 100 mM nicotinamide using time points at 11, 16, 20, 25, 30, 35, 40 and 45 min.

7.14 The effect of duration of exposure, in L1210 cells exposed to 3 MHz, 1.0 Wcm^{-2}, CW ultrasound, on PARP activity

7.14.1 Background and experimental protocol

In order to investigate the effect of duration of exposure of insonation at a frequency of 3 MHz the ultrasound exposure system shown in 4.2.3 was employed. Insonation itself was the only method of cellular permeabilisation. Cells were exposed for 10, 5 or 3 min in triplicate. Temperature rises were similar to those seen in 5.3, final

temperatures were between 32 and 37 °C in the 10 min samples, 24 and 29 °C in the 5 min samples and in the 3 min samples all flasks rose to 18 °C. Following insonation, the 10 min samples were 64, 63 and 57 % permeable, the 5 min samples were 48, 52 and 40 % permeable and finally the 3 min samples were 27, 18 and 12 % permeable. PARP assays were conducted on all cells and in one sample from each group a PARP assay was conducted in the presence of nicotinamide.

7.14.2 Results

Figure 7.15 describes the results of the PARP assays. No clear trend in PARP activity is apparent as far as the effect of duration of exposure to ultrasound is concerned, although it is clear that PARP activity was induced by exposure to ultrasound using these parameters. Since activity can be observed in all samples but the magnitude of this is indistinguishable between durations of exposure it is likely that total PARP activity is greater in the 10 min exposures as the proportion of cells which become permeable is far greater. However, it is impossible to say what goes on in those cells which do not suffer permeability as a result of insonation.

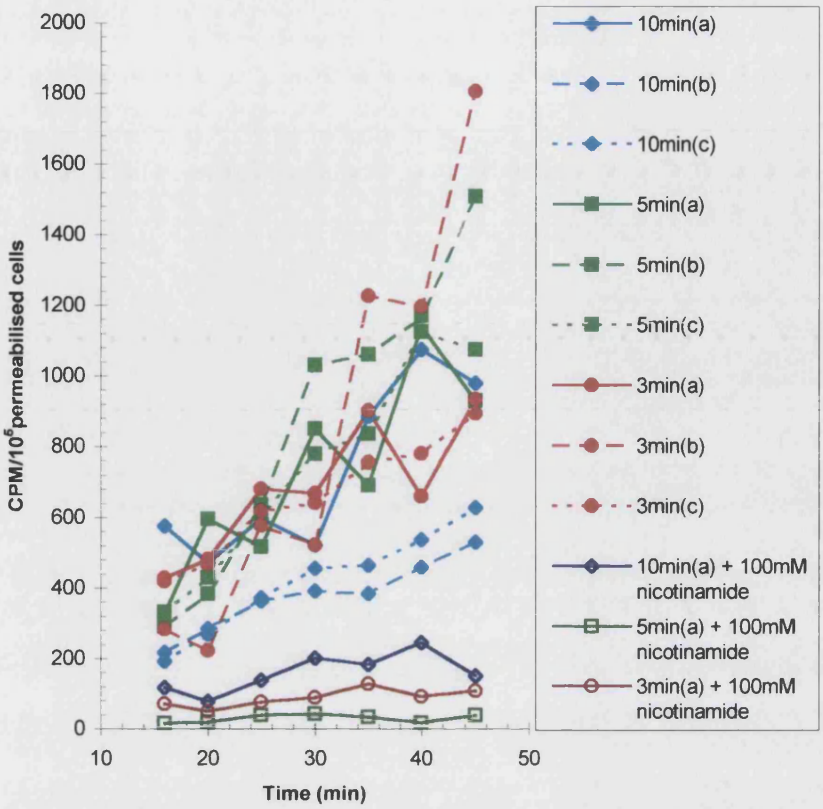

Figure 7.15: The effect of duration of exposure, in L1210 cells exposed to 3 MHz, 1.0 Wcm^{-2}, CW ultrasound, on PARP activity.

L1210 cells were exposed to 10, 5, 3 min insonation at 3 MHz, 1.0 Wcm^{-2}, CW in triplicate. PARP assays were performed on all samples and one sample from each duration in the presence of 100 mM nicotinamide. Time points for these assays were 16, 20, 25, 30, 35, 40, 45 min.

7.15 The effect of duration of exposure, in L1210 cells exposed to 1 MHz, 1.0 Wcm^{-2}, CW ultrasound, on PARP activity

7.15.1 Experimental protocol and results

This experiment was carried out in exactly the same way as that described in 7.14, with the exception of the frequency. Again, temperatures rises were in line with those observed in 5.5. In the 10 min samples the temperatures rose to 25-29 °C, in the five min samples they rose to 22-25 °C, while in the 3 min samples they rose to 16-17 °C. The permeabilities of the cells post-insonation were 93, 96 and 88 % in the 10 min

samples, 99, 95, 96 % in the 5 min samples and 92, 93 and 93 % in the 3 min samples. PARP assays were conducted as in 7.14 and are illustrated in figure 7.16. Again it is impossible to distinguish between the durations of exposure, but it is clear that insonation under these conditions does cause PARP activity as can be seen by the inhibition due to 100 mM nicotinamide. At this frequency cells are permeabilised to a similar degree regardless of the duration of exposure in the range used here, however, at longer exposures more cells will be lost completely (chapter 5). It is possible therefore that the overall number of mere DNA strand breaks is uniform under these conditions and hence will produce similar levels of PARP activity. It seems that in general PARP activity induced at this frequency is greater than at 3 MHz (7.14), although comparison between experiments is not reliable.

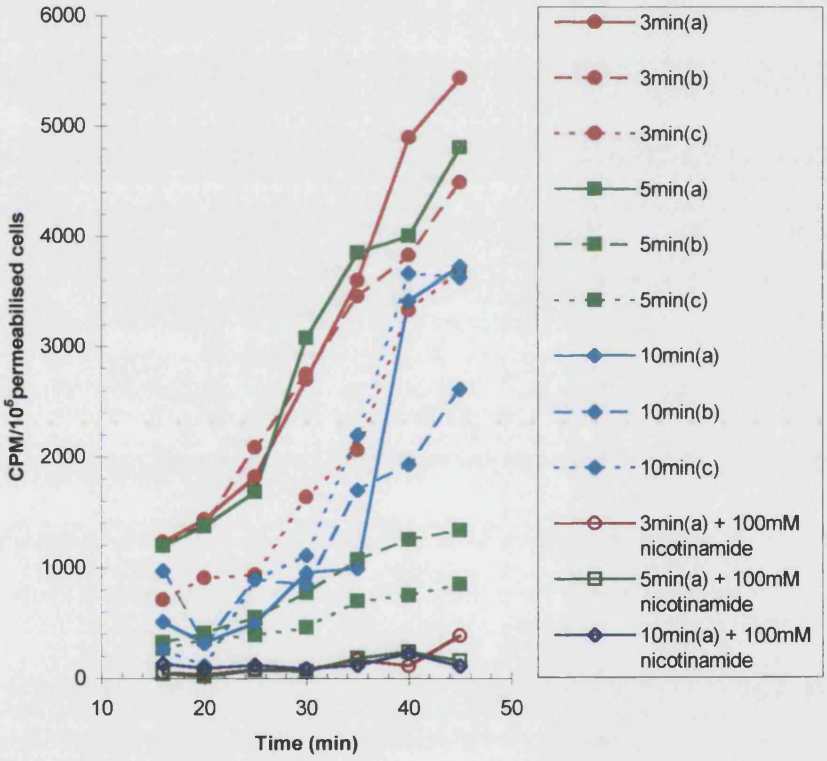

Figure 7.16: The effect of duration of exposure, in L1210 cells exposed to 1 MHz, 1.0 Wcm^{-2}, CW ultrasound, on PARP activity.

L1210 cells were exposed to 10, 5, 3 min insonation at 1 MHz, 1.0 Wcm^{-2}, CW in triplicate. PARP assays were performed on all samples and one sample from each duration in the presence of 100 mM nicotinamide. Time points for these assays were 16, 20, 25, 30, 35, 40, 45 min.

7.16 Effect of beam intensity on PARP activity following L1210 cell exposure to 3 MHz, 1.0 W cm^{-2}, CW ultrasound

7.16.1 Experimental protocol and results

This experiment was carried out using the same method as described in 7.14, with the exception that the duration of exposure was 5 min in all samples. Cells were exposed to intensities of 0.4, 0.8 and 1.6 Wcm^{-2} in triplicate. Temperature rises were similar to those seen in 5.3. Final temperatures were 17-19 °C in 0.4 Wcm^{-2} samples, 20-21 °C in 0.8 Wcm^{-2} samples and 39-45 °C in 1.6 Wcm^{-2} samples. Post-insonation permeabilities were 8, 6 and 8 % in the 0.4 Wcm^{-2} samples, 23, 18 and 25 % in the 0.8 Wcm^{-2} samples and 77, 60 and 91 % in the 1.6 Wcm^{-2} samples. In view of the very low numbers of permeable cells at the lower intensities it was not possible to add the standard 2.4 x 10^5 cells per PARP assay and lower numbers had to be used. The results were still corrected to CPM/10^5permeable cells and are displayed in figure 7.17. Again, the results are diverse and indistinguishable, although there is very definitely some PARP activity induced in response to these ultrasonic parameters.

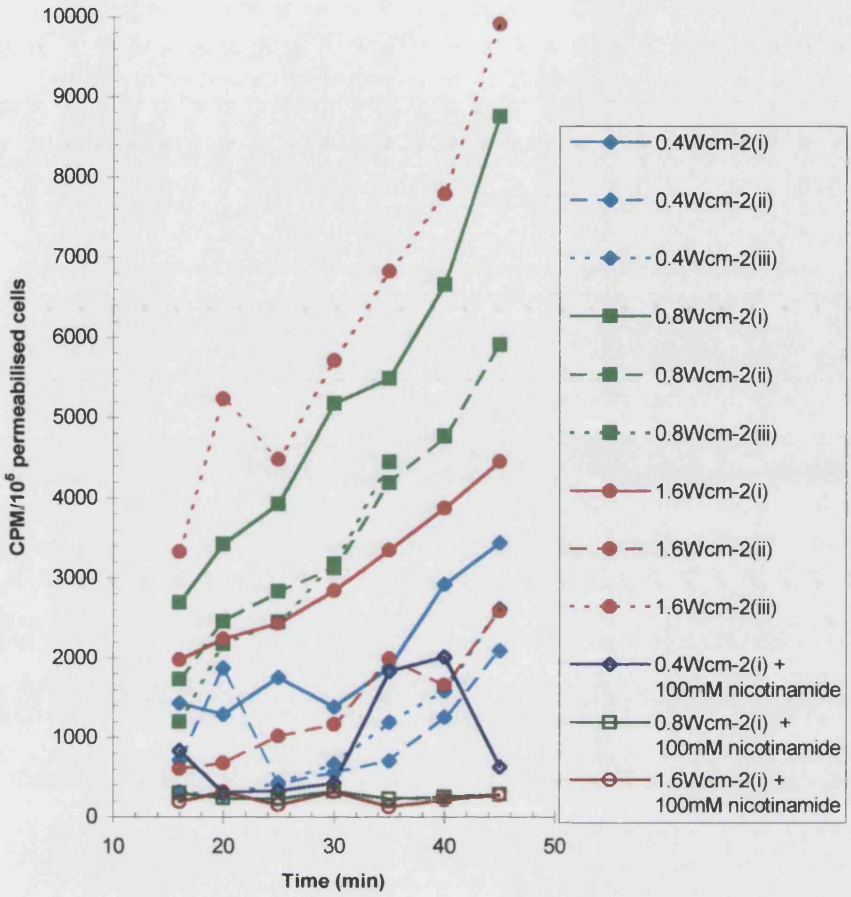

Figure 7.17: Effect of beam intensity on PARP activity following L1210 cell exposure to 3 MHz, 1.0W cm^{-2}, CW ultrasound.

L1210 cells were exposed to 0.4, 0.8 or 1.6 Wcm^{-2} insonation at 3 MHz, CW for 5 min in triplicate. PARP assays were performed on all samples and one sample from each duration in the presence of 100 mM nicotinamide. Time points for these assays were 16, 20, 25, 30, 35, 40, 45 min.

7.17 Effect of beam intensity on PARP activity following L1210 cell exposure to 1 MHz, 1.0 W cm^{-2}, CW ultrasound

7.17.1 Experimental protocol and results

The protocol for this experiment was exactly the same as in 7.16, but was conducted at 1 MHz not 3 MHz. Temperatures rises were again in-line with those observed in 5.5 and were as follows: 0.4 Wcm^{-2} samples 19-20 °C, 0.8 Wcm^{-2} samples 20-22 °C

and 1.6Wcm^{-2} samples 27-32°C. The post-insonation permeabilites were 89, 88 and 78 % in the 0.4 Wcm^{-2} samples, 93, 94 and 98 % in the 0.8 Wcm^{-2} samples and 97, 97 and 98 % in the 1.6 Wcm^{-2} samples. Figure 7.18 depicts the results of the PARP assays and again no clear trends can be identified despite insonation in general clearly inducing PARP activity.

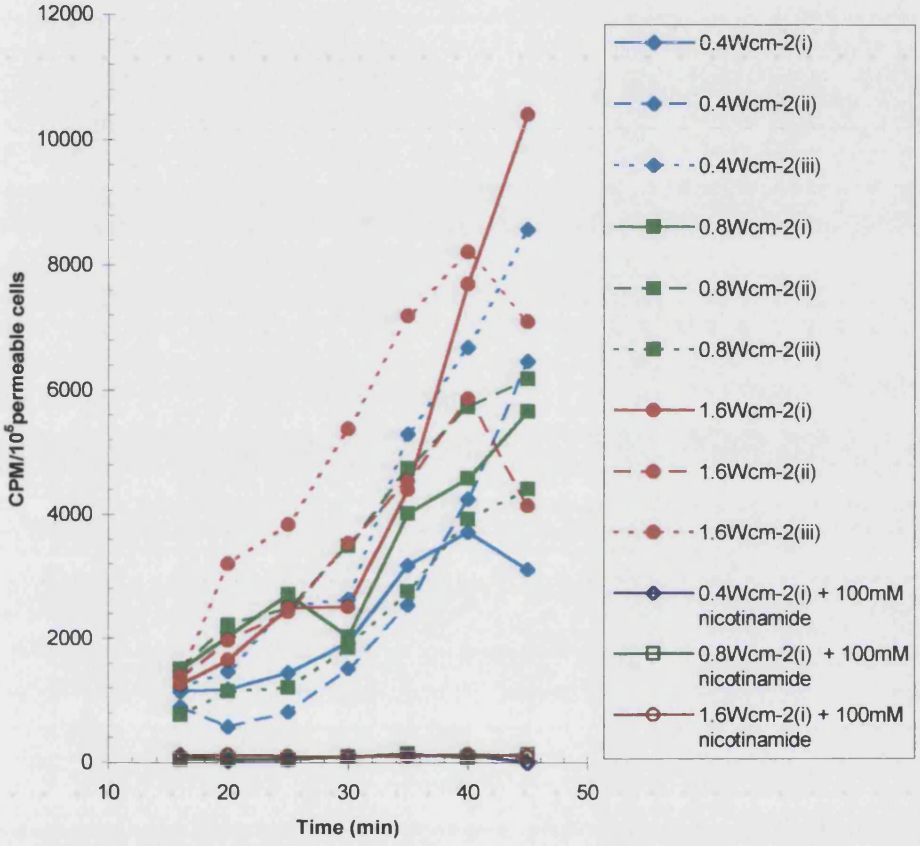

Figure 7.18: Effect of beam intensity on PARP activity following L1210 cell exposure to 1 MHz, 1.0W cm^{-2}, CW ultrasound.

L1210 cells were exposed to 0.4, 0.8 or 1.6 Wcm^{-2} insonation at 1 MHz, CW for 5 min in triplicate. PARP assays were performed on all samples and one sample from each duration in the presence of 100 mM nicotinamide. Time points for these assays were 16, 20, 25, 30, 35, 40, 45 min.

7.18 The Effect of 50 IU/ml SOD and 1000 IU/ml catalase (alone or together) on PARP activity following L1210 exposure to 1 MHz, 1.0 Wcm^{-2}, CW ultrasound

7.18.1 Background and experimental protocol

In an attempt to decipher the mechanism by which insonation produces DNA damage and subsequent PARP activity ultrasound exposure of L1210 cells was conducted in the presence of SOD (5.11) and/or catalase (5.9). The experimental protocol was as described in 7.14, briefly, L1210 cells were exposed to 1 MHz, 1.0 Wcm^{-2}, CW ultrasound for a period of 3 min. Insonations were carried out in triplicate in the presence of SOD, catalase, catalase and SOD or in the absence of either of these chemicals. The concentrations of SOD and catalase were as detailed in 5.11. PARP assays were then carried out on each sample and on one replicate from each group in the presence of nicotinamide.

7.18.2 Results

Temperature rises throughout the samples were as seen in 5.5 and were not different between the groups, although they ranged from 13-19 °C. Insonations resulted in the following permeabilites: control samples, 98, 97 and 89 %; catalase samples, 94, 84 and 88 %; SOD samples 97, 75 and 83 % and catalase + SOD samples, 94, 94 and 82 %.

The results of the PARP assays are shown in figure 5.20. In the presence of nicotinamide all samples produce little or no PARP activity. Control samples and samples insonated in the presence of SOD produce similar amounts of PARP activity, while catalase alone and catalase and SOD produce a reduction in PARP activity. This suggests that catalase has a protective effect and reduces the amount of DNA damage induced in L1210 cells in response to insonation, despite reducing cell numbers slightly as compared to controls (also seen in 5.10 and 5.11). The implication is that the DNA damage produced under these conditions is due to the action of H_2O_2.

However, catalase did not reduce PARP activity to that observed in the presence of nicotinamide suggesting that H_2O_2 is not the sole causative agent.

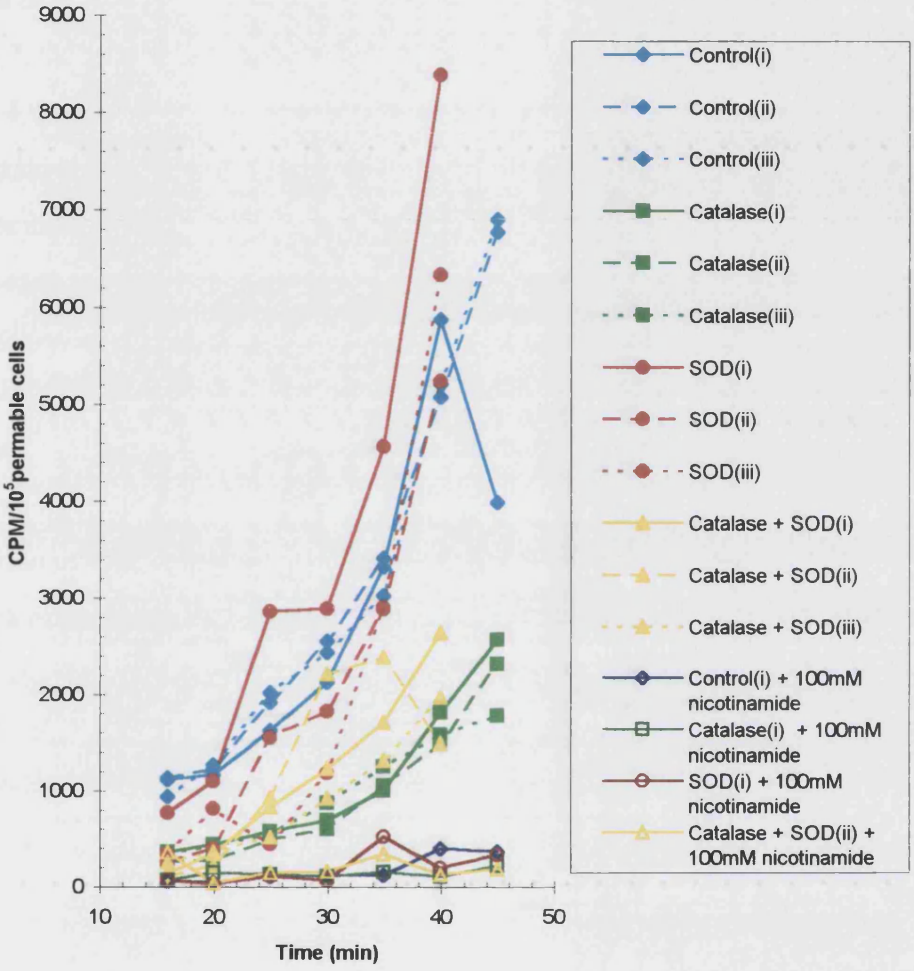

Figures 7.20: The Effect of 50 IU/ml SOD and 1000 IU/ml catalase (alone or together) on PARP activity following L1210 exposure to 1 MHz, 1.0 Wcm^{-2}, CW ultrasound.

L1210 cells were exposed to 1 MHz, 1.0 Wcm^{-2}, CW ultrasound for 3 min the absence of catalase and SOD (control), in the presence of 50 IU/ml SOD (SOD), in the presence of 1000 IU/ml catalase (catalase) or in the presence of both 50 IU/ml SOD and 1000 IU/ml catalase (SOD + catalase) in triplicate. PARP assays were the conducted on all samples and in one replicate per group in the presence of 100 mM nicotinamide. Time points were 16, 20, 25, 30, 35, 40 and 45 min.

7.19 Conclusions

It is clear that insonation induces PARP activity in the system used in the latter part of the chapter (4.2.3), although it does not do so in the system used in the former section (4.2.1). Despite the clear activation of PARP by insonation using the system described in 4.2.3, it proved impossible to differentiate between subtle changes in the ultrasonic parameters as regards degrees of enzymatic activity. However, it can be said that insonation under certain circumstances led to the activation of PARP, indicating the strand breaks have been induced in the DNA of exposed cells. Indeed, the final section in this chapter throws light on the mechanism which is producing this PARP activity and subsequently the reason that it was observed in one exposure system and not in the other. The protection that cells enjoyed in the presence of catalase suggests that H_2O_2 is involved in the induction of strand breaks which in turn induce the observed PARP activity. Furthermore this implicates cavitation as the mechanism of action responsible for cellular DNA damage induced by ultrasound. These findings are in agreement with much of the work described in 7.1 and in particular with Miller, Thomas and Buschbom (1995) who also observed that within their system the addition of catalase was not sufficient to abolish all DNA damage as was seen in 7.20. Since cavitation is not likely to occur in the exposure system detailed in 4.2.1, this accounts for the lack of induction in PARP activity observed within the earlier sections of this chapter.

CHAPTER EIGHT

COMPARISON OF PERMEABILISATION TECHNIQUES BY SCANNING ELECTRON MICROSCOPY

8.1 Introduction

In view of the results obtained in chapter 7, where permeabilisation techniques themselves induced PARP activity within L1210 cells, it was decided that observing the physical appearance of cells which had undergone these procedures may prove useful. Scanning electron microscopy was therefore employed to picture the damage that occurred to the cell plasma membrane in response to hypotonic shock, digitonin treatment and insonation at two frequencies.

8.2 Methods

8.2.1 Permeabilisation techniques

L1210 cells underwent hypotonic shock as described in 7.2, digitonin treatment as in 7.8.2 or insonation using the system in 4.2.3 at 1.0 Wcm^{-2} and either 1 or 3 MHz, CW ultrasound for 3 min. A control sample which was not permeabilised by any of these methods, but was exposed to the centrifugations involved in the other treatments was also performed. Following treatment, 1 %(v/v) glutaraldehyde (Sigma-Aldrich,) was added to all preparations as a fixative.

8.2.2 Scanning electron microscopy (SEM)

Cryo-SEM or low temperature SEM (-100-180°C) was performed on all samples in accordance with the methods of Read (1991). Briefly, cells were quickly mounted on filter paper and immediately washed with saline. Samples were then cryofixed to arrest biological processes by plunging into sub-cooled liquid nitrogen. Water crystals were not formed during this process. In the preparation stage of the microscope, samples were subjected to a vacuum to prevent a gas phase insulating the cells. Within the microscope samples were heated (-180-60°C) to remove frost before being returned to the preparation stage to be gold coated at -120°C under vacuum. Finally the samples were returned to the main stage of the microscope to be examined and photographed.

It should be noted that the background in the photographs within this chapter depicts the fibres of the filter paper.

8.3 Results

The control unpermeabilised cells were 10 % permeable to trypan blue following treatment, while the hypotonically shocked cells were 80 % permeable and the digitonin treated cells were 100 % permeable. In the insonated cells, those exposed to 3 MHz ultrasound were 58 % permeable, while those exposed to 1 MHz were 99 % permeable.

Figure 8.1 depicts the untreated cells as seen upon viewing under the electron microscope (EM). In both figures 8.1(a) and 8.1(b) the plasma membrane appears to be 'fluffy' and is intact. Figure 8.2 shows another untreated cell; the plasma membrane in close up (Figure 8.2(a)) and less magnified as a whole (Figure 8.2(b)). Again the cell appears 'fluffy' and intact and is representative the other cells examined in this sample.

Figure 8.3 shows two separate cells (a) and (b) which have undergone hypotonic shock. It is clear that the surface of these cells have lost their 'fluffy' appearance. In figure 8.4(a) a further 2 cells which have been treated in the same way are seen, again they appear less 'fluffy' than the normal cells. Figure 8.4(b) shows a close up of the surface of the cell on the right in figure 8.4(a). The smoothness of the cell is again apparent here. Pores in the cell membrane can be observed on the bottom left and the upper right of the cell. Figure 8.5(a) depicts two hypotonically treated cells which seem to be linked together. The cell on the left appears to be relatively normal but has a smooth appearance while the cell on the right has suffered severe damage. The three cells depicted in figure 8.5(b) can be described in a hierachy of damage starting with the one in the middle which is grossly damaged, followed be the one at the top which is relatively badly damaged and finally the one at the bottom which is partially damaged. Overall, some of the cells observed in this sample were normal in appearance with the exception of their smooth surface and the presence of some pores, while others appeared to be more seriously damaged. This may be a function of the fact that not all cells excluded trypan blue following the permeabilisation treatment implying that some retained an intact plasma membrane.

Figure 8.6 shows two cells ((a) and (b)) that had experienced treatment with digitonin. The surface of these cells seems to be smooth in the similar way to those treated by hypotonic shock. Small pores are present in both cell membranes. Figure 8.7 (a) illustrates another two cells also exposed to digitonin, it is of note that the one on the right displays particularly large pores. These cells are also smooth in appearance. Interestingly, one cell was observed where the plasma membrane and cytoskeleton appear to have collapsed around the nucleus (Figure 8.7(b)). Figure 8.8 shows a number of cells also exposed to the same digitonin treatment which have undergone various degrees of damage as a result. The two cells in the centre of the picture which appear to be joined have suffered severe damage and display large pores. A number of similar cells were observed within this sample.

The pictorial results of the cells which underwent insonation at 3 MHz and were subsequently viewed by SEM are shown in figures 8.9 to 8.11. It is clear that the cells shown in figure 8.9 have retained their 'fluffy' appearance, although the cell in figure

8.9(a) appears to have a large pore in the middle. The cell featured in figure 8.9(b) seems to be relatively intact although some poring has occurred. In figure 8.10(a) the surface of a cell is viewed in close up, it is apparent that the cell has retained its 'fluffy' texture although pores have been formed. Figure 8.10(b) depicts two further cells which have been exposed to 3 MHz ultrasound. Here the one on the right hand side has a similar appearance to that just described although at lower magnification, while the one on the left, displays cavernous pores while still at least partially 'fluffy'. Three more cells are shown in figure 8.11(a), the two cells on either side appear to be relatively intact, although associated with the cell in the middle, which is more damaged than any of the cells described in this group so far. In part (b) of the same figure, all of the cellular material on the left hand side may have been from the same cell and may represent cellular splitting. This effect seems likely as neither of the parts of this mass are large enough to represent an individual cell. Cells seen here which have been exposed to 3 MHz ultrasound were in general 'fluffy' with a small amount of poring, although a number were observed to be damaged to a greater degree. The fact that some cells appeared substantially more damaged than others may be a result of the partial permeability of the sample.

Cells which were exposed to 1 MHz were largely observed to be very damaged upon SEM examination. In figure 8.12 and 8.13 four individual cells are pictured. They were all seriously pored, although they still appeared to display a slightly 'fluffy' texture. No intact cells were observed within this sample and indeed a large amount of cell debris was observed throughout this sample, examples of this are shown in figure 8.14.

(a)

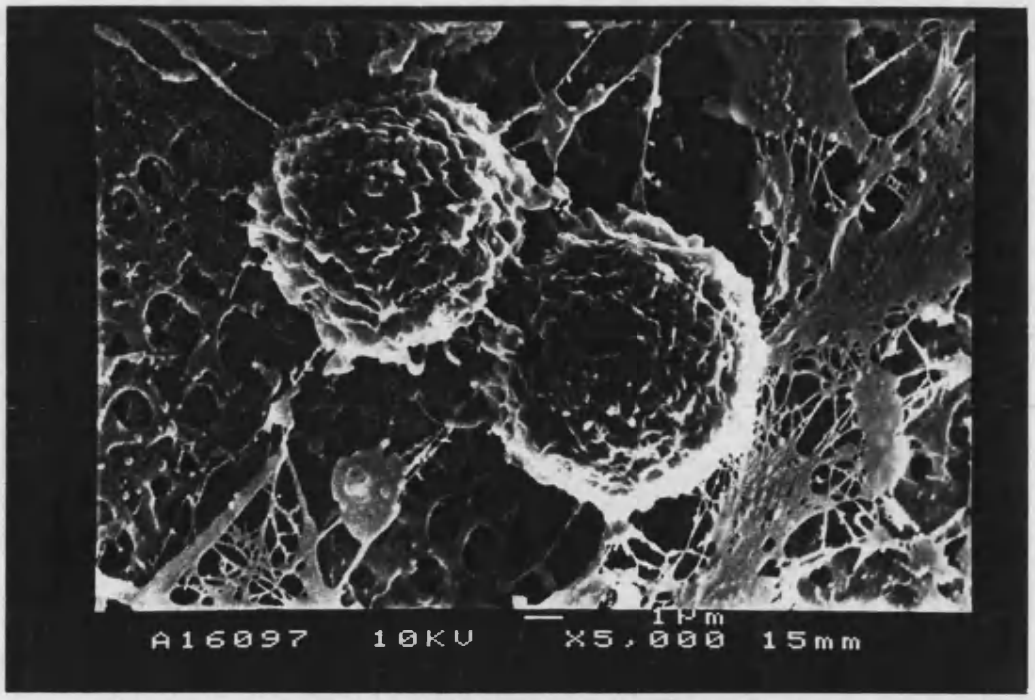

(b)

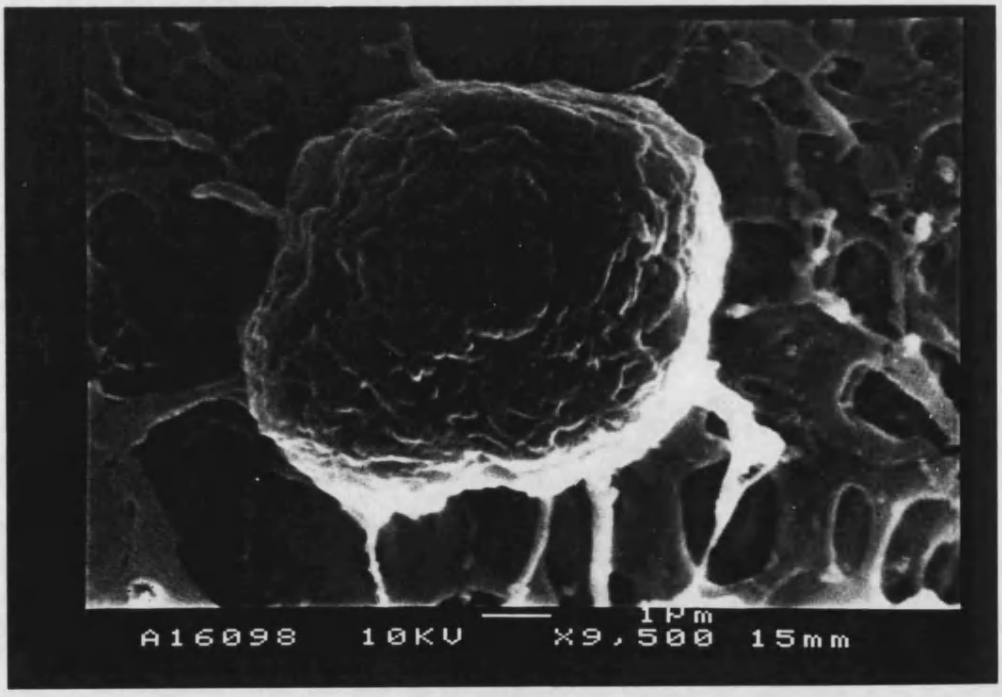

Figure 8.1: Normal (unpermeabilised) L1210 cells as viewed by SEM.

(a) Two cells depicted at a magnification of x5,000, (b) another cell depicted at a magnification of x9,500.

(a)

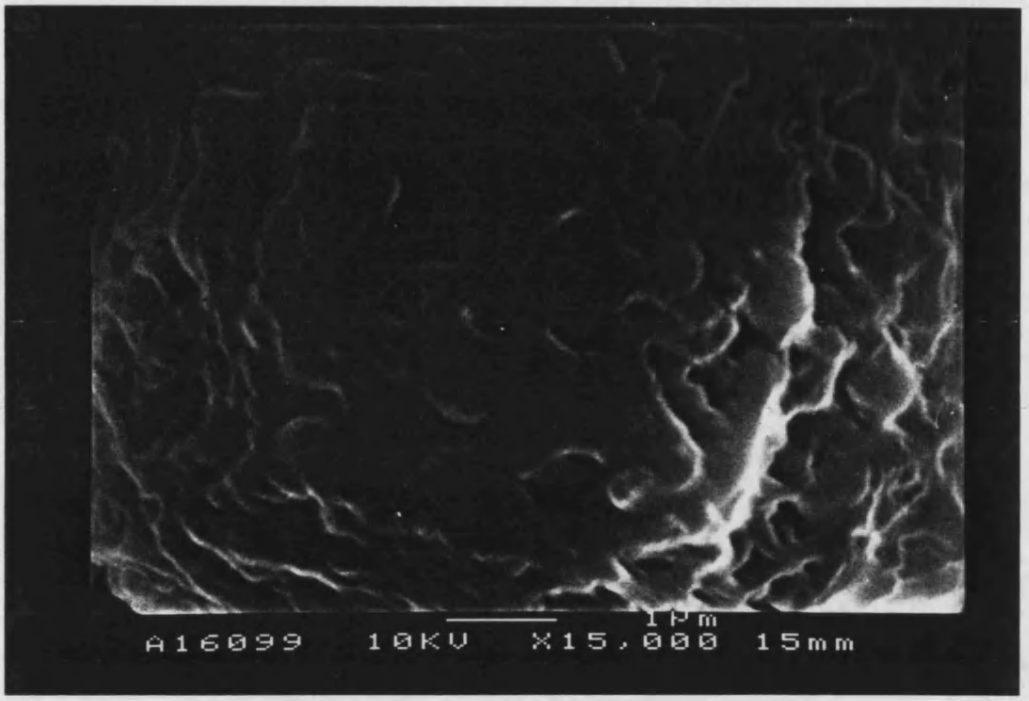

(b)

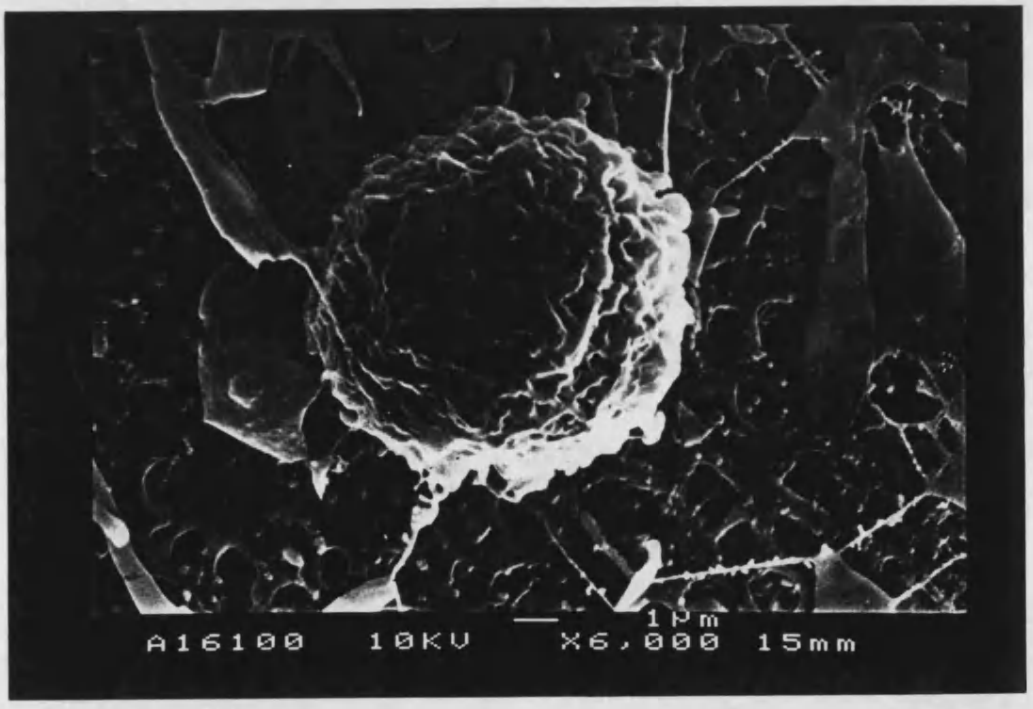

Figure 8.2: A normal (unpermeabilised) L1210 cell as viewed by SEM.

(a) A cell depicted at a magnification of x15,000, (b) the same cell depicted at a magnification of x6,000.

(a)

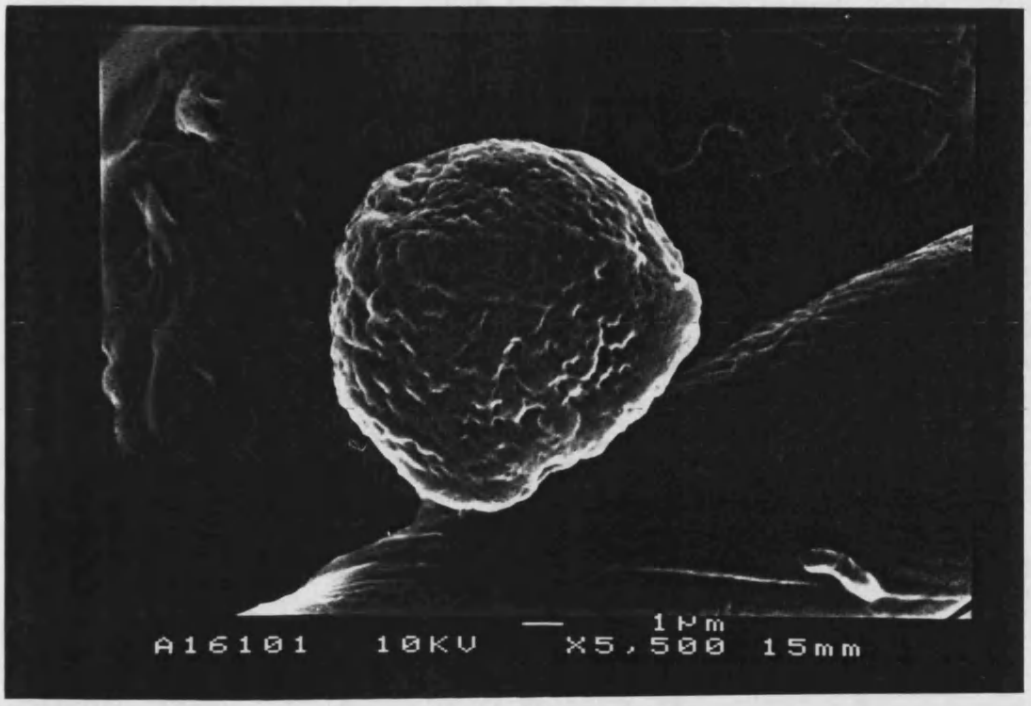

(b)

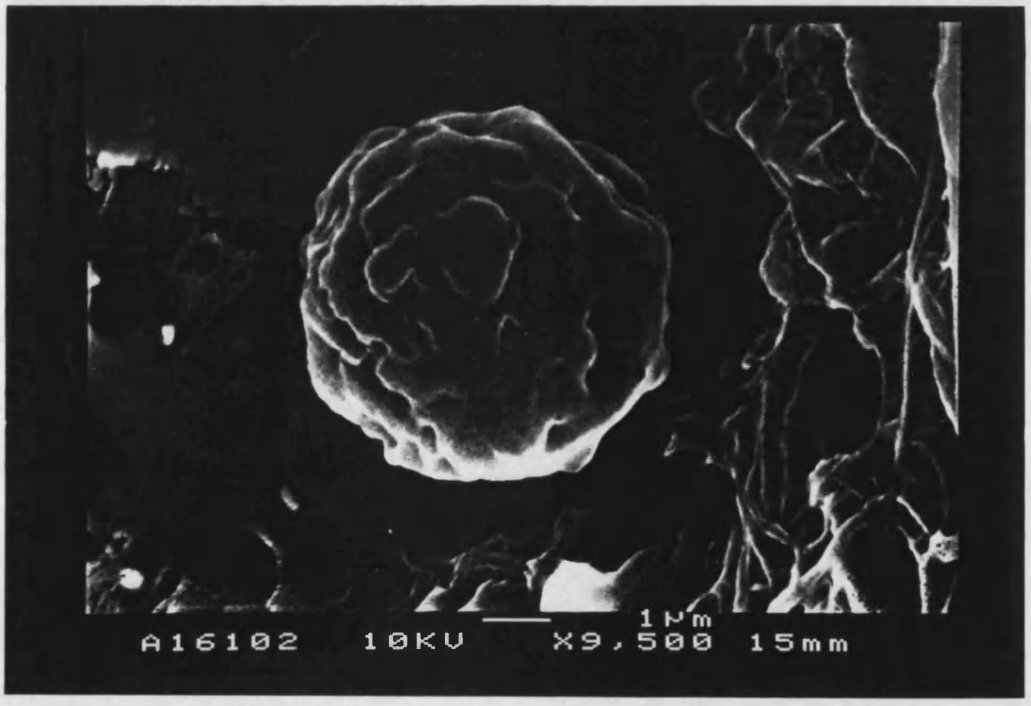

Figure 8.3: L1210 cells treated by hypotonic shock as viewed by SEM.

(a) A cell depicted at a magnification of x 5,500, (b) another cell depicted at a magnification of x9,500.

(a)

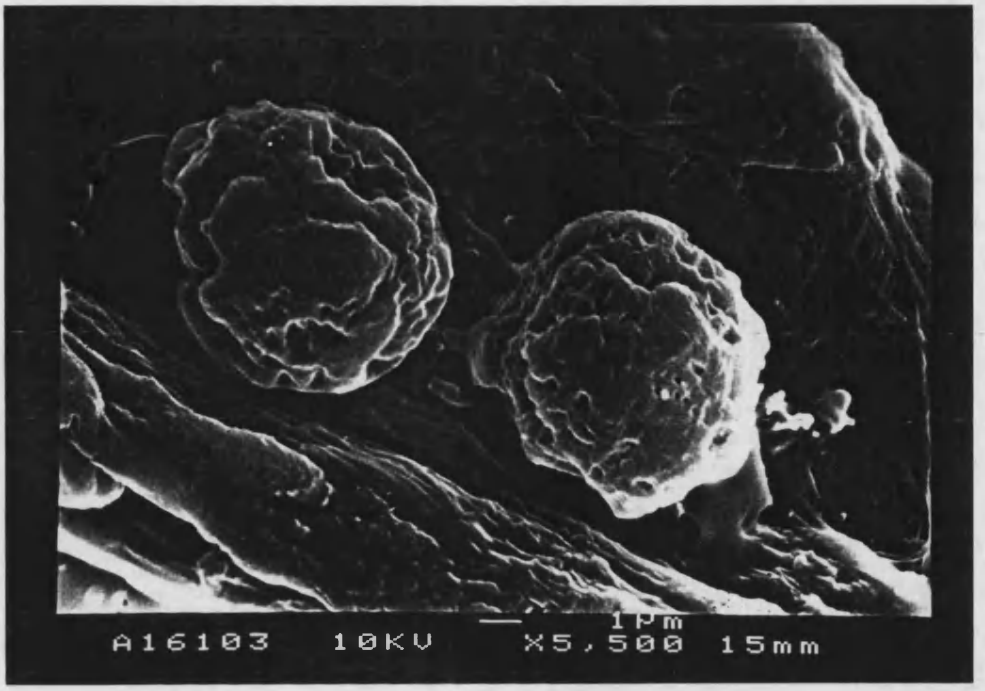

(b)

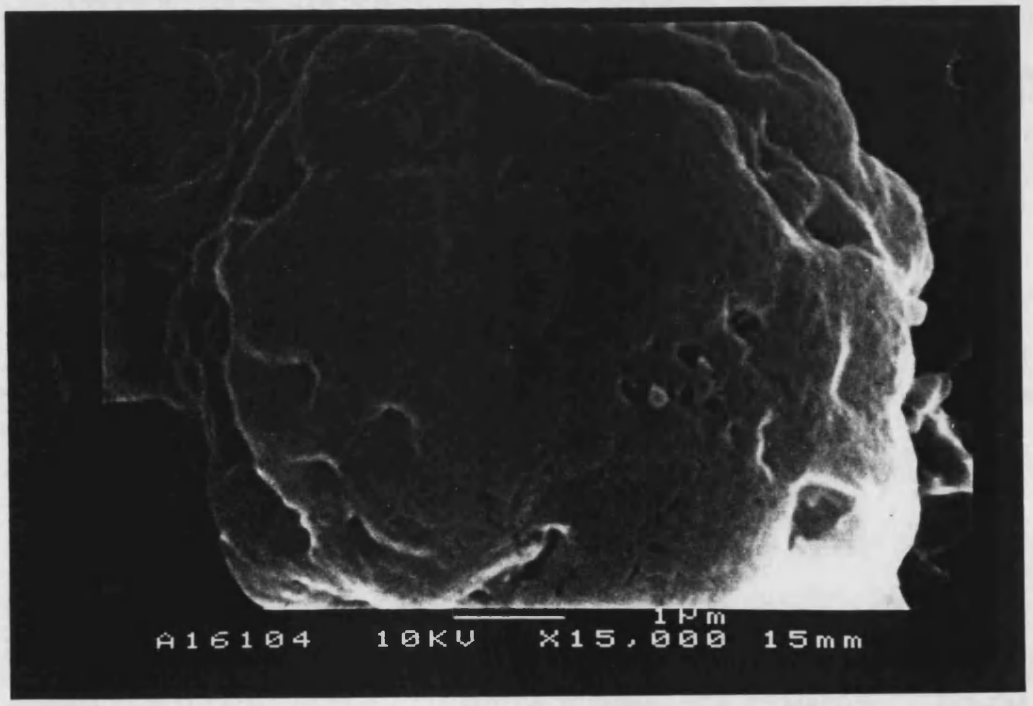

Figure 8.4: L1210 cells treated by hypotonic shock as viewed by SEM.

(a) Cells depicted at a magnification of x 5,500, (b) the cell on the right depicted at a magnification of x15,000.

(a)

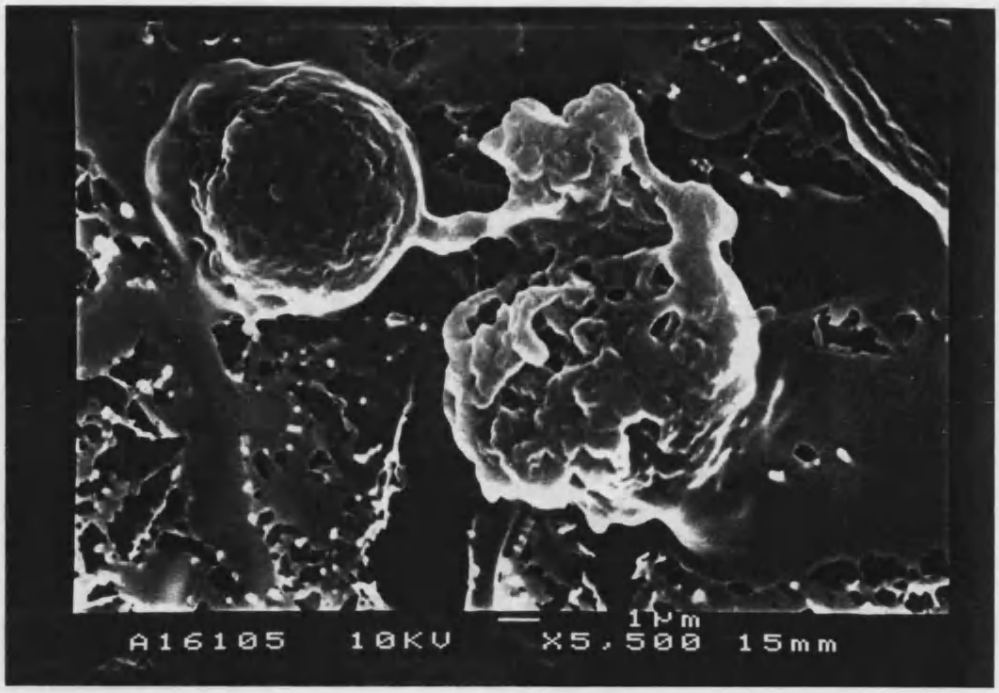

(b)

Figure 8.5: L1210 cells treated by hypotonic shock as viewed by SEM.

(a) Two cells depicted at a magnification of x5,500, (b) three different cells depicted at a magnification of x3,300.

(a)

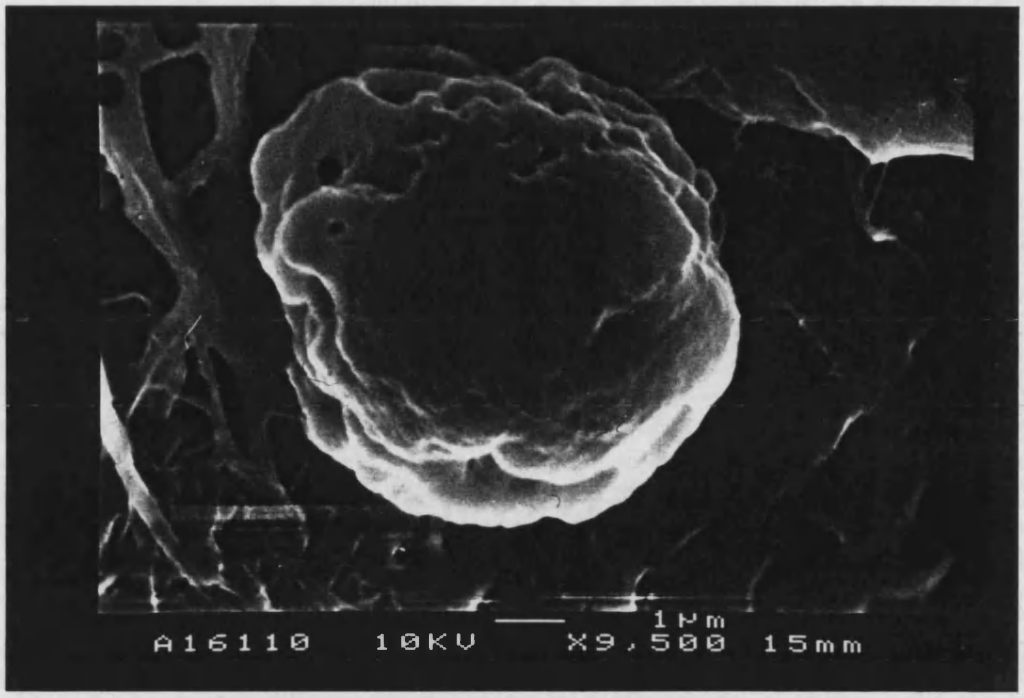

(b)

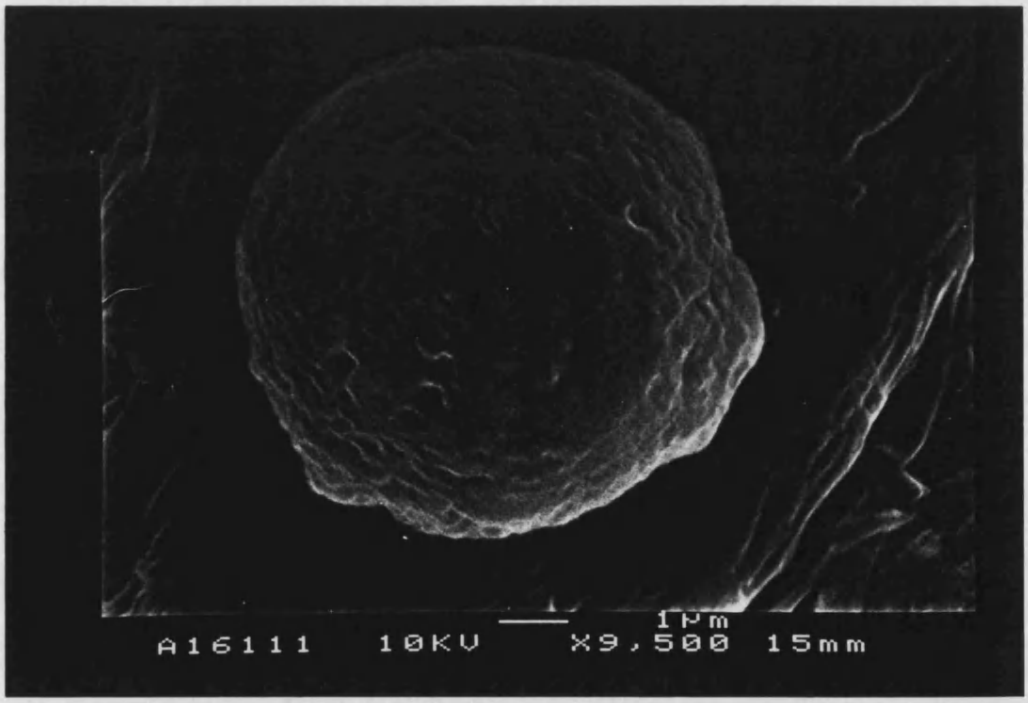

Figure 8.6: L1210 cells treated with digitonin as viewed by SEM.

(a) A cell depicted at a magnification of x9,500, (b) another cell depicted at the same magnification.

(a)

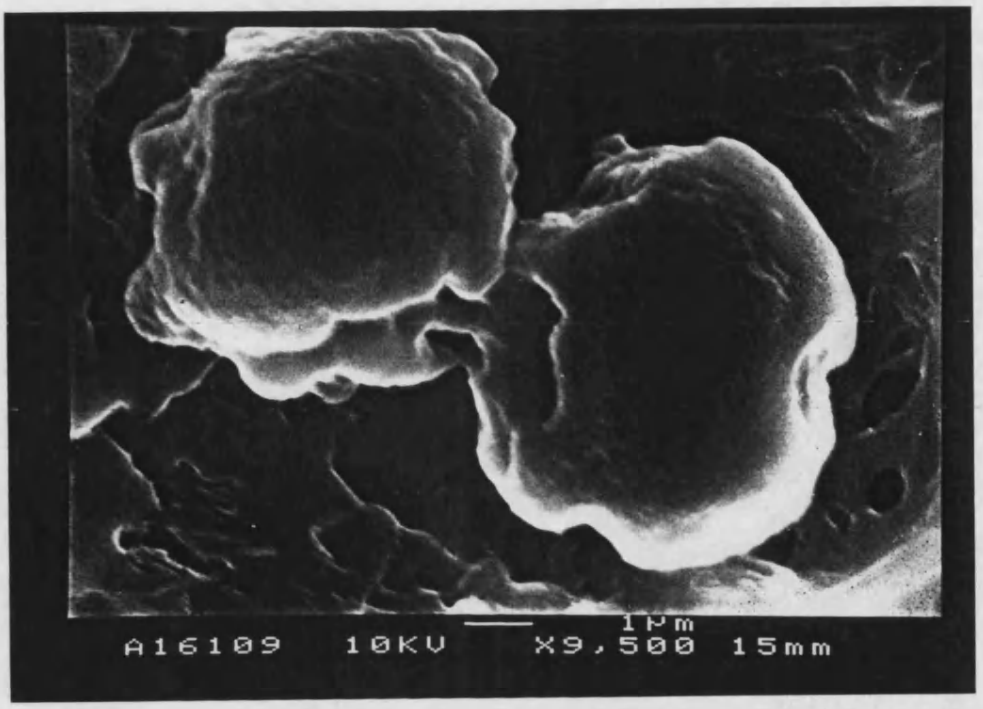

(b)

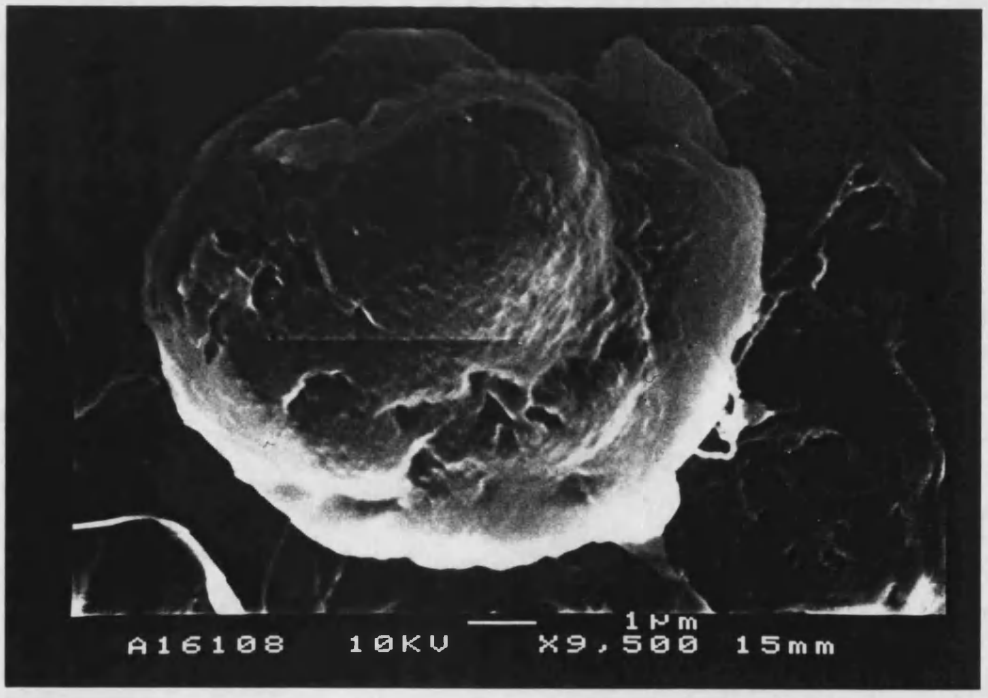

Figure 8.7: L1210 cells treated with digitonin as viewed by SEM.

(a) Two cells depicted at a magnification of x9,500, (b) another cell depicted at the same magnification.

Figure 8.8: L1210 cells treated with digitonin as viewed by SEM.

Several cells depicted at a magnification of x3,000.

(a)

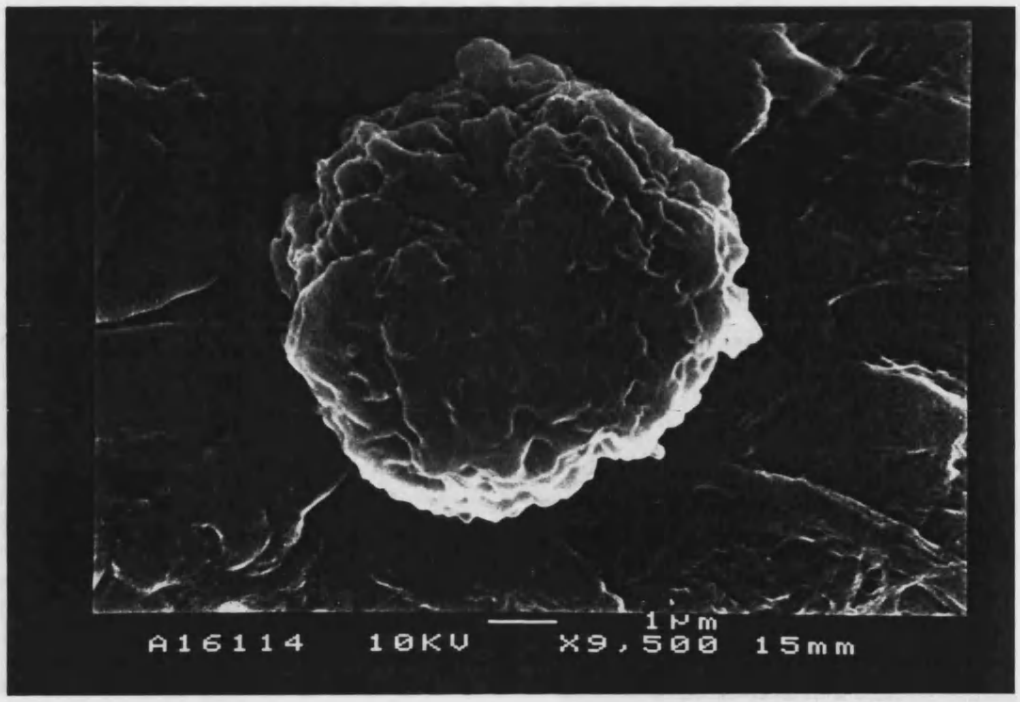

(b)

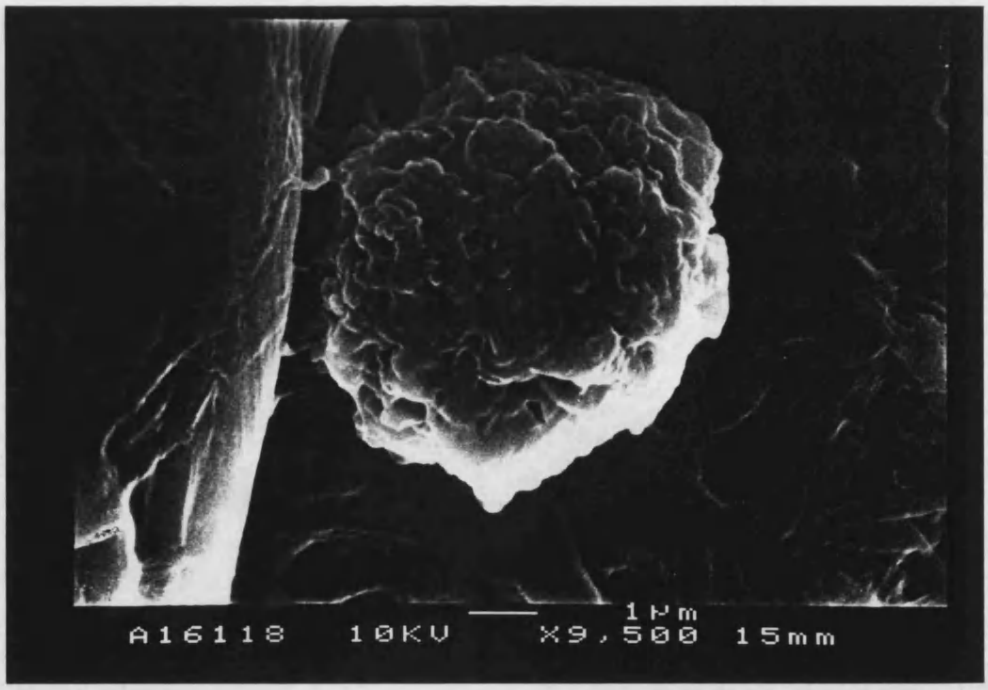

Figure 8.9: L1210 cells insonated at 3 MHz, 1.0 Wcm^{-2}, CW for 3 min, as viewed by SEM.

(a) A cell depicted at a magnification of x9,500, (b) another cell depicted at the same magnification.

(a)

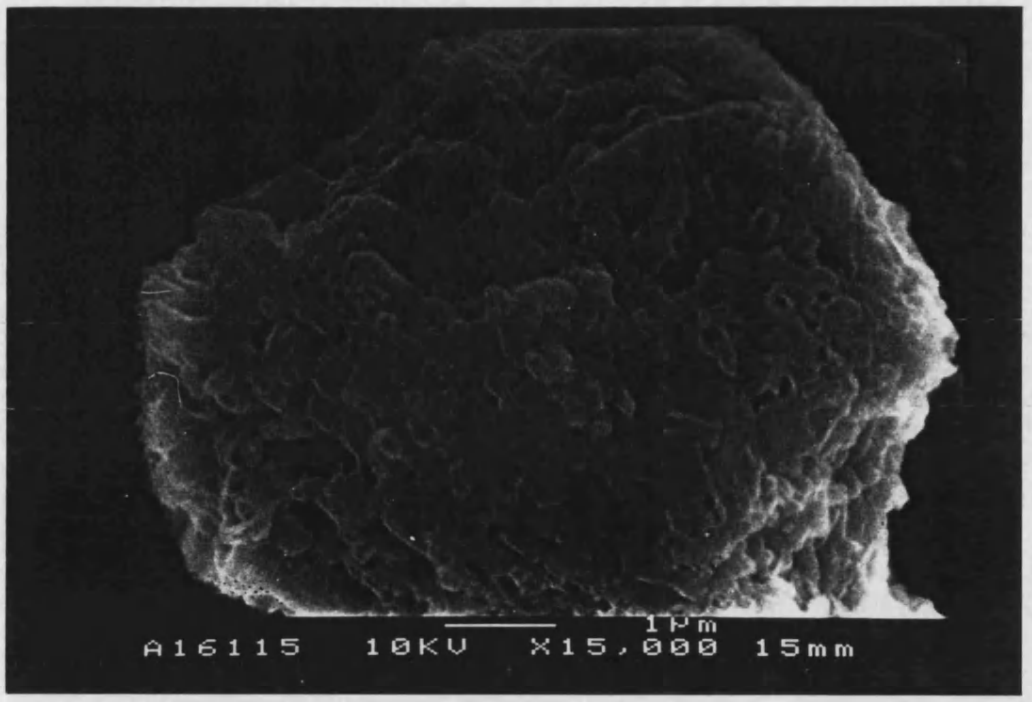

(b)

Figure 8.10: L1210 cells insonated at 3 MHz, 1.0 Wcm^{-2}, CW for 3 min, as viewed by SEM.

(a) A cell depicted at a magnification of x15,000, (b) and two cells depicted at a magnification of x5,500.

(a)

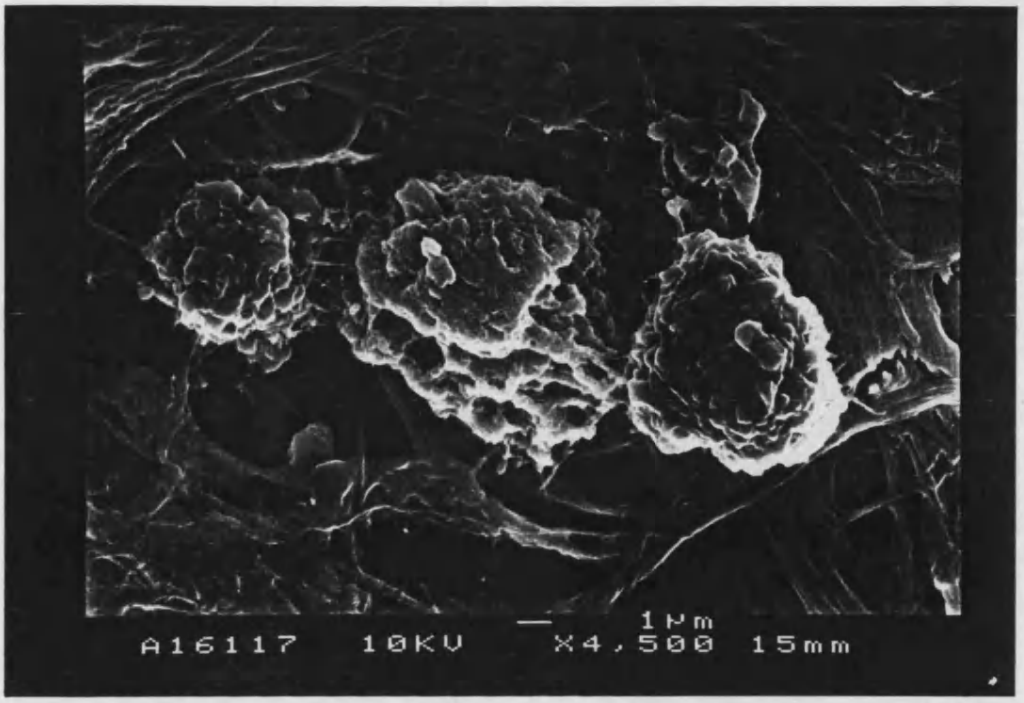

(b)

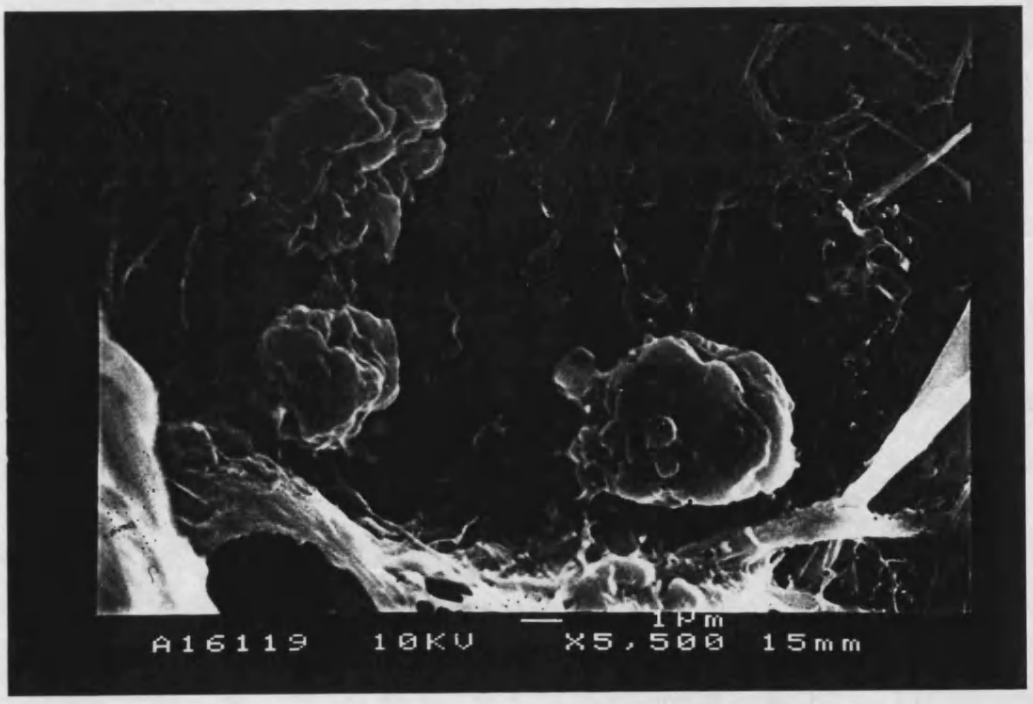

Figure 8.11: L1210 cells insonated at 3 MHz, 1.0 Wcm^{-2}, CW for 3 min, as viewed by SEM.

(a) Cells depicted at a magnification of x4,500, (b) another group of cells depicted at a magnification of x5,500.

(a)

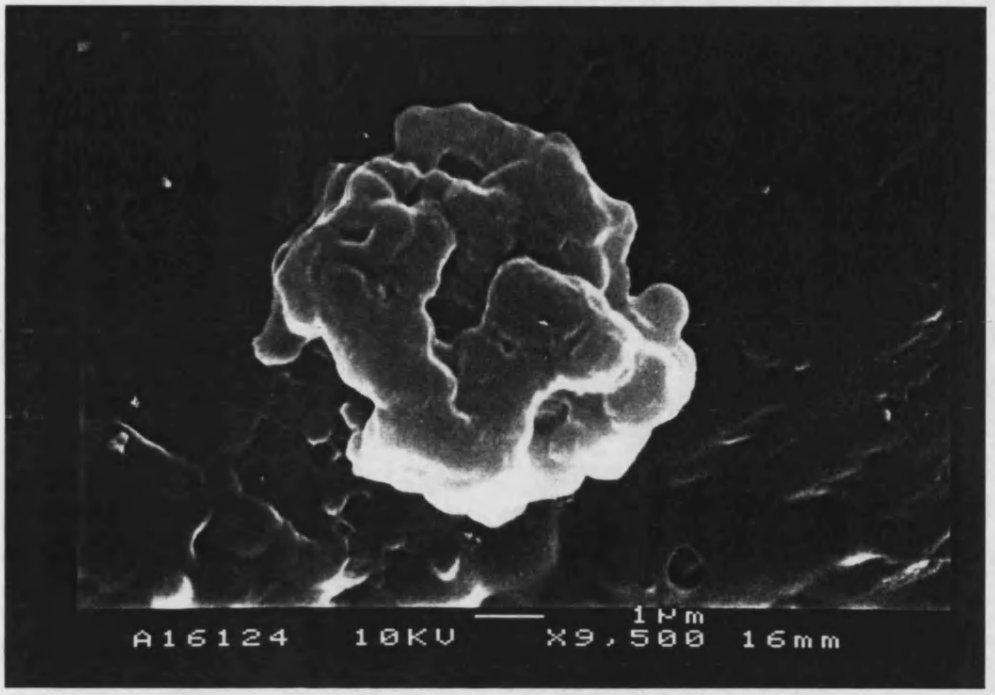

(b)

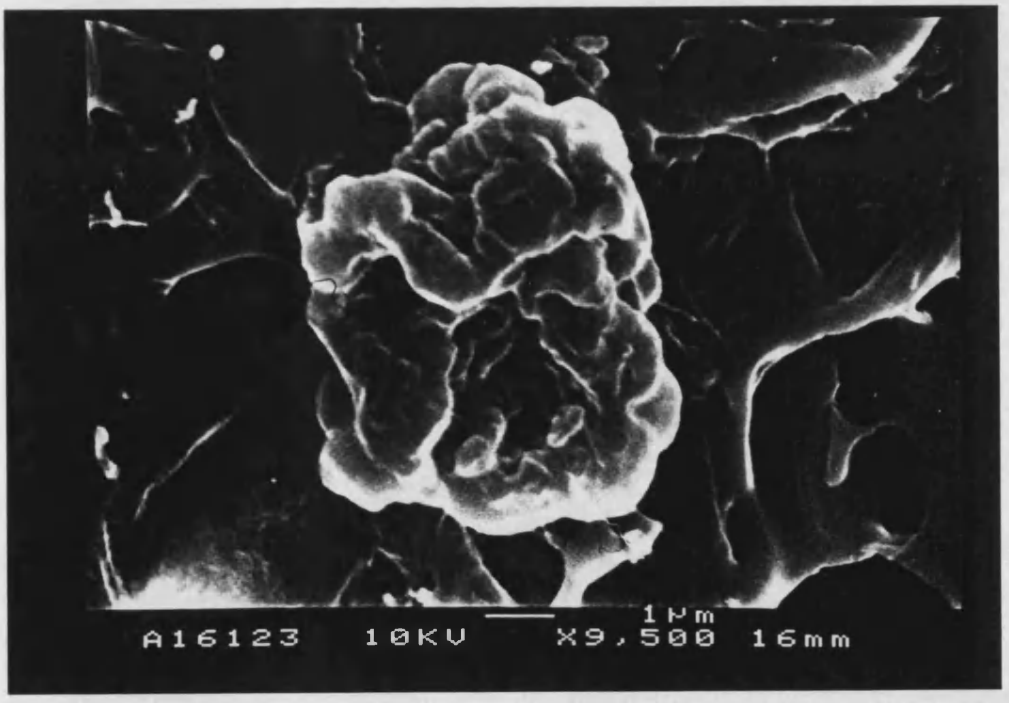

Figure 8.12: L1210 cells insonated at 1 MHz, 1.0 Wcm^{-2}, CW for 3 min, as viewed by SEM.

(a) A cell depicted at a magnification of x9,500, (b) another cell depicted at the same magnification.

(a)

(b)

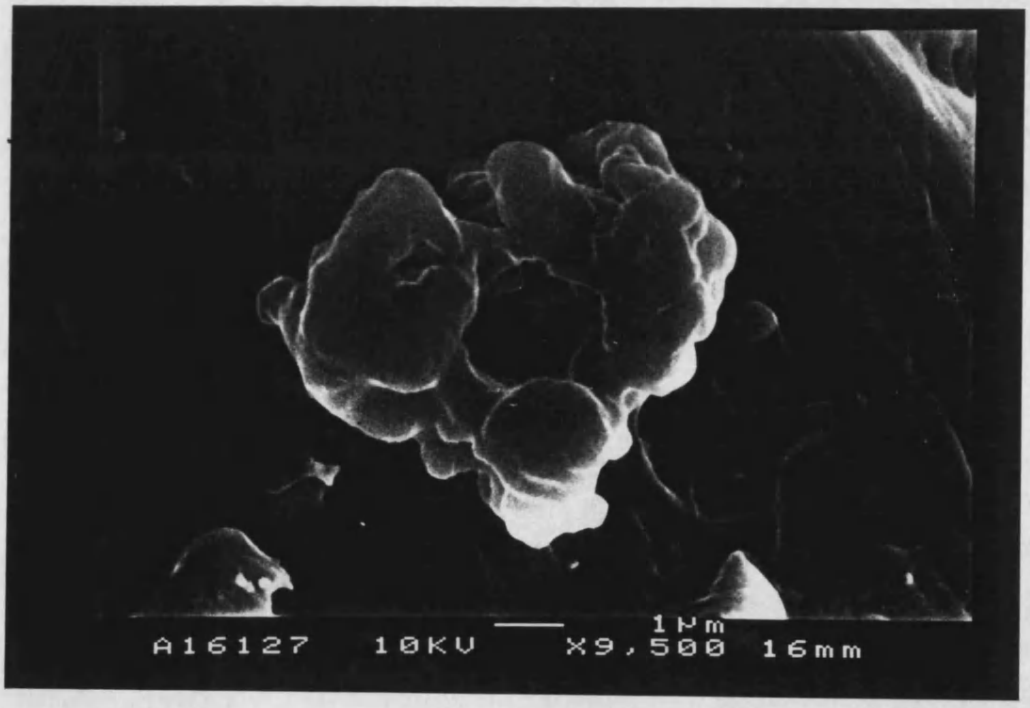

Figure 8.13: L1210 cells insonated at 1 MHz, 1.0 Wcm^{-2}, CW for 3 min, as viewed by SEM.

(a) A cell depicted at a magnification of x15,000, (b) another cell depicted a magnification of x9,500.

(a)

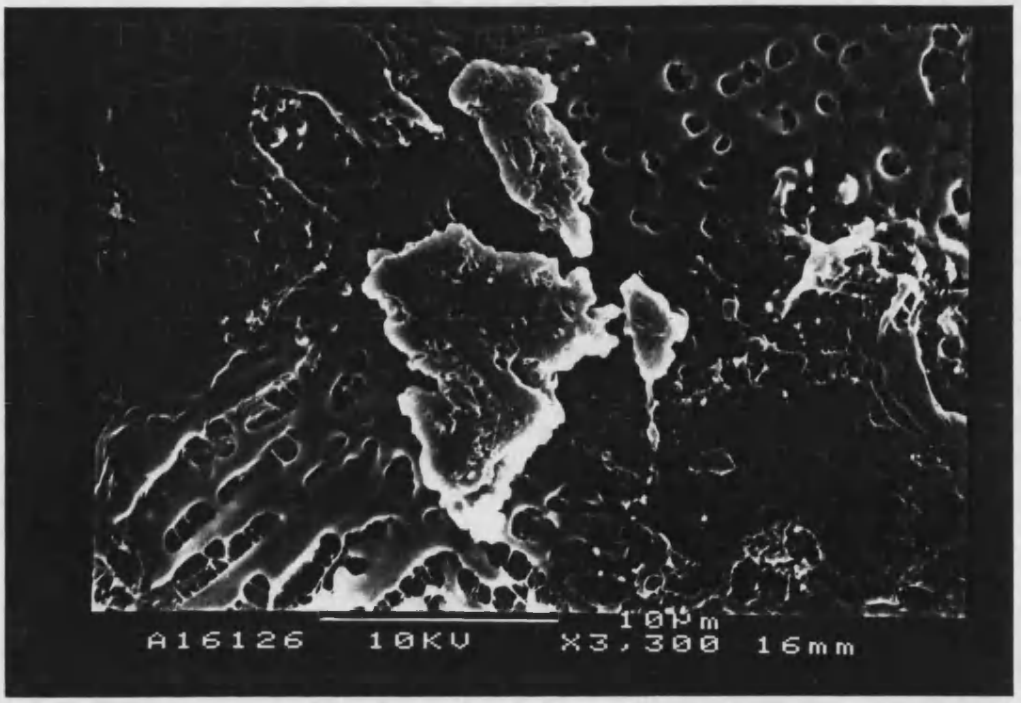

(b)

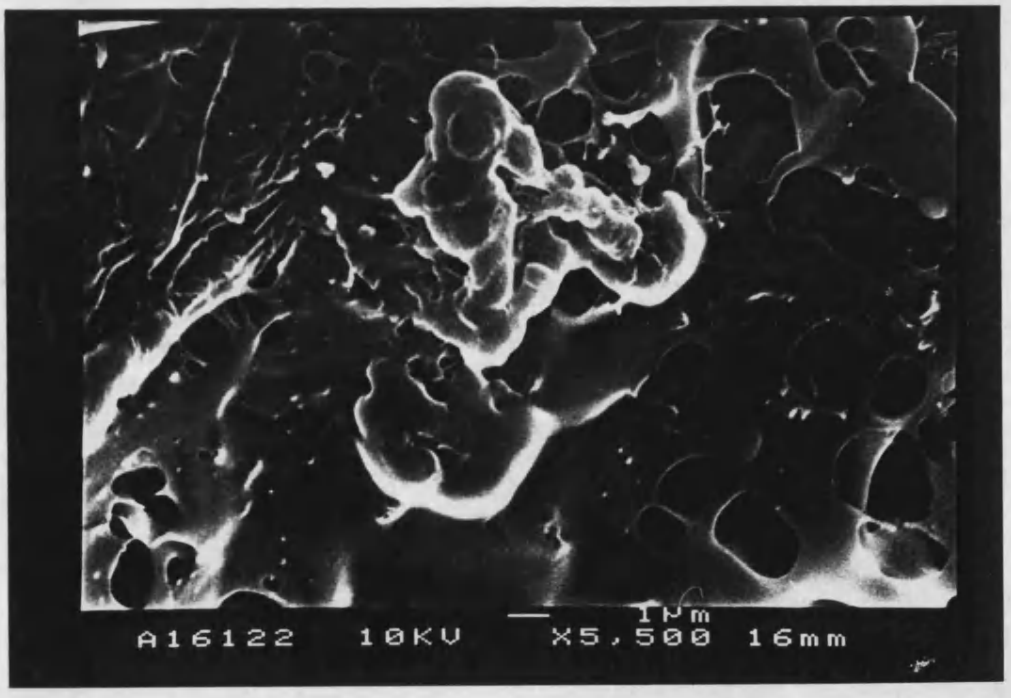

Figure 8.14: L1210 cells insonated at 1 MHz, 1.0 Wcm^{-2}, CW for 3 min, as viewed by SEM.

(a) Cell debris at a magnification of x3,300, (b) more cell debris depicted at a magnification of x5,500.

8.4 Conclusions

The electron micrographs described in this chapter have produced some very interesting results. In both hypotonically shocked and digitonin exposed cells there was a 'smoothing' of the cell surface, perhaps suggesting that some kind of lipid stripping is involved in permeabilisation by these techniques. It was also clear that considerable physical damage was induced in both of these samples which accounts for the observed elevation in PARP activity seen in chapter 7. Unfortunately, it was not possible to confidently conclude that one of these techniques produced more damage than the other.

In the insonated cells, there seemed to be a retention of the 'fluffy' outer surface regardless of whether or not cells were damaged. This is interesting as during counting under the light microscope hypotonically shocked and digitonin treated cells were dark blue and discrete upon trypan blue staining while insonated cells were paler blue and far less discrete. The retention of this 'fluffy' exterior may well be due to the fact that permeabilisation by insonation is physical and instant in nature while both of the other methods are chemical and involve incubations.

There is a clear difference in the amount of cell damage seen at different ultrasonic frequencies. At 3 MHz cells were less permeable and accordingly were less damaged when viewed under the EM, in fact some cells were still pretty much intact. At 1 MHz, cells were almost totally permeable and were very damaged upon viewing under the EM. Cells in this sample were very diffuse and large amounts of debris were observed. This increase in cellular damage observed at lower frequencies suggests that cavitation is responsible for the effects observed in insonated cells, since the cavitation threshold rises with frequency. This is in agreement with the conclusion of chapter 5 (5.13) in that sonoporation is likely to be a cavitational effect and furthermore it is probably due to mechanical effects rather than sonochemicals.

It is curious that in some cases a severely damaged cell was observed to be associated with another healthy cell (Figure 8.5(a) and (b), Figure 8.8, Figure 8.11(a)). The

reason for this is unknown, although the phenomenon was observed across the spectrum of permeabilisation techniques. However, cell-splitting was only observed within the insonated samples (Figure 8.11(b)) and is thought to occur due to either the classical mechanical effects of ultrasound or the mechanical effects associated with cavitation bubbles. It is likely that this kind of cell splitting and disintegration is responsible for the large amounts of debris observed within the 1 MHz sample.

Further study using electron microscopy in the presence of free radical scavengers and under different ultrasonic parameters is likely to yield useful and illuminating results.

CHAPTER NINE

CONCLUSIONS

Mathematical modelling has clearly shown that therapeutic ultrasound incident on polystyrene microcarriers cannot provide sufficient energy to sustain temperatures compatible with cell growth under biofermentation conditions. Unfortunately, while alterations in the ultrasonic parameters are likely to produce the required heat elevations in polystyrene beads, simultaneous adverse cellular effects are almost inevitable. Microcarriers constructed from a more dense material would also allow satisfactory heating to occur but would lack buoyancy. Unless an acceptable balance of alterations can be determined it seems that ultrasound has no future as a heating mechanism in biofermentation. Despite the results of these unfavourable calculations it was possible to maintain cell health under certain ultrasonic conditions. The waterbath system (4.2.1) allowed cells to survive unperturbed, at least when measured by the methods of damage detection in this thesis, to the extent that other less 'kind' systems had to be designed in order to observe bioeffects.

Therapeutic ultrasound was confirmed as an agent with a great deal of potential to cause adverse bioeffects depending on both the biological and the physical exposure conditions. Damage was shown to occur at different sites in the cell by employing a range of biological detection methods, while maintaining similar types of exposure, an approach which has not been described elsewhere in the literature.

Alterations in the integrity of the cell membrane were observed by trypan blue exclusion and the successful stable transfection of foreign DNA into host cells. The latter also indicated that DNA breaks were induced, at least transiently, and there was also evidence of an upregulation in the rate of integration. While trypan blue exclusion was important in the identification of ultrasonic parameters which influenced the

magnitude of membrane damage, such as, duration of exposure, intensity of the beam, frequency and to a lesser extent cell density. Increases in PARP activity showed that chromatin structure was quite clearly damaged by cellular insonation, although it was impossible to differentiate between subtle changes in the ultrasonic parameters by enzyme activity. PARP activity had not previously been used as a tool to measure ultrasonic damage and proved to be somewhat difficult to harness, despite the fact that it is extremely sensitive to small numbers of DNA single strand breaks.

Electron microscopy revealed the severity of the physical damage insonation can produce. Cells were clearly holed, divided or fragmented. Comparison with other methods of permeabilisation showed that ultrasonic damage allowed the 'fluffy' cellular coat to remain, where chemical techniques did not. The dramatic effects illuminated by this technique have not previously been described.

Although the exact mechanism of a particular bioeffect was extremely difficult to elucidate, probable candidates were identified as mechanical, in the case of cell lysis and sonoporation, the mechanical effects associated with cavitation regarding membrane permeabilisation, and free radical generation where DNA damage was induced.

The implications of this work for the use of ultrasound in medicine are complex and should be considered with caution. The key to experimentation rests in the identification of the potential ultrasonic bioeffect inducing phenomena which may occur as a result of a particular type of examination. Thereafter an experimental system must be designed to investigate the resultant effects on cells. However, this is a far from easy process and the effects of ultrasound on the patients who are exposed remains largely unknown.

Al-Karmi, A. M., Dinno, M. A., Stoltz, D. A. *et al.* (1994) Calcium and the effects of ultrasound on frog skin. *Ultrasound Med. Biol.* 20(1):73-81.

Althaus, F. R. and Richter, C. (1987) *ADP-ribosylation of Proteins, Enzymology and Biological Significance.* Springer Verlag, Berlin.

Alvarez-Gonzalez, R and Althaus, F. R. (1989) Poly(ADP-ribose) catabolism in mammalian cells exposed to DNA damaging agents. *Mutation Res.* 218:67-74.

Alvarez-Gonzalez, R. and Jacobson M. K. (1987) Characterization of polymer ADP-ribose generated *in vitro* and *in vivo. Biochem.* 26:3218-3224.

Andersson, L. C., Nilsson, K. and Gahmberg, C. G. (1979) K562-A human erythroleukemic cell line. *Int. J. Cancer* 23:143-147.

Armour, E. P. and Corry, P. M. (1982) Cytotoxic effects of ultrasound *in vitro*: dependence on gas content, frequency, radical scavengers and attachment. *Radiat. Res.* 89:369-380.

Bachtold, M. R., Rinaldi, P. C., Jones, J. P. *et al.* (1998) Focused ultrasound modifications of neural circuit activity in a mammalian brain. *Ultrasound Med. Biol.* 24(4):557-565.

Baggs, R. Penney, D. P., Cox., C. *et al.* (1996) Thresholds for ultrasonically induced lung hemorrhage in neonatal swine. *Ultrasound Med. Biol.* 22(1):119-128.

Bao, S., Thrall, B. D. and Miller, D. L. (1997) Transfection of a reporter plasmid into cultured cells by sonoporation *in vitro. Ultrasound Med. Biol.* 23(6):953-959.

Barnett, S. B., Rott, H-D., ter Haar, G. R. *et al.* (1997) The sensitivity of biological tissue to ultrasound. *Ultrasound Med. Biol.* 23(6):805-812.

Barnett, S. B., ter Harr, G. R., Ziskin, M. C. *et al.* (1994) Current status of research on biophysical effects of ultrasound. *Ultrasound Med. Biol.* 20(3):205-218.

Benjamin, R. C. and Gill, D. M. (1980) Poly(ADP-ribose) synthesis *in vitro* programmed by damaged DNA. *J. Biol. Chem.* 255(21):10502-10508.

Boundy, R. H. and Boyer, R. F. (1952) *Styrene. Its Polymers, Co-polymers and Derivatives.* Reinhold Publishing Corporation. New York.

Boyer, R. F., Keskkula, H. and Platt, A. E. (1970) *Styrene Polymers*. John Wiley and Sons Inc., London.

Brayman, A. A., Church, C. C. and Miller, M. W. (1996) Re-evaluation of the concept that high cell concentrations "protect" cells *in vitro* from ultrasonically induced lysis. *Ultrasound Med. Biol.* 22(4):497-514.

Carstensen, E. L., Kelly, P., Church, C. C. *et al.* (1993) Lysis of erythrocytes by exposure to CW ultrasound. *Ultrasound Med. Biol.* 19(2):147-165.

Chandraratna, P. A. N., Gallet, J., Jones, J. P. *et al.* (1998) An investigation of possible effects of high-frequency ultrasound on cellular integrity of cultured fibroblasts. *Ultrasound Med. Biol.* 24(6):911-914.

Chapman, I. V., M^{ac}Nally, N. A. and Tucker, S. (1979) Ultrasound-induced changes in the rates of influx and efflux of potassium ions in rat thymocytes *in vitro*. *Ultrasound Med. Biol.* 6:47-58.

Chen, L., ter Harr, G., Hill, C. R. *et al.* (1998) Treatment of implanted liver tumors with focused ultrasound. *Ultrasound Med. Biol.* 24(9):1475-1488.

Coleman, A. J. and Saunders, J. E. (1992) A review of the physical properties and biological effects of the high amplitude acoustic fields used in extracorporeal lithotripsy. *Ultrasonics* 31(2):75-89.

Dalecki, D., Raeman, C. H., Child, S. Z. *et al.* (1996) A test for cavitation as a mechanism for intestinal hemorrhage in mice exposed to a piezoelectric lithotripter. *Ultrasound Med. Biol* 22(4):493-496.

Debus, J., Spoo, J., Jenne, J. *et al.* (1999) Sonochemically induced radicals generated by pulsed high-energy ultrasound *in vitro* and *in vivo*. *Ultrasound Med. Biol.* 25(2):301-306.

De Deyne, P. G. and Kirsch-Volders, M. (1995) *In vitro* effects of therapeutic ultrasound on the nucleus of human fibroblasts. *Phys. Therapy* 75:629-634.

Delacretaz, G., Rink, K., Pittomvils, G. *et al.* (1995) Importance of the implosion of ESWL-induced cavitation bubbles. *Ultrasound Med. Biol.* 21(1):97-103.

De Murcia, G., Menissier-de Murcia, J. and Schreiber, V. (1991) Poly(ADP-ribose) polymerase: molecular biological aspects. *BioEssays* 13(9):455-462.

De Murcia, G., Schreiber, V., Molinete, M., *et al.* (1994) Structure and function of poly(ADP-ribose) polymerase. *Mol. Cell. Biochem.* 138:15-24.

Dinno, M. A., Crum, L. A. and Wu, J. (1989) The effect of therapeutic ultrasound on electrophysiological parameters of frog skin. *Ultrasound Med. Biol.* 15(5):461-470.

Dinno, M. A., Dyson, M., Young, S. R. *et al.* (1989) The significance of membrane changes in the safe and effective use of therapeutic and diagnostic ultrasound. *Phys. Med. Biol.* 34(11):1543-1552.

Doida, Y., Brayman, A. A. and Miller, M. W. (1992) Modest enhancement of ultrasound-induced mutations in V-79 cells *in vitro*. *Ultrasound Med. Biol.* 18(5):465-469.

Doida, Y. Marcello, K. R., Brayman, A. A. *et al.* (1998) Sonochemicals increase the mutation frequency of V79 cells *in vitro*. *Ultrasound Med. Biol.* 24(8):1209-1213.

Doida, Y., Miller, M. W., Cox, C. *et al.* (1990) Confirmation of an ultrasound-induced mutation in two *in-vitro* mammalian cell lines. *Ultrasound Med. Biol.* 16(7):699-705.

Durkacz, B. W., Omidiji, O., Gray, D. A. *et al.* (1980) $(ADP\text{-}ribose)_n$ participates in DNA excision repair. *Nature* 283:593-596.

Dyson, M. and Young, S. R. (1988) Acceleration of tissue repair by low intensity ultrasound applied during the inflammatory phase. *Phys. Therapy.* 68(5):812,R186.

Earle, W. R. (1943) Production of malignancy *in vitro*. IV. The mouse fibroblast cultures and changes seen in the living cells. *J. Nat. Cancer Inst.* 4:165-212.

Edmonds, P. D. and Sancier, K. M. (1983) Evidence for free radical production by ultrasonic cavitation in biological media. *Ultrasound Med. Biol.* 9(6):635-639.

Edwards, R. (1999) Shadow of a doubt. *New Scientist* 12th June:4.

Ellwart, J. W., Brettel, H. and Kober, L. O. (1988) Cell membrane damage by ultrasound at different cell concentrations. *Ultrasound Med. Biol.* 14(1):43-50.

Ernst, E. (1995) Ultrasound for cutaneous wound healing. *Phlebology* 10(1):2-4.

Ewigman, B., Green, J. and Lumley, J. (1993) Ultrasound during pregnancy: A Discussion. *Birth Issues in Perinatal Care* 20(4):212-215.

Fahnestock, M., Rimer, V. G., Yamawaki, R. M. *et al.* (1989) Effects of ultrasound exposure *in vitro* on neuroblastoma cell membranes. *Ultrasound Med. Biol.* 15(2):133-144.

Felger, P. L. and Ringbold, G. M. (1989) Cationic liposome-mediated transfection. Nature 337:387-388.

Fiskum, G., Craig, S. W., Decker, G. L. *et al.* (1980) The cytoskeleton of digitonin-treated rat hepatocytes. *PNAS* 77(6):3430-3434.

Foley, G. E., Drolet, B. P., M°Carthy, R. E. *et al.* (1960) Isolation and serial propagation of malignant and normal cells in semi-defined media. Origins of CCRF cell lines. *Cancer Res.* 20:930-939.

Fry, F. J., Sanghvi, N. T., Foster, R. S. *et al.* (1995) Ultrasound and microbubbles: their generation, detection and potential utilization in tissue and organ therapy-experimental. *Ultrasound Med. Biol.* 21(9):1227-1237.

Fuciarelli, A. F., Sisk, E. C., Thomas, R. M. *et al.* (1995) Induction of base damage in DNA solutions by ultrasonic cavitation. *Free Rad. Biol. Med.* 18(2):231-238.

Goldberg, R. B. and Kimmelman, B. A. (1988) *Medical Diagnostic Ultrasound: A Retrospective on its 40th Anniversary.* Rochester: Eastman Kodak Company.

Gray, R. J. M., Quayle, A. A., Hall, C. A. *et al.* (1994) Physiotherapy in the treatment of temporomandibular joint disorders: a comparative study of four treatments. *Br. Dent. J.* 176(7) 257-261.

Greenleaf, W. J., Bolander, M. E., Sarkar, G. *et al.* (1998) Artificial cavitation nuclei significantly enhance acoustically induced cell transfection. *Ultrasound Med. Biol.* 24(6):587-595.

Halldorsson, H., Gray, D. A. and Shall, S. (1978) Poly(ADP-ribose) polymerase activity in nucleotide permeable cells. *FEBS Lett.* 85(2):349-352.

Hatakeyama, K., Nemoto, Y., Ueda, K. *et al.* (1989) Poly(ADP-ribose) glycohydrolase and ADP-ribosyl group turnover. In, *ADP-riboseTtransfer Reactions. Mechanisms and Biological Significance.* (edited by Jacobson, M.K. and Jacobson, E.L.), Springer-Verlag, New York. 47-52.

Holland, C. K., Deng, C. X., Apfel, R. E. *et al.* (1996) Direct evidence of cavitation *in vivo* from diagnostic ultrasound. *Ultrasound Med. Biol.* 22(7):917-925

Hrazdira, I., Sulcova, A., Kellnerova, R. *et al.* (1995) Prenatal application of diagnostic ultrasound in mice. *Ultrasound Med. Biol.* 21(3):427-430.

Hutchison, D. J., Ittensohn, O. L. and Bjerregaard, M. R. (1966) Growth of L1210 mouse leukemia cells *in vitro*. *Expt. Cell Res.* 42:147-160.

ImaRx Pharmaceutical Corp., Tuson, Arizona, U.S.A. (1997) *Technical Report:Drug and Gene Delivery.*

Joersbo, M. and Brunstedt, J. (1990) Direct gene transfer to plant protoplasts by mild sonication. *Plant Cell Reports* 9:207-210.

Joersbo, M. and Brunstedt, J. (1992) Sonication: A new method for gene transfer to plants. *Physiologia Plantarum* 85:230-234.

Kameshita, I., Matsuda, Z., Taniguchi, T. *et al.* (1984) Poly(ADP-ribose) synthetase. Separation and identification of three proteolytic fragments as the substrate-binding domain, the DNA-binding domain, and the automodification domain. *J. Biol. Chem.* 259(8):4770-4776.

Kappus, S. (1997) *Nuclear ADP-ribosylation.* Ph.D. Thesis, University of Bath.

Kaufman, G. E. (1985) Mutagenicity of ultrasound in cultured mammalian cells. *Ultrasound Med. Biol.* 11(3):497-501.

Kaufman, G. E. and Miller, M. W. (1978) Growth retardation in Chinese hamster V-79 cells exposed to 1 MHz ultrasound. *Ultrasound Med. Biol.* 4:139-144.

Kaye, G. W. C. and Laby, T. H. (1973) *Tables of Physical and Chemical Constants and Some Mathematical Functions.* 14th Edition. Longmans, London.

Khan, A. U. and Wilson, T. (1995) Reactive oxygen species as cellular messengers. *Chemistry and Biology* 2:437-445.

Kim, H. J., Greenleaf, J. F., Kinnick, R. R. *et al.* (1996) Ultrasound-mediated transfection of mammalian cells. *Human Gene Therapy* 7:1339-1346.

Kondo, T. and Kano, E. (1988) Effect of free radicals induced by ultrasonic cavitation on cell killing. *Int. J. Radiat. Biol.* 54:955-962.

Kruman, I. I., Gukovskaya, A. S., Petrunyaka, V. V. *et al.* (1992) Apoptosis of murine BW 5147 thymoma cells induced by cold shock. *J. Cell. Physiol.* 153:112-117.

Le Rhun, Y., Kirkland, J. B. and Shan, G. M. (1998) Cellular responses to DNA damage in the absence of poly(ADP-ribose) polymerase. *Biochem. Biophys. Res. Comm.* 245:1-10.

Lindal, T., Satoh, M. S., Poirier, G. G. *et al.* (1995) Post-translational modification of poly(ADP-ribose) polymerase induced by DNA strand breaks. *TIBS* 20:405-412.

Love, L. A. and Kremkau, F. W. (1980) Intracellular temperature distribution produced by ultrasound. *J. Accoust. Soc. Am.* 67(3):1045-1050.

Malcolm, A. L. and ter Harr, G. R. (1996) Ablation of tissue volumes using high intensity focused ultrasound. *Ultrasound Med. Biol.* 22(5):659-669.

Margulies, N., Abraham, V., Way, J. S. *et al.* (1991) Reversible biochemical changes in the developing rat central nervous system following ultrasound exposure. *Ultrasound Med. Biol.* 17(4):383-390.

Martin, A. O., Madsen, E. L., Dyer, A.R. *et al.* (1991) Sister chromatid exchange analysis of human cells exposed to diagnostic levels of ultrasound. *J. Ultrasound Med.* 10:665-670.

Matthews, J. C., Harder, W. L., Richardson, W. K. *et al.* (1993) Inactivation of firefly luciferase and rat erythrocyte ATPase by ultrasound. *Membrane Biochem.* 10:213-220.

Matulonis, U. A., Dosiou, C., Lamont, C. *et al.* (1995) Role of B7-1 in mediating an immune response to myeloid leukemia cells. *Blood* 85(9):2507-2515.

Maxwell, L., Collecutt, T., Gledhill, M. *et al.* (1994) The augmentation of leucocyte adhesion to endothelium by therapeutic ultrasound. *Ultrasound Med. Biol.* 20(4):383-390.

M^{c}Creery, T. P., Sweitzer, R. H., Caldwell, V. E. *et al.* (1998a) Ultrasound enhanced lipofection in fish and mice. *J. Ultrasound Med.* 16:S1-S148,8542.

M^{c}Creery, T. P., Sweitzer, R. H., Caldwell, V. E. *et al.* (1998b) Upregulation of mRNA levels and repair gene expression after exposure to ultrasound.. *J. Ultrasound Med.* 16:S1-S148,8310.

Meidan, V. M., Walmsley, A. D. and Irwin, W. J. (1995) Phonophoresis - is it a reality? *Internat. J. Pharm.* 118:129-149.

Merritt, C. R. B., Kremkau, F. W. and Hobbins, J. C. (1992) *Diagnostic ultrasound: bioeffects and safety*. Ultrasound. Obset. Gynecol. 2:366-374.

Miller, D. L., Bao, S. and Morris, J. E. (1999) Sonoporation of cultured cells in the rotating tube exposure system. *Ultrasound Med. Biol.* 25(1):143-149.

Miller, D. L., and Gies, R. A. (1998) Gas-body-based contrast agent enhances vascular bioeffects of 1.09 MHz ultrasound on mouse intestine. *Ultrasound Med. Biol.* 24(8):1201-1208.

Miller, M. W., Miller, D.L. and Brayman, A. A. (1996) A review of *in vitro* bioeffects of inertial ultrasonic cavitation from a mechanistic perspective. *Ultrasound Med. Biol.* 22(9):1131-1154.

Miller, D. L. and Thomas, R. M. (1993) A comparison of hemolytic and sonochemical activity of ultrasonic cavitation in a rotating tube. *Ultrasound Med. Biol.* 19(1):83-90.

Miller, D. L. and Thomas, R. M. (1995) Ultrasound contrast agents nucleate inertial cavitation *in vitro*. *Ultrasound Med. Biol.* 21(8):1059-1065.

Miller, D. L., Thomas, R. M. and Buschbom, R.L. (1995) Comet assay reveals DNA strand breaks induced by ultrasonic cavitation *in vitro*. *Ultrasound Med. Biol.* 21(6):841-848.

Miller, D. L., Thomas, R. M. and Frazier, M. E. (1991a) Single strand breaks in CHO cell DNA induced by ultrasonic cavitation *in vitro*. *Ultrasound Med. Biol.* 17(4):401-406.

Miller, D. L., Thomas, R. M. and Frazier, M .E. (1991b) Ultrasonic cavitation indirectly induces single strand breaks in DNA of viable cells *in vitro* by the action of residual hydrogen peroxide. *Ultrasound Med. Biol.* 17(7):729-735.

Mortimer, A. J. and Dyson, M. (1988) The effect of therapeutic ultrasound on calcium uptake in fibroblasts. *Ultrasound Med. Bio.* 14(6):499-506.

National Council on Radiation Protection and Measurements (NCRP) (1992a) Exposure criteria for medical diagnostic ultrasound. *NCRP Report No. 113*. Bethesda, M.D., U.S.A.

National Council on Radiation Protection and Measurements (NCRP) (1992b) Exposure criteria for medical diagnostic ultrasound. Part I: Criteria based on thermal mechanisms. Chapter 4: Calculations of Temperature Elevation: Basic Theory. *NCRP Report No. 113*. Bethesda, M.D., U.S.A.

Ohgushi, H., Yoshihara, K. and Kamiya, T. (1980) Bovine thymus poly(adenosine diphosphate ribose) polymerase. *J. Biol. Chem.* 255(13):6205-6211.

Ohtsu, E. and Nishizuka, Y. (1971) Nicotinamide phosphoribosyltransferase and NAD pyrophosphorylase from *Lactobacillus fructosus. Methods Enzymol.* 18B:127-132.

Onik, G. M., Downey, D. B. and Fenster, A. (1996) Three-dimensional sonographically monitored cryosurgery in a prostate phatom. *J. Ultrasound Med.* 16:267-270.

Perkins, M. A. (1989) A versatile force balance for ultrasound power measurement. *Phys. Med. Biol.* 34(11):1645-1651.

Pohl, P, Antonenko, Y. N. and Rosenfeld, E. (1993) Effect of ultrasound on pH profiles in the unstirred layers near planar bilayer lipid membranes measured by microelectrodes. *Biochimica et Biophysica Acta.* 1152:155-160.

Pohl, E. E., Rosenfeld, E. H., Pohl, P. *et al.* (1995) Effects of ultrasound on agglutination and aggregation of human erythrocytes *in vitro. Ultrasound Med. Biol.* 21(5):711-719.

Preiss, J., Schlaeger, R. and Hilz, H. (1971) Specific inhibition of poly ADP-ribose polymerase by thymidine and nicotinamide in HeLa cells. *FEBS Lett.* 19(4):244-246.

Preston, R. C. (1988) The NPL Ultrasound Beam Calibrator. *IEEE Transactions on Ultrasonics, Ferroelectronics, and Frequency Control.* 35(2):122-139.

Prise, K. M., Davies, S. and Michael, B. D. (1989) Cell killing and DNA damage in Chinese hamster V79 cells treated with hydrogen peroxide. *Int. J. Radiat. Biol.* 55(4):583-592.

Ramnarine, K. V., Nassiri, D. K., M^{c}Carthy, A. *et al.* (1998) Effects of pulsed ultrasound on embryonic development: an *in vitro* study. *Ultrasound Med. Biol.* 24(4): 575-585.

Read, N. D. (1991) Low-temp scanning electron microscopy of fungi and fungus-plant interactions. In, *Electron Microscopy of Plant Pathogens.* (edited by Mendgen, K. and Lesemada, D.,E.), Springer-Verlag, Berlin 17-29.

Reher, P., Elbeshir, E. I., Harvey, W. *et al.* (1997) The stimulation of bone formation *in vitro* by therapeutic ultrasound. *Ultrasound Med. Biol.* 23(8):1251-1258.

Riesz, P. and Kondo, T. (1992) Free radical formation induced by ultrasound and its biological implications. *Free Rad. Biol. Med.* 13:247-270.

Rumley, A. G. and Paterson, J. R. (1998) Analytical aspects of antioxidants and free radical activity in clinical biochemistry. *Ann. Clin. Biochem.* 35:181-200.

Sacks, P. G., Miller, M. W. and Sutherland, R. M. (1983) Response of multicell spheroids to 1-MHz ultrasonic irradiation: cavitation-related damage. *Radiat. Res.* 93:545-559.

Salvesen, K. A., Valten, L. J., Eiknes, S. H. *et al.* (1993) Routine ultrasonography *in-utero* and subsequent handedness and neurological development. *B.M.J.* 307:159-164.

Salz, H., Rosenfeld, E. H. and Wussling, M. (1997) Effect of ultrasound on the contraction of isolated myocardial cells of adult rats. *Ultrasound Med. Biol.* 23(1):143-149.

Sanford, K. K., Earle, W. R. and Likely, G. D. (1948) The growth *in vitro* of single isolated tissue cells. *J. Nat. Cancer Inst.* 9:229-246.

Schmidt, P., Rosenfeld, E. and Millner, R. (1987) Theoretical and experimental studies on the influence of ultrasound on immobilized enzymes. *Biotechnology and Bioengineering* 30:928-935.

Scovassi, A. I., Izzo, R., Franchi, E. *et al.* (1986) Structual analysis of poly(ADP-ribose) polymerase in higher and lower eukaryotes. *Eur. J. Biochem.* 159:77-84.

Stark, C. R., Orleans, M., Haverkamp, A. D., *et al.* (1984) Short- and long-term risks after exposure to diagnostic ultrasound *in utero*. *Obset. Gyn.* 63:194-200.

Sundstrom, C. and Nilsson, K. (1976) Establishment and characterization of a human histiocytic lymphoma cell line (U-937). *Int. J. Cancer* 17:565-577.

Suslick, K. S. (1988) *Ultrasound: Its Chemical, Physical and Biological Effects.* VCH Verlagsgesellschaft mBH, Weinheim.

Szoka, F. and Paphadjopoulos, D. (1978) Procedure for preparation of liposomes with large internal aqueous space and high capture by reverse-phase evaporation. *Proc. Natl. Acad. Sci.* 75(9):4194-4198.

Tata, D. B., Biglow, J., Wu, J. *et al.* (1996) Ultrasound-enhanced hydroxyl radical production from two clinically employed anti-cancer drugs, adriamycin and mitomycin C. *Ultrasonics Sonochemistry* 3:39-45.

Tata, D. B., Dunn, F. and Tindall, D. J. (1997) Selective clinical ultrasound signals mediate differential gene transfer and expression in two human prostate cancer cell lines: LnCap and PC-3. *Biochem. Biophys. Res. Com.* 234:64-67.

Ter Harr, G. R. and Daniels, S. (1981) Evidence for ultrasonically induced cavitation *in vivo*. *Phys. Med. Biol.* 26(6):1145-1149.

This Morning (1999) Granada Television. 15th June.

TV Quick (1997) Letters. 3-9th May:Issue 18.

Umemura, S., Kawabata, K., Yumita, N. *et al.* (1992) Sonodynamic approach to tumor treatment. *IEEE Ultrasonics Symposium* 1231-1240.

Unger, E. C., M^{c}Creery, T. P. and Sweitzer, R. H. (1997) Ultrasound enhances gene expression of liposomal transfection. *Investigative Radiology* 32(12):723-727.

Wallace, W. (1996) Could Ultrasound damage your baby? *The Independent.* 13th August Section 2:6-7.

Williams, A. R. (1983) *Ultrasound: Biological Effects and Potential Hazards.* Academic Press Inc., London.

Williams, A. R., Miller, D. L. and Gross, D. R. (1986) Haemolysis *in vivo* by therapeutic intensities of ultrasound. *Ultrasound Med. Biol.* 12(6):501-509.

World Federation for Ultrasound in Medicine and Biology (1992) WFUMB Symposium on safety and standardization of medical ultrasound. *Ultrasound. Med. Biol.* 18(9):736-750.

World Federation for Ultrasound in Medicine and Biology (1998) WFUMB Symposium on safety of ultrasound in medicine. *Ultrasound Med. Biol.* 24:Supp 1.

Yamanaka, H., Penning, C. A., Willis, E. H. *et al.* (1988) Characterisation of human poly(ADP-ribose) polymerase with autoantibodies. *J. Biol. Chem.* 263(8):3879-3883.

Young., S.R. and Dyson, M. (1990) Macrophage responsiveness to therapeutic ultrasound. *Ultrasound Med. Biol.* 16(8):809-816.